

IMA9-2018

IMA9 - 9th Conference of the International Marangoni Association

Interfacial Fluid Dynamics and Processes



August 31 – September 5, 2018, Guilin, China

ORGANIZATIONS

ORGANIZED BY:

- International Marangoni Association (IMA);
- Institute of Mechanics, Chinese Academy of Sciences;
- Guilin University of Electronic Technology.

CO-ORGANIZERS:

- Institute of Process Engineering, CAS;
- College of Power Engineering, Chongqing University.

SPONSORED BY:

- National Natural Science Foundation of China (NSFC);
- Chinese Academy of Sciences.

TOPICS:

- ✧ Marangoni effects
- ✧ Contact angle and contact angle dynamics
- ✧ Interfacial instabilities and surface waves
- ✧ Interfacial phenomena with phase change
- ✧ Thermo- and solutocapillary flows
- ✧ Thin films and multiple-layer systems
- ✧ Boiling and evaporation
- ✧ Heat pipes
- ✧ Droplets and spreading
- ✧ Binary mixtures and surfactants
- ✧ Coating processes
- ✧ Microfluidics
- ✧ Liquid bridges
- ✧ Applications in material processing
- ✧ Applications in bio-fluid systems

SCIENTIFIC COMMITTEE:

- S. Amiroudine (France)
- E. Benilov (Ireland)
- M. Besthorn (Germany)
- C. Dang Vu-Delcarte (France)
- K. Eckert (Germany)
- H. Kuhlmann (Austria)
- S. Kumar (USA)
- Q.-S. Liu (China)
- M. Medale (France)
- A. Mizev (Russia)
- R. Narayanan (USA)
- A. Nepomnyashchy (Israel)
- K. Nishino (Japan)
- A. Oron (Israel)
- R. Savino (Italy)
- D. Schwabe (Germany)
- V. Shevtsova (Belgium)
- V. Starov (UK)
- I. Ueno (Japan)
- A. Viviani (Italy)

Advisory Committee:

H. Kuhlmann (Austria)
R. Narayanan (USA)
A. Oron (Israel)
D. Schwabe (Germany)

ORGANIZING COMMITTEE:

Q-S Liu (China)
H. Kuhlmann (Austria)
A. Oron (Israel)
M. Besthorn (Germany)
V. Shevtsova (Belgium)
F. Duan (Singapore)

ORGANIZING SECRETARY:

Ya-Sha LIU Institute of Mechanics/CAS, China
Xue CHEN Guilin University of Electronic Technology.

LOCAL ORGANIZING COMMITTEE:

Q-S Liu (IM/CAS) (Chair)	C. Yang (IPE/CAS) (Co-Chair)	Y-R Li (CQU) (Co-Chair)
G-D Yang (GUET) (Co-Chair)	X-Y. Gao (GUET)	Y-Y Mo (GUET)
Q-S Chen (IM/CAS)	X Chen (GUET)	J. Chen (IPE/CAS)
J-J Guo (IM/CAS)	Y-S Liu (IM/CAS)	C-M Wu (CQU)
Y-M Yong (IPE/CAS)	D-W Zhang (IM/CAS)	Z-Q Zhu (IM/CAS)

Introduction

Conference of the International Marangoni Association (IMA) is coordinated by International Marangoni Association. The main objective of the 9th Conference of the International Marangoni Association (IMA9) is to provide opportunities for scientists and engineers, working on the Interfacial Fluid Dynamics and Processes, to exchange their knowledge and ideas, and to renew their friendship. Previous conferences were held successfully in Rauschholzhausen (2001), Brussels (2004), Gainesville FL (2006), Tokyo (2008), Florence (2010), Haifa (2012), Vienna (2014) and the most recent one in Bad Honnef (2016). The 9th Conference of the International Marangoni Association (IMA9) will take place at the City Centre “Lijiang Waterfall Hotel”, Guilin, China on August 31-September 5, 2018.

On behalf of the 9th Conference of the International Marangoni Association (IMA9) and the Organizing Committee, it is our privilege to invite you to the 9th Conference of the International Marangoni Association- Interfacial Fluid Dynamics and Processes, August 31 – September 5, 2018, Guilin, China. We are honored to host this event, and look forward to welcoming all friends and colleagues from around the world.

We would like to thank all the institutions of organizers and sponsors, especially to the National Natural Science Foundation of China (NSFC) for its financial support.

Enjoy your time in Guilin.

Prof. Qiu-Sheng Liu
Chair of the Symposium Scientific and Organizing Committees.

Contents

Part I	1
General Information	3
Venue	3
IMA9 Program Overview	7
Full Program	8
Poster Program	15
Social Program	17
Part II	19
THE ABSTRACTS	19
Ratchet flows in thin liquid films under two-frequency asymmetric tangential forcing	21
Elad Sterman-Cohen, Michael Bestehorn and Alex Oron	21
The spreading of liquid droplets upon impact on a hard surface	22
Alexey Fedyushkin, Aleksey Rozhkov	22
Solutal-Marangoni-induced apparent contact angles for evaporating sessile drops of binary liquids	23
Jehan Charlier, Alexey Rednikov, Sam Dehaeck, Pierre Colinet and Denis Terwagne	23
Transient gas flow in elastic microchannel	24
Shai Elbaz, Hila Jacob and Amir Gat	24
Unsteady Conjugate Mass Transfer between a Deformable Droplet and a Creeping Extensional Flow in a Cross-slot	25
Anjun Liu, Jie Chen, Zhenzhen Wang, Chao Yang, Jingtao Wang, and Zai-Sha Mao	25
Formation of frozen waves on miscible interface	26
Ilya B. Simanovskii, Antonio Viviani.....	26
Effect of Pool Rotation on Thermal-solutal Marangoni Convection in a Shallow Annular Pool with Radial Temperature and Concentration Gradients	27
Cheng-Zhi Zhu, Lan Peng, Li Ma and Jian Gao	27
Linear stability of thermocapillary liquid layers on an inclined plane	28
Chen-Yi Yan, Kai-Xin Hu	28
Short-Wave Marangoni instability in thin films	29
Dipin S. Pillai, R. Narayanan	29
The role of physical science in material design	30
Dominika Zabiegaj, Nicasio Gerald.....	30
Elastic deformation instability in soft microfluidic configurations induced by non-uniform electro-osmotic flow	31



Evgeniy Boyko, Amir D. Gatand Moran Bercovici.....	31
Controlling Coffee Ring Drying from a Sessile Colloidal Droplet through Diffusion-Limited Aggregation Approach	32
Junheng Ren, Alexandru Crivoi, and Fei Duan	32
Numerical Study of Marangoni Effect and Buoyancy Effect in Enclosed Cavity with a Fluid Phase Change Interface.....	33
Guo-Feng Xu and Qiu-Sheng Liu	33
Crystallization controlled by Marangoni Flows	35
Hans Riegler, Stephan Eickelmann, Bingbing Sun, and Junbai Li.....	35
Surface Ondulations of Ultrathin Liquid Films Induced by Marangoni Flows	36
Hans Riegler, Stefan Karpitschka, and Stephan Eickelmann.....	36
Effect of rotating magnetic field on the thermocapillary flow instability in a liquid bridge	37
Hao Liu, Zhong Zeng, Long Qiao	37
Surface waves in a circular channel: experiment and simulation	38
Ion Dan Borcia, Rodica Borcia, Michael Bestehorn, Wenchao Xu, and Uwe Harlander.....	38
Bénard-Marangoni Instability Patterns in Evaporating Sessile Droplet at Constant Contact Angle Mode on a Heated Substrate	39
Ji-Long Zhu , Wan-Yuan Shi	39
Mass transfer and fluid dynamics in disperse multiphase systems: Interfacial phenomena in the presence of surfactants	40
Joschka M. Schulz, Lutz Böhm and Matthias Kraume.....	40
Linear stability of thermocapillary liquid layers of non-Newtonian fluids	41
Kai-Xin Hu, Chen-Yi Yan.....	41
Electrohydrodynamic Instabilities in Microchannels for non-Newtonian Liquids	42
Seymen İlke Kaykanat, Berkay Keklik and Kerem Uguz.....	42
Surface Heat Dissipation Dependence of Thermocapillary Convection in Shallow Annular Pool.....	43
Li Zhang, You-Rong Li and Chun-Mei Wu	43
Experimental Study of Thermocapillary Convection of Liquid Layer with an Evaporating Interface	44
Li-Li Qiao, Qiu-Sheng Liu and Zhi-Qiang Zhu.....	44
Thermocapillary Flow at the Evaporating Interface of a Liquid Pool Powered by an Interfacial Line Heater	46
Lu Qiu, Fei Duan.....	46
Effect of using mixed working fluid on the performance of open pulsating heat pipe (OLPHP)	47
Meilan Zhou, Caihang Liang.....	47
Dimension-Reduced Model for DeepWater Waves	50
Michael Bestehorn and Peder A. Tyvand.....	50

Thermal Marangoni convection for particle assembling in colloidal films	51
Mohammed Al-Muzaiqer, Victor Fliagin, Natalia Ivanova.....	51
Thermocapillary deformation of a pinned sessile droplet caused by a laser beam	52
Sergey Semenov, Alexander Malyuk and Natalia Ivanova	52
Laser-induced thermocapillary rupture of a thin liquid layer laying on a liquid substrate	53
Natalia Ivanova, Denis Klyuev, Victor Fliagin.....	53
Humidity-induced breath of droplets: Marangoni-driven against sorption-driven mechanisms	54
Nikolay Kubochkin, Natalia Ivanova	54
Radiative heat transfer from the surface of thermocapillary liquid bridges of high-Prandtl-number fluids in microgravity	55
Nobuhiro Shitomi, Taishi Yano and Koichi Nishino	55
Thermocapillary flow instability in low Pr fluid pool: Effects of Pr and pool geometry.....	56
Nobuyuki Imaishi, M.K. Ermakov and W.Y. Shi	56
Structures of film flow with phase transitions.....	57
Oxana A. Frolovskaya and Vladislav V. Pukhnachev.....	57
Mathematical Models of Polymer Solutions Motion	58
Oxana A. Frolovskaya and Vladislav V. Pukhnachev.....	58
Two- and three-dimensional numerical simulations of sessile droplets.....	59
Paul G. Chen, Jalil Ouazzani and Qiusheng Liu.....	59
Cohesion of natural cave sediments in the presence of thin liquid films	60
Perrine Freydier, Frédéric Doumenc, Jérôme Martin, Béatrice Guerrier, Pierre-Yves Jeannin	60
Velocity profiles in the front of viscoplastic surges: experimental-theoretical comparisons	61
Perrine Freydier, Guillaume Chambon	61
Image super resolution reconstruction based on deep parallel convolution neural network ...	62
Qiang Yu, Liu Xiaoke.....	62
Study on combined buoyancy-Marangoni convection heat and mass transfer of nanofluids in porous media	63
Y.J. Zhuang, Q.Y. Zhu.....	63
Effect of rod-rotating on stability of thermocapillary flows under microgravity conditions....	64
Q.-S. Chen, P. Zhu, M. He, K.-X. Hu.....	64
Phase-Changed Interfacial Formation of Evaporation and Condensation under Microgravity Condition onboard Space Platforms TZ-1	65
Qiusheng Liu, Zhiqiang Zhu, Wenjun Liu, Zhengzhi Zhang, Guofeng Xu, Jingchang Xie	65
Electrostatically Forced Interfacial Instability.....	66
Ranga Narayanan, Nevin Brosius, Kevin Ward, Dipin Pillai, and Satoshi Matsumoto.....	66
Liquid pumping induced by transverse forced vibrations of an elastic beam: A lubrication approach.....	67



Rodica Borcia and Michael Bestehorn	67
Breath Figures on ice films	68
Ruddy Urbina and Wenceslao González-Viñas	68
Melting Dynamics of Phase Change Materials under Thermocapillarity	69
Santiago Madruga.....	69
Direct Numerical Simulation of the Navier-Stokes equations	70
Sebastian Richter and Michael Bestehorn	70
Experimental investigation of thermocapillary deformation of thin liquid films on heated structured substrates.....	71
Iman Nejati, Cihat Ates, Timm Schröder, Peter Stephan and Tatiana Gambaryan-Roisman.....	71
Marangoni-induced isothermal levitation of n-butanol droplet above n-butanol-silicone oil solutions.....	72
Natalia Ivanova, Tair Esenbaev and Denis Klyuev	72
Thermocapillary Convection in High-Prandtl-Number Liquid Bridges with Free Surface Cooling/Heating by Ambient Gas Flow	73
Taishi Yano, Makoto Hirotsu and Koichi Nishino.....	73
Rayleigh-Benard-Marangoni instability in a system of two superposed horizontal layers of immiscible fluids with deformable interface	74
Tatyana Lyubimova , Yanina Parshakova	74
Rayleigh-Taylor and Kelvin-Helmholtz Instabilities of a Miscible Interfaces.....	75
Tatyana Lyubimova , Anatoly Vorobev, Sergei Prokopev and Andrey Ivantsov	75
Thermocapillary dipole in a Hele-Shaw cell.....	77
Formation of frozen waves on miscible interface	78
Valentina Shevtsova, Aliaksandr Mialdun and Yuri Gaponenko	78
Influence of internal energy of the interface on a stationary flow and its stability	79
Victor Andreev and Victoria Bekezhanova.....	79
Thermocapillary convection in a liquid layer induced by local heating	81
Victoria Bekezhanova and Alla Ovcharova.....	81
Critical characteristics of the two-layer convective flows with evaporation in a 3D channel... 82	82
Victoria Bekezhanova and Olga Goncharova	82
Measurement of the thermocapillary deformations of liquid layers using the laser-scanning method.....	83
Viktor M. Fliagin, Natalia A. Ivanova, Vasily V. Vostrikov.....	83
Numerical Study of the Diffusion of Two Gases Equally Diluted by Third Component	84
Vladimir Kossov, Olga Fedorenko, Dauren Zhakebayev and Asylzhan Kizbaev	84
Modelling of heat transfer and mass transfer in cryogenic propellant tank pressurization process under microgravity environment.....	85
WANG Yanhui, GA Yongjing, LUO Shu, WANG Haosu, ZHOU Binghong	85

Instabilities of thermocapillary-buoyancy-driven flow in a rotating annular pool of medium Prandtl number liquid.....	86
Wan-Yuan Shi, Han-Ming Li and Michael Ermakov	86
Growth mechanisms of Breath Figures with a humidity sink	87
Mathan K. Raja and Wenceslao González-Viñas	87
A Method of Measuring Gas Density By Digital Holography	88
Wei Song, Qiu-Sheng Liu, Jin-Chang Xie, Yong-Xiang Xv, Wen-Jun Liu, Li-Li Qiao	88
Experimental Investigation of Quasi-Static Liquid Layer Evaporation	90
Wen-Jun Liu and Qiu-Sheng Liu	90
The influence of different scale on thermocapillary convection in sessile droplet: experimental study	92
Xue CHEN', Zhiqiang ZHU, Qiu-Sheng LIU	92
Effect of Rotation on Thermal-Solutal Capillary Convection of Binary Fluid Mixture in a Czochralski Configuration	94
Wu Chunmei, Yuan Bo, Li Yourong and Lin Ding	94
Unsteady flow and heat transfer of MHD nanofluid thin film over a stretching sheet with Marangoni convection	96
Yan Zhang , Bo Yuan , Min Zhang and Yu Bai	96
Influence of confinement on the linear stability of a falling liquid film.....	99
Yiqin Li, Sophie Mergui, Gianluca Lavallo and Georg F. Dietze	99
Effect of gas temperature on instability in liquid bridge.....	100
Yury Gaponenko, Viktor Yasnou, Aliaksandr Mialdun and Valentina Shevtsova	100
Numerical Simulation of Marangoni Convection in a Sessile Droplet Evaporating in Pure Vapor	101
Yu Zhang, You-Rong Li and Jia-Jia Yu	101
Spontaneous motion of a floating droplet on liquid layer	102
Zhenzhen Wang, Jie Chen, Anjun Liu , Chao Yang, and Zai-Sha Mao.....	102
The double-diffusive Marangoni convection in opened two-layer rectangular cavity.....	103
Zheng Feng, Zheng Lin	103
Preliminary Results of Droplet Evaporation Experiments onboard TZ-1 Cargo Spaceship .	106
Wen-Jun Liu, Zhi-Qiang Zhu and Qiu-Sheng Liu	106
Part III.....	108
LIST OF PARTICIPANTS	109



Part I

THE CONFERENCE

General Information

Venue

The conference will be held in “Lijiang Waterfall Hotel” located at the City Centre of Guilin, (Guangxi Province, China).

Lectures will be given in the “Li Jiang Hall” which is located at 4th floor of the hotel.

Lijiang Waterfall Hotel

Located near Diecai Hill Park, Guilin Lijiang Waterfall Hotel is in close vicinity of the picturesque Lijiang River, the gently flowing Cedar Lake, the symbolic Elephant Trunk Hill, the bustling Zhengyang Pedestrian Street and Central Square (nicknamed as the Parlor of the City). From here, it's only 25 km to Guilin Liangjiang International Airport and 3 km to Guilin Railway Station. The huge man-made waterfall at the back of the hotel, referred to as Milky Way, is a must-see sight for tourists flocking into Guilin. The waterfall measures 45 meters high, 72 meters wide at the top and 75 meters at the bottom, which enables its entry into the Guinness World Record. A total of 652 guestrooms are elegantly designed with light and natural colors and built with environment-friendly materials. Special care to details is also given to ensure customer satisfaction. With a total of 1800 seats, the dining section inside the hotel serves a great variety of delicious dishes and its 21 boxes are all in different decorative styles. The hotel also boasts a whole range of advanced facilities for conferences, exhibitions and business activities. Its multi-functional hall can hold 400 diners or 500 conference participants and is equipped with a six-channel simultaneous interpretation conference system. Other options are available, including the five meeting rooms of different types and sizes. Health and sports facilities are also found here, including an indoor heated swimming pool, a roof garden, a VIP fitness club, a sauna and massage parlour as well as a beauty salon. Since its opening, the hotel has received numerous honors, including National Golden Leaf Green Hotel which made it one of the first hotels in Guangxi that won such a recognition. With reasonable pricing and high-quality service, Guilin Lijiang Waterfall Hotel is your top choice for a trip either on business or for pleasure.

Hotel Address: No.1 Shanhu North Road, Xiufeng District, Xiufeng, 541001 Guilin, China

Phone: (0773)2822881

Post: 541001

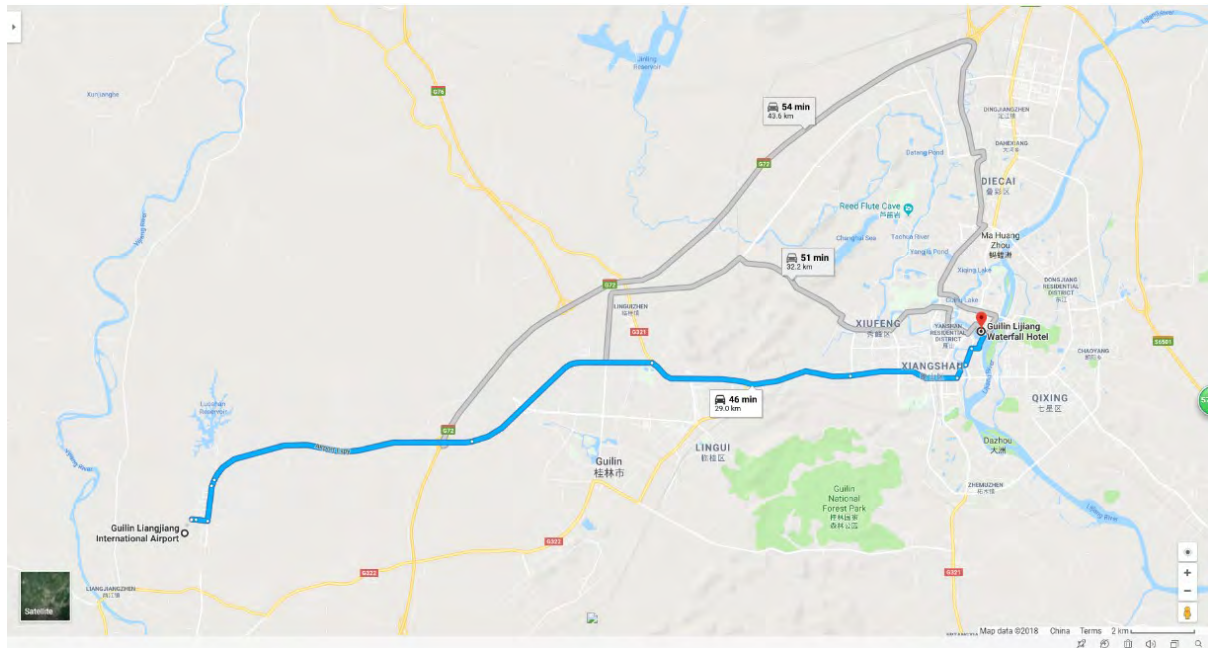
Web-site: http://www.waterfallguilin.com/en/index_main.html

Transportation

Guilin Lijiang Waterfall Hotel is located in the center of Guilin city, “Center Landscape Zone near both Mountain and River”, which is very close to the beautiful Lijiang River, green-waving Sequoia Lake, the badge of Guilin, the Elephant Trunk Hill, the “Hall of Guilin” — the Central Square, and the prosperous Zhengyang Commercial Street. Walk out of the hotel to feel the bustling Guilin, and enter into the hotel to enjoy tranquility.

The hotel integrates business and entertainment functions, just 3 kilometers from the train station, 2 kilometers to the bus station, 30 km away from the Guilin Liangjiang International Airport, about

40-50 minutes by taxi.



Contact Address

Conference Chair: Prof. Qiusheng LIU (liu@imech.ac.cn)

Institute of Mechanics, Chinese Academy of Sciences
Address: No.15 Beisihuanxi Road, Beijing, 100190 (China)
TEL: 8610-82544095, FAX: 8610-82544096

Conference Secretary: Ms. Yasha LIU (liyasha@imech.ac.cn)

Institute of Mechanics, Chinese Academy of Sciences
Address: No.15 Beisihuanxi Road, Beijing, 100190 (China)
TEL: 8610-82543650, FAX: 8610-82544096

Email Address: ima9@imech.ac.cn

Registration Desk

The registration desk is located at the hall of the Lijiang Waterfall Hotel (the first floor of the hotel)

The opening hours will be:

Friday 31 August 10:00–20:00

Saturday 1 September 08:30–12:00

Information for Presenting Authors

- Please contact the chairman of your session before the session starts. He must make sure that all presenting authors are present.
- Please stick to the time table. The time available for oral presentations is 15 minutes including discussion, for poster presentation it is 3 minutes.
- For poster presentation, please check the relative board code written in the poster sessions' program. We will offer the panel of
W90 cm x H120 cm in size. Please prepare your poster within the above size in vertical shape
- If you have a computer presentation, please transfer your presentation to the conference laptop in



the meeting room. Please make sure that all features of your presentation are working correctly.

- You can transfer your presentation to the conference laptop from 08:00 to 08:30 in the morning, or from 13:00 to 14:00. Alternatively, if you want to use your personal laptop, please make sure that it is well adaptable to the projection system in the meeting room. Any delay will reduce your presentation time.

Information for Chairs

- _ Please reserve 3 minutes for the discussion at the end of each oral presentation.
- _ Poster presentations do not need to reserve any official time for discussion.
- _ Please keep the schedule strictly.

Phone Numbers

- Chinese country code: +86
- Guilin area code: (0)773
- Emergency 120
- Police 110
- Fire 119

IMA9 Program Overview

Aug.31 Friday	10:00-20:00	Registration, Welcome reception (Dinner)	
Sep.1 Saturday	8:45-9:15	Registration	
	9:15-9:30	Opening Session	Chairman: Q.S. Liu
	9:30-10:30	Session 1- Thin Films and Marangoni Effects-I	Chairman: R. Narayanan
	10:30-11:00	Coffee Break	
	11:00-12:00	Session 2- Interfacial Instability and Waves	Chairman: P. G. Chen
	12:00-14:00	Lunch	
	14:00-15:15	Session 3- Drops and Spreading	Chairmen: M.Bestehorn & C. Yang
	15:15-15:45	Poster Session I–Short Presentation	Chairman: K. Nishino
	15:45-16:15	Coffee Break	
	16:15-17:15	Session 4- Liquid Bridges	Chair: V. Shevtsova
	17:15-17:30	Presentation of IMA10	R. Borcia
18:00-20:00	Dinner		
Sep.2 Sunday	9:00-10:30	Session 5- Gravity and Marangoni Effects	Chairmen: N. Imaishi & W.Y. Shi
	10:30-11:00	Coffee Break	
	11:00-12:15	Session 6- Thin Films and Marangoni Effects-II	Chairman: A. Oron
	12:15-14:00	Lunch	
	14:00-15:00	Session 7- Evaporation and Condensation	Chairman: F. Duan
	15:00-15:30	Poster Session II- Short Presentation	Chairman: A. Viviani
	15:30-16:00	Coffee Break	
	16:00-17:00	Session 8- Electric-Field Effects	Chairman: Kerem Uguz
	17:00-18:00	Poster Session I & II	
18:00-19:45	Dinner		
20:00-22:00	Social Program in the evening		
Sep.3 Monday	9:00-10:30	Session 9- Thermocapillary Flow	Chairmen: Y.R. Li & C.M. Wu
	10:30-11:00	Coffee Break	
	11:00-12:00	Session 10- Capillary Interfacial Deformation	Chair: R. Borcia
	12:00-14:00	Lunch	
	14:00-15:15	Session 11- Solutocapillary Flow and Effect of Surfactants	Chair: T. Lyubimova
	15:15-15:45	Coffee Break	
	15:45-16:45	Session 12- Numerical Simulations	Chairman: Q.S. Chen
	16:45-17:30	Session 13- Heat Transfer and Phase Change	Chairman: I. Borcia
20:00-21:30	Banquet		

Full Program

Friday, 31/8

10:00-20:00 Registration, Welcome reception/ Dinner



Saturday, 1/9

8:45-9:15 Registration

9:15-9:30 Opening Session (Chairman: Q.S. Liu)

9:30-10:30 Session 1- Thin Films and Marangoni Effects-I (Chairman: R. Narayanan)

9:30 Short-wave Marangoni instability in thin films

Dipin S. Pillai and R. Narayanan

9:45 Liquid pumping induced by transverse forced vibrations

of an elastic beam: A lubrication approach

R. Borcia and M. Bestehorn

10:00 Thermal Marangoni convection for particle assembling in colloidal films

M. Al-Muzaiqer, V. Fliagin and N. Ivanova

10:15 Linear stability of thermocapillary liquid layers on an inclined plane

C.Y. Yan and K.X. Hu

10:30-11:00 Coffee Break

T11:00-12:00 Session 2- Interfacial Instability and Waves (Chairman: P. G. Chen)

11:00 Formation of frozen waves on miscible interface

V. Shevtsova, A. Mialdun and Y. Gaponenko

11:15 Dimension-reduced model for deep water waves

M. Bestehorn and P. A. Tyvand

11:30 Velocity profiles in the front of viscoplastic surges: experimental- theoretical comparisons.

P. Freydier and G. Chambon

11:45 Surface waves in a circular channel: experiment and simulation

Ion D. Borcia, R. Borcia, M. Bestehorn, W. Xu and U. Harlander

12:00-14:00 Lunch

14:00-15:15 Session 3- Drops and Spreading (Chairmen: M. Bestehorn & C. Yang)

14:00 Controlling coffee ring drying from a sessile colloidal droplet through diffusion-limited aggregation approach

F. Duan

14:15 Preliminary results of droplet evaporation experiments onboard TZ-1 cargo spaceship

Z.Q. Zhu, W.J. Liu and Q.S. Liu

14:30 The spreading of liquid droplets upon impact on a hard surface

A. Fedyushkin and A. Rozhkov

14:45 Numerical simulation of Marangoni convection in a sessile droplet evaporating in pure vapor

Y. Zhang, Y.R. Li and J.J. Yu

15:00 Gas flows in elastic microchannels

S. Elbaz, H. Jacob and A. Gat

15:15-15:45 Poster Session I – Short Presentation (Chairman: K. Nishino)

15:45-16:15 Coffee Break

16:15-17:15 Session 4- Liquid Bridges (Chair: V. Shevtsova)

16:15 Effect of gas temperature on instability in liquid bridge

Y. Gaponenko, V. Yasnou, A. Mialdun and V. Shevtsova

16:30 Radiative heat transfer from the surface of thermocapillary liquid bridges of high-Prandtl-number fluids in microgravity

N. Shitomi, T. Yano and K. Nishino

16:45 Effect of rotating magnetic field on the thermocapillary flow instability in a liquid bridge

H. Liu, Z. Zeng and L. Qiao

17:00 Thermocapillary convection in high-Prandtl-number liquid bridges with free surface cooling/heating by ambient gas flow

T. Yano, M. Hirotsu and K. Nishino

17:15-17:30 Presentation of IMA10 (R. Borcia)

18:00-20:00 Dinner

Sunday, 2/9

9:00-10:30 Session 5- Gravity and Marangoni Effects (Chairmen: N. Imaishi & W.Y. Shi)

- 9:00 The influence of spatial temperature modulation of the interfacial heat release on convective flows in a two-layer system
Ilya B. Simanovskii and A. Viviani
- 9:15 Rayleigh-Benard-Marangoni instability in a system of two superposed horizontal layers of immiscible fluids with deformable interface
T. Lyubimova and Y. Parshakova
- 9:30 The double-diffusive Marangoni convection in open two-layer rectangular cavity
Zheng Feng and Zheng Lin
- 9:45 Numerical study of Marangoni effect and buoyancy effect in enclosed cavity with a fluid phase change interface
G.F. Xue and Q.S. Liu
- 10:00 Study on combined buoyancy-Marangoni convection heat and mass transfer of power-law nanofluids in porous fibrous media
Y.J. Zhuang and Q.Y. Zhu
- 10:15 Experimental investigation of quasi-static liquid layer evaporation
W.J. Liu and Q.S. Liu

10:30-11:00 Coffee Break

11:00-12:15 Session 6- Thin Films and Marangoni Effects-II (Chairman: A. Oron)

- 11:10 Influence of confinement on the linear stability of a falling liquid film
Y.Q. Li, S. Merguil, G. Lavalle and G. F. Dietze
- 11:15 Ratchet flows in thin liquid films under two-frequency asymmetric tangential forcing
E. Sterman-Cohen, M. Bestehorn and A. Oron
- 11:30 Surface undulations of ultrathin liquid films induced by Marangoni flows
H. Riegler, S. Karpitschka and S. Eickelmann
- 11:45 Breath figures on ice films
R. Urbina and W. González-Viñas
- 12:00 Unsteady flow and heat transfer of MHD nanofluid thin film overstretching sheet with Marangoni convection
Y. Zhang, B. Yuan, M. Zhang and Y. Bai

12:15-14:00 Lunch

14:00-15:00 Session 7- Evaporation and Condensation (Chairman: F. Duan)

- 14:00 Phase-changed interfacial formation of evaporation and condensation under microgravity condition onboard space platforms TZ-1
Q.S. Liu, Z.Q. Zhu, W.J. Liu, and J.C. Xie
- 14:15 Growth mechanisms of breath figures with a humidity sink

M.K. Raja and W. González-Viñas

14:30 Critical characteristics of the two-layer convective flows with evaporation in a 3D channel

V.B. Bekezhanova and O.N. Goncharova

14:45 Bénard-Marangoni instability patterns in evaporating sessile droplet at constant contact angle mode on a heated substrate

J.L. Zhu and W.Y. Shi

15:00-15:30 Poster Session II -Short Presentation (Chairman: A. Viviani)

15:30-16:00 Coffee Break

16:00-16:45 Session 8- Electric-Field Effects (Chairman: K. Uguz)

16:00 Electrostatically forced interfacial instability

R. Narayanan

16:15 Electrohydrodynamic instabilities in microchannels for non-Newtonian liquids

S. İlke Kaykanat, B. Keklik and K. Uguz

16:30 Elastic deformation instability in soft microfluidic configurations induced by non-uniform electro-osmotic flow

E. Boyko, A. D. Gat and M. Bercovici

17:00-18:00 Poster Session I & II

18:00-19:45 Dinner

20:00-22:00 Social Program in the evening

Accompanying Persons Activities (one full day)

Monday, 3/9

9:00-10:30 Session 9- Thermocapillary Flow (Chairman: Y.R. Li & Chair: C.M. Wu)

9:00 Thermocapillary flow instability in low Pr fluid pool: Effects of Pr and pool geometry

N. Imaishi, M.K. Ermakov and W.Y. Shi

9:15 Effect of rod-rotation on stability of thermocapillary flows under microgravity conditions

Q.-S. Chen, P. Zhu, M. He and K.-X. Hu

9:30 Thermocapillary convection in a liquid layer induced by local heating

V.B. Bekezhanova and A.S. Ovcharova

9:45 Linear stability of thermocapillary liquid layers of non-Newtonian fluids

K.X. Hu and C.Y. Yan

10:00 Surface heat dissipation dependence of thermocapillary convection in shallow annular pool

L. Zhang, Y.R. Li and C.M. Wu

10:15 Thermocapillary dipole in a Hele-Shaw cell
V. Frumkin and M. Bercovici

10:30-11:00 Coffee Break

11:00-12:00 Session 10- Capillary Interfacial Deformation (Chair: R. Borcia)

11:00 Experimental investigation of thermocapillary deformation of thin liquid films on heated structured substrates
I. Nejati, C. Ates, T. Schröder, P. Stephan and T. Gambaryan-Roisman

11:15 Thermocapillary deformation of a pinned sessile droplet caused by a laser beam
S. Semenov, A. Malyuk and N. Ivanova

11:30 Interface of a liquid pool powered by an interfacial line heater
L. Qiu, F. Duan

11:45 Measurement of the thermocapillary deformations of liquid layers using the laser-scanning method
V. Fliagin, D. Klyuev and N. Ivanova

12:00-14:00 Lunch

**14:00-15:00 Session 11- Solutocapillary Flow and Effect of Surfactants
(Chair: T. Lyubimova)**

14:00 Effect of rotation on thermal-solutal capillary convection of binary fluid mixture in a Czochralski configuration
C.M. Wu, B. Yuan, Y.R. Li and D. Lin

14:15 Solutal-Marangoni-induced apparent contact angles for evaporating sessile drops of binary liquids
J. Charlier, A. Rednikov, S. Dehaeck, P. Colinet and D. Terwagne

14:30 Unsteady conjugate mass transfer between a deformable droplet and a creeping extensional flow in a cross-slot
A. Liu, J. Chen, Z.Z. Wang, C. Yang, J.T. Wang and Z.S. Mao

14:45 Mass transfer and fluid dynamics in disperse multiphase systems: Interfacial phenomena in the presence of surfactants
J. M. Schulz, L. Böhm and M. Kraume

15:00 Effect of pool rotation on thermal-solutal Marangoni convection in a shallow annular pool with radial temperature and concentration gradients
C.Z. Zhu, L. Peng, L. Ma and J. Gao

15:15-15:45 Coffee Break

15:45-16:45 Session 12- Numerical Simulations & Experiment (Chairman: Q.S. Chen)

15:45 Direct numerical simulation of the Navier-Stokes equations
S. Richter and M. Bestehorn

16:00 Two- and three-dimensional numerical simulations of sessile droplets

P. G. Chen, J. Ouazzani and Q.S. Liu

16:15 Modelling of heat transfer and mass transfer in cryogenic propellant tank pressurization process under microgravity environment

Y.H. Wang and B.H. Zhou

16:30 Micro/Nano Satellite: Space Science Experiment Solution

Z.Q. Ju and W.J. Ren

16:45-17:30 Session 13- Heat Transfer and Phase Change (Chairman: I. Borcia)

16:45 Structures of film flow with phase transitions

O. A. Frolovskaya and V. V. Pukhnachev

17:00 Effect of using mixed working fluid on the performance of open pulsating heat pipe(OLPHP)

M.L. Zhou and C. Liang

17:15 Melting dynamics of phase change materials under thermocapillarity

S. Madruga

Banquet (20:00-21:30)

Tuesday, 4/9



Excursion to Lijiang River and Yangshuo County

(Full day's excursion out of Guilin City)

Wednesday, 5/9

Leaving from Guilin

Poster Program

1. **Linear stability of thermocapillary liquid layers on an inclined plane**
Chen-Yi Yan, Kai-Xin Hu
2. **The role of physical science in material design**
Dominika Zabiegaj, Nicasio Geraldí
3. **Experimental Study of Thermocapillary Convection of Liquid Layer with an Evaporating Interface**
Li-Li Qiao, Qiu-Sheng Liu and Zhi-Qiang Zhu
4. **Thermocapillary deformation of a pinned sessile droplet caused by a laser beam**
Sergey Semenov, Alexander Malyuk and Natalia Ivanova
5. **Marangoni-induced isothermal levitation of n-butanol droplet above n-butanol-silicone oil solutions**
Natalia Ivanova, Tair Esenbaev and Denis Klyuev
6. **Laser-induced thermocapillary rupture of a thin liquid layer laying on a liquid substrate**
Natalia Ivanova, Denis Klyuev, Victor Fliagin
7. **Humidity-induced breath of droplets: Marangoni-driven against sorption-driven mechanisms**
Nikolay Kubochkin, Natalia Ivanova
8. **Numerical Study of the Diffusion of Two Gases Equally Diluted by Third Component**
Vladimir Kossov, Olga Fedorenko, Dauren Zhakebayev and Asylzhan Kizbaev
9. **Mathematical Models of Polymer Solution Motion**
Oxana A. Frolovskaya and Vladislav V. Pukhnachev
10. **Cohesion of natural cave sediments in the presence of thin liquid films**
Perrine Freydier, Frédéric Doumenc, Jérôme Martin, Béatrice Guerrier, Pierre-Yves Jeannin
11. **Image super resolution reconstruction based on deep parallel convolution neural network**
Qiang Yu, Liu Xiaoke
12. **A Method of Measuring Gas Density By Digital Holography**
Wei Song, Qiu-Sheng Liu, Jin-Chang Xie, Yong-Xiang Xv, Wen-Jun Liu, Li-Li Qiao
13. **The effect of axial vibrations of finite frequency and amplitude on thermocapillary flow in a liquid zone**
Tatyana Lyubimova, Yanina Parshakova, Robert Skuridyn
14. **Rayleigh-Taylor and Kelvin-Helmholtz Instabilities of a Miscible Interfaces**
Tatyana Lyubimova, Anatoly Vorobev, Sergei Prokopev and Andrey Ivantsov
15. **Numerical Simulation of Marangoni Convection in a Sessile Droplet Evaporating in Pure Vapor**
Yu Zhang, You-Rong Li and Jia-Jia Yu
16. **Influence of internal energy of the interface on a stationary flow and its stability**
Victor Andreev and Victoria Bekezhanova
17. **Instabilities of thermocapillary-buoyancy-driven flow in a rotating annular pool of medium Prandtl number liquid**
Wan-Yuan Shi, Han-Ming Li and Michael Ermakov
18. **The influence of different scale on thermocapillary convection in sessile droplet: experimental study**
Xue CHEN, Zhiqiang ZHU, Qiusheng LIU
19. **Spontaneous motion of a floating droplet on liquid layer**
Zhenzhen Wang, Jie Chen, Anjun Liu, Chao Yang, and Zai-Sha Mao
20. **MARANGONI EFFECT IMAGES FROM EXPERIMENTS IN SPACE**
Antonio VERGA



Social Program

Li River

"The river winds like a green silk ribbon, while the hills are like jade hairpins"

--- by HanYu (768-824), a famous Chinese poet of Tang Dynasty (618-907)



Lijiang, China's rivers and mountains of a beautiful pearl is the essence of Guilin scenery is the soul of Guilin scenery is the essence of Guilin scenery. Has long been famous, known for the world. Lijiang is located in the eastern part of Guangxi Zhuang Autonomous Region in southern China is the Pearl River water system. Li River originates in "the first peak in southern China," the more the city north ridge, it is a show Lin Wood, fresh air, excellent local ecological environment. Upper reaches of the Lijiang River mainstream, said six-dong; Nanliu Secretary to the front of Xing'an County near satisfied Huangbai East River, West by Chuanjiang, merging said Jiang

Yong; by Town Meeting dissolved water, flowing through Lingchuan, Guilin, Yangshuo, to Ping music, into the West River, 437 kilometers in length. From Guilin to Yangshuo, about 83 kilometers of the water-way, said Li.

Lijiang Xing'an County originated from Guilin to Yangshuo, 83 kilometers of water-way, winding like a jade belt Lijiang, wrapped in green Qifeng, the good fortune to the world's largest and most beautiful karst scenery scenic. Pan-boat tour of Lijiang, Qifeng considerable reflection, clear water and Castle Peak, cowboy songs and death, gain free hanging, ancient people of the countryside, breathing fresh - everything is so poetic. Currently approved open a three-Lijiang Tour: Urban Water Tour, Lijiang Highlights Tour, Yangshuo, Li River water upstream.

The cave is a typical karst topography, cross-peaks 12, a floor-style cave, inside a collection of different geological ages the growth of stalactites, sparkling, white and flawless, like the night sky and under the tilt of the Milky Way, blinking out like silver, shine like diamonds, so called." Inside dozens of attractions, the most famous landscape: snow-capped mountains, music, Shi Ping, Yao Chi Wonderland; Sambo: Buddha on the economic, pearl umbrella, Chingtien Mot. Uncanny workmanship of nature here has been thoroughly demonstrated, it is known as the "wonders of the world's cave." At the same time, the World Tourism natural scenic resort, human landscape in one; before the vast fields, handsome small Castle Peak, Mountain Village and the North Korea where they stand, forget it; the Song Dynasty Kennedy, a hero of anti-law of Chen legend, adding many more scenic color humanities.



scenic spots full of green. The mountains are green, water is green is green, trees are green, green fields, for which the person was scenic as "representatives of Guilin landscape."

Two Rivers and Four Lakes



Two Rivers and Four Lakes include Liriver, Taohua river and Ronghu lake, Shanhu lake, Guihu lake, Mulong lake. It is extending 7.33km and covering an area of 385.9 thousand square meters.

In 1998, the Two Rivers and Four Lake Project was implemented. The water system cruise has become one of the Guilin's tourist attractions. It starts from Zhiyin Dock, via Shan, Rong, Gui, Mulong, joins the Liriver, ending at the Liberation Bridge.

In middle of Shan lake, there are two pagodas, we call Yan Ta. At night, with the colorful lights glittering on it and the music

fountain nearby, it's very impression for us.

Part II

THE ABSTRACTS

Ratchet flows in thin liquid films under two-frequency asymmetric tangential forcing

Elad Sterman-Cohen*, Michael Bestehorn** and Alex Oron*

* Faculty of Mechanical Engineering, Technion-Israel Institute of Technology,
Haifa, 32000, Israel
meroron@technion.ac.il

**Department of Theoretical Physics, Brandenburg University of Technology, 03044 Cottbus, Germany

We study the dynamics of the system consisting of a thin liquid film placed on the underside of a horizontal planar wall driven by a two-frequency tangential forcing with the acceleration imparted to the substrate by $b(t) = B\omega^2[\cos(\omega t) + \alpha \sin(\omega t)]$, where B and ω are displacement amplitude and frequency of forcing, respectively, and t is time. The longwave limit is employed to derive a set of evolution equations describing the nonlinear spatiotemporal dynamics of the system as in Bestehorn et al. (2013) and Bestehorn (2013) in terms of the local instantaneous dimensionless film thickness h and flow rate q . Linear stability properties of the system are consistent with those arising from the Navier-Stokes equations for disturbances with a sufficiently long wavelength and for small to moderate values of the asymmetry factor α .

A numerical investigation of the nonlinear evolution of the system is carried out and the emergence of ratchet flow under Rayleigh-Taylor instability conditions in periodic domains is revealed. The results demonstrate a feasibility to develop such flow by applying asymmetric forcing to the substrate, and stimulating the system to the subdomain of nonlinear saturated waves. The flow intensity Q is defined as the flow rate q averaged spatially over a periodic domain and temporally over a forcing period in the long time limit. The emergence of ratchet flows is demonstrated here for thin films of water and silicone oil. We reveal that in the long-time regime the flow intensity Q is independent of time and tends to a constant depending on the forcing parameters, film geometry and the liquid. Variation of Q with the fundamental wavenumber of the domain is presented in Fig. 1.

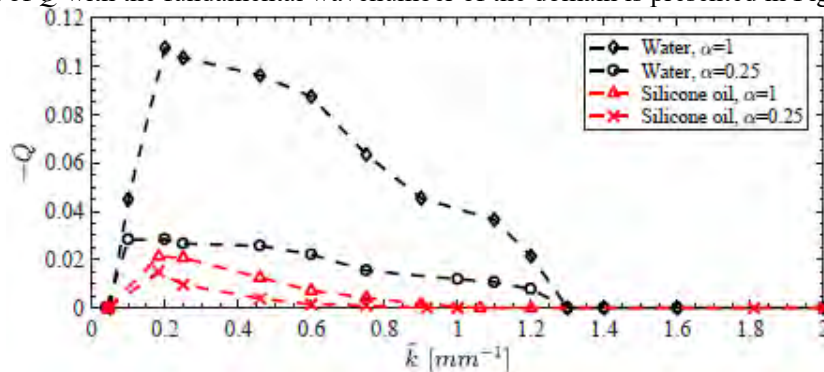


Figure 1: Variation of flow intensity Q with the fundamental wavenumber of the periodic domain for $B=2$ mm and $\omega=125$ rad/s in the water and silicone oil films of $d=0.1$ mm thick.

We find that ratchet flow is created only in the linearly unstable region of the parameter domain. This feature implies that a driving mechanism of the directional flow rate emerges through the presence of interfacial waves created and sustained by an asymmetric substrate vibration, and not by the vibration itself. We show the existence of a threshold frequency beyond which no increase in flow rate is achieved, due to local thinning in the film thickness. This mechanism, enhanced by an increase in the vibration frequency and amplitude, chokes the flow and eventually causes film rupture similarly to what was described as inertial mode of rupture (Sterman-Cohen et al, 2017). Finally, we elucidate the impact of fluid inertia on the emergence of ratchet flow under a tangential forcing which breaks the left-right symmetry. In the presence of inertia, this symmetry breaking creates ratchet flow in the opposite direction with respect to the case of the inertia neglected. If the fluid inertia is accounted for, the flow intensity turns to be a much higher than without it.

The research was partially supported by Grant 1228-405.10 from the Germany-Israel Foundation (GIF) to M. B. and A. O., and by the David T. Siegel Chair in Fluid Mechanics to A. O.

References

- M. Bestehorn, Q. Han, and A. Oron, Phys. Rev. E 88, 023025 (2013).
- M. Bestehorn, Phys. Fluids 25, 114106 (2013).
- E. Sterman-Cohen, M. Bestehorn, and A. Oron, Phys. Fluids 29, 052105 (2017).

The spreading of liquid droplets upon impact on a hard surface

Alexey Fedyushkin, Aleksey Rozhkov

Ishlinsky Institute for Problems in Mechanics of the Russian Academy of Sciences

101/1, Prospect Vernadskogo, Moscow 119526, Russia

E-mails fai@ipmnet.ru, rozhkov@ipmnet.ru

The experimental and numerical investigation of the impact and spreading of liquid drops on solid surface (Fig.1) for various properties, contact angle, diameters d_i , and impact velocities v_i of the drops for different conditions was carried out. Mathematical simulation is performed on the numerical solutions of unsteady 2D and 3D Navier-Stokes equations for flows of incompressible two-phase systems and phase fraction equation.

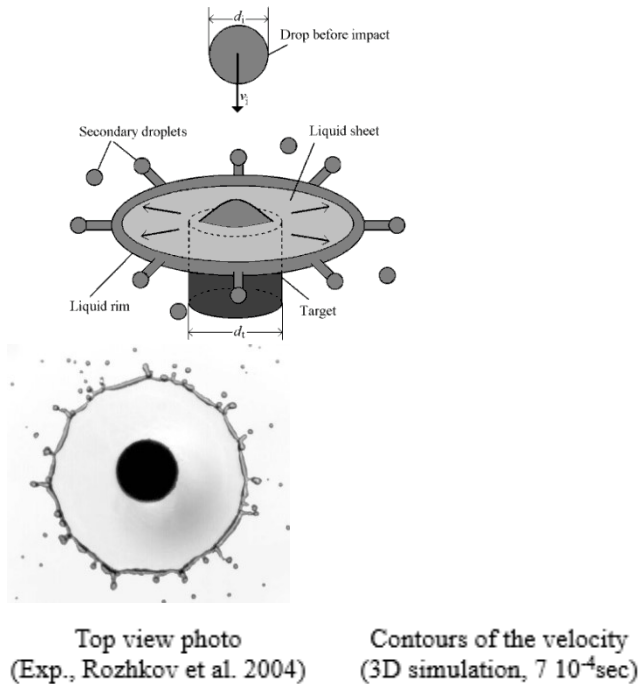


Figure 1: The scheme of the motion.

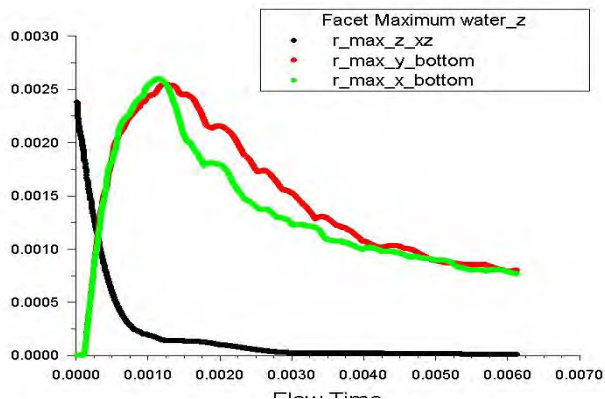


Figure 2: Maximums of distances (m) of falling and spreading water drop ($v_i=3.87$ m/s, $d_i=1$ mm) from zero along coordinates during time (sec) (3D numerical simulation).

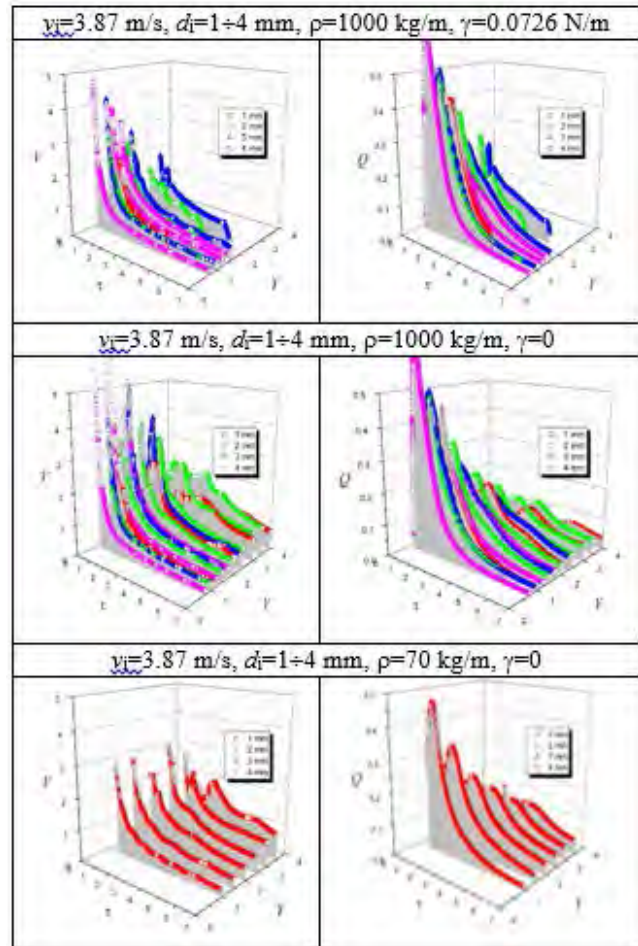


Figure 3: Universality of the flow in the impacting drop (it is resulted on numerical data): the dimensionless velocity $V=v/v_i$ and dimensionless flow rate $Q=q/(\pi d_i v_i/6)$ as functions of dimensionless coordinate $Y=r/d_i$ and dimensionless time $\tau=t/(d_i/v_i)$, respectively; t is the time, r , the radial coordinate (Fig. 1), v , the local velocity, and q , the local flow rate defined as the amount of liquid that flows through a circular contour of radius r per unit time, i.e., $q=2\pi r h v$ with h the local film thickness.

The results of 3D simulation of falling and spreading water drop on solid surface are presented in Fig. 2. Universality diagrams of the flows of spreading liquid drops on solid surfaces are shown in Fig.3. Impact conditions (v_i , d_i , liquid density ρ and surface tension γ) are shown in the Fig.3.

References

- Rozhkov A., Prunet-Foch B., Vignes-Adler M. Impact of water drops on small targets. Physics of Fluids, Vol. 14, N. 10, pp. 3485-3504, (2002)
- Rozhkov A., Prunet-Foch B., Vignes-Adler M. Dynamics of a liquid lamella resulting from the impact of a water drop on small target. Proc. Roy.Soc. London . A. Vol. 460. N. 2049, pp. 2681-2704, (2004)
- Fedyushkin A., Rozhkov A. Investigation of the impact and spreading of drops on solid surface for Ground and Space conditions. Sixth Int. Conf. on Two-phase systems for Ground and Space applications, Italy, 2011. p. 32.

Solutal-Marangoni-induced apparent contact angles for evaporating sessile drops of binary liquids

Jehan Charlier¹, Alexey Rednikov², Sam Dehaeck², Pierre Colinet² and Denis Terwagne¹

Université Libre de Bruxelles, Avenue F.D. Roosevelt, 50, Brussels, 1050, Belgium

¹trioS.lab, CP 223, ²TIPs Laboratory, CP 165/67

E-mail: aredniko@ulb.ac.be

It is known that evaporating sessile drops can possess finite apparent contact angles even in the case of perfect wetting. Accordingly, a (fast) initial spreading eventually stops, giving rise to a quasi-steady stage with a slow retraction governed by evaporation mass loss due to evaporation. Most typically, the dynamical factor behind the finite angles is the flow kinematically induced in the drop by the evaporation process, singular towards the contact line (e.g. Colinet and Rednikov 2011, Morris 2014). In a binary-liquid drop, however, it is rather a solutal Marangoni flow that can become the predominant dynamical factor provided that a more volatile component possesses higher surface tension as e.g. for a water-propylene glycol drop (Cira et al. 2015). It is the latter case that is in the focus of the present study. On the experimental side, our interferometric methods (Dehaeck et al. 2015) helped to reveal and quantify an underlying peculiar shape of such drops (figure 4 left), with an inflection point present in a close vicinity of the contact line. The effect is here much more pronounced than its thermal Marangoni counterpart in the drops of pure liquids (Tsoumpas et al 2015). On the theoretical side, an effective new fitting-parameter-free approach based on the lubrication approximation and Taylor dispersion in the liquid was developed, manifesting a fair agreement with experiment (figure 4 right). Remarkably, unlike the case of thermal Marangoni influence in pure-liquid drops (Tsoumpas et al 2015), the formation of the apparent contact angle here proves to be localizable in a distinguished small vicinity of the contact line, similar to evaporation-induced angles studied by Colinet and Rednikov (2011) and Morris (2014), and thus a fully local approach can be pursued. A simpler version of the theory can be used for large water concentrations, when the evaporation flux distribution along the drop can merely be borrowed/adjusted from the known pure-liquid results. Otherwise, a full coupling with vapor diffusion in the air is required, which can also be accomplished within a local approach.

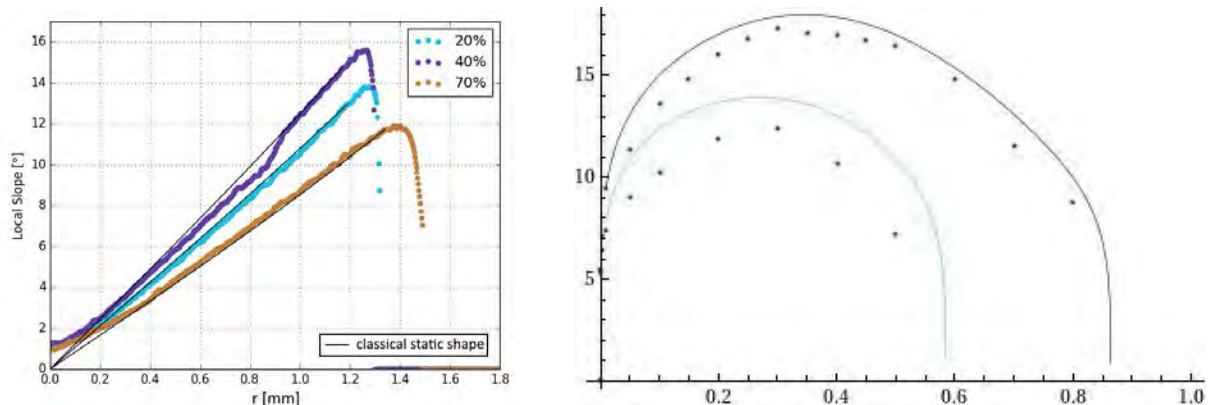


Figure 1: (Left) Slope profiles of 0.5 μl sessile drops at various propylene glycol mass fractions in water and 27.4% relative humidity. (Right) Apparent contact angles ($^\circ$) for such drops as a function of the (average) propylene glycol mass fraction. Measured values from [Cira2015] (dots) and present theoretical results (curves). 75% and 40% relative humidities (upper and lower dots and curves, respectively).

We are grateful to the support from BELSPO & ESA PRODEX projects and F.N.S.-FNRS.

References

- N.J. Cira, A. Benusiglio and M. Prakash, “Vapour-mediated sensing and motility in two-component droplets”, *Nature* 519, 446-450 (2015).
- P. Colinet and A. Rednikov, 2011 “On integrable singularities and apparent contact angles within a classical paradigm. Partial and complete wetting regimes with or without phase change”, *Eur. Phys. J. Special Topics* 197, 89-113 (2011).
- S. Dehaeck, Y. Tsoumpas and P. Colinet, “Analyzing closed-fringe images using two-dimensional fan wavelets”, *Applied Optics* 54, 2939-2952 (2015).
- S.J.S. Morris, “On the contact region of a diffusion-limited evaporating drop: a local analysis”, *J. Fluid Mech.* 739, 308-337 (2014).
- Y. Tsoumpas, S. Dehaeck, A. Rednikov and P. Colinet, “Effect of Marangoni flows on the shape of thin sessile droplets evaporating into air”, *Langmuir* 31, 13334 (2015).

Transient gas flow in elastic microchannel

Shai Elbaz, Hila Jacob and Amir Gat

Faculty of Mechanical Engineering, Technion-Israel Institute of Technology,
Technion City, Haifa, 32000, Israel.
amirgat@technion.ac.il

We study pressure-driven propagation of gas into a two-dimensional microchannel bounded by linearly elastic substrates. Relevant fields of application include lab-on-a-chip devices, soft robotics and respiratory flows. Applying the lubrication approximation, the flow field is governed by the interaction between elasticity and viscosity, as well as weak rarefaction and low-Mach-number compressibility effects, characteristic of gaseous microflows. A governing equation describing the evolution of channel height is derived for the problem. Several physical limits allow simplification of the governing equation and solution by self-similarity. These limits, representing different physical regimes and their corresponding time-scales, include compressibility-elasticity-viscosity, compressibility-viscosity and elasticity-viscosity dominant balances. Transition of the flow field between these regimes and corresponding exact solutions is illustrated for the case of an impulsive mass insertion in which the order-of-magnitude of the deflection evolves in time. For an initial channel thickness which is similar to the elastic deformation generated by the background pressure, a symmetry between compressibility and elasticity allows us to obtain a self-similar solution which includes weak rarefaction effects. The presented results are validated by numerical solutions of the evolution equation.

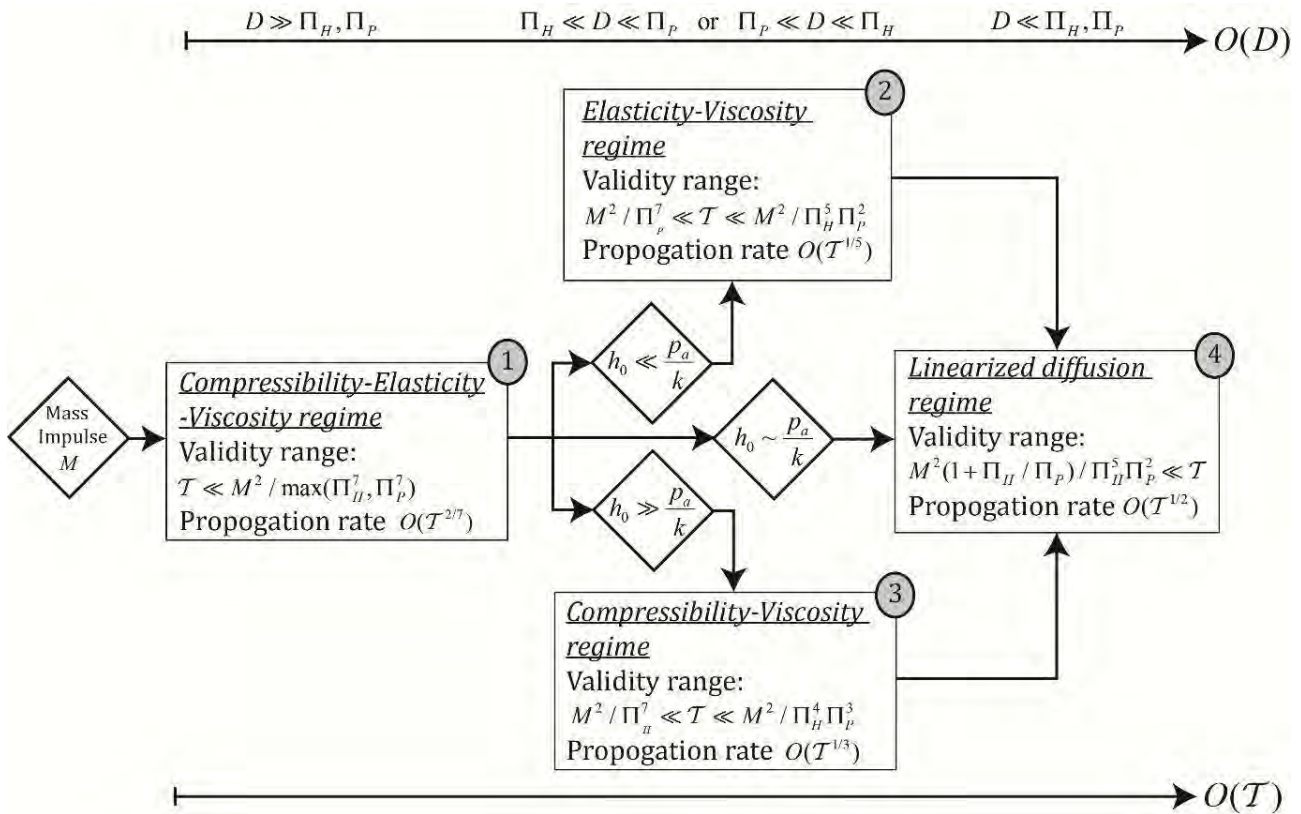


Figure 1: Flowchart diagram of impulse driven transient gaseous flow in a two-dimensional microchannel bounded by linearly elastic substrates. The diagram describes the transition in time between the various propagation regimes associated with different dominant balances of the governing evolution equation (shown in the top scale of the order-of-magnitude of the nondimensional deflection D and its relation to the scale prewetting thickness ratio Π_H and the scaled compression ratio Π_p). Dimensional parametric conditions involving initial channel thickness h_0 , channel stiffness k and background pressure p_0 are also given. The regimes are labeled in grey ellipse numberings as follows: (1) - Compressibility-Elasticity-Viscosity, (2) - Elasticity-Viscosity, (3) - Compressibility-Viscosity, (4) - Linearized diffusion.

Unsteady Conjugate Mass Transfer between a Deformable Droplet and a Creeping Extensional Flow in a Cross-slot

Anjun Liu^{1,2}, Jie Chen^{2,3*}, Zhenzhen Wang^{2,3}, Chao Yang^{2,3*}, Jingtao Wang¹, and Zai-Sha Mao²

¹ School of Chemical Engineering and Technology, Tianjin University, Tianjin 300350, China;

² CAS Key Laboratory of Green Process and Engineering, Institute of Process Engineering, Chinese Academy of Sciences, Beijing 100190, China;

³ University of Chinese Academy of Sciences, Beijing 100049, China

*Corresponding authors: jchen@ipe.ac.cn (J. Chen), chaoyang@ipe.ac.cn (C. Yang)

With the development of the micro-reactors in the food, chemical and pharmaceutical industry, the interface hydrodynamics and transport process of a single drop and simple extensional flow in the micro-channels has been attracted the attentions of the academics and practitioners to demonstrate the enhanced transport performance in micro-channels (Abdollahi et al. 2017). This work was aimed to investigate the unsteady conjugate interafce mass transfer process between a deformable drop and the extensional flow in a cross-slot. The droplet would be trapped in the center of the cross-slot and deform under the extensional flow field. In such a system, it is of great difficulty for experimental observations to predict concentration variation detailedly and precisely. Therefore, we established the mathematical model on the basic of the Stokes equation solved by spectral boundary element method (Dimitrakopoulos et al. 2007), which could describe the deformable interface and its disturbances on the flow field, and the convection-diffusion equation solved by the finite difference method (Yang et al. 2005) to determine the unsteady conjugate interphase mass transfer. The simulation results show that the mass transfer rate, which was characterized by mean concentration variation and Sherwood number Sh , was significantly affected by Capillary number Ca , Peclet number Pe , viscosity ratio λ , interior-to-exterior diffusivity ratio K and distribution coefficient m .

Acknowledgment: This work was supported by the National Key Research and Development Program (2016YFB0301701), National Natural Science Foundation of China (21606234, 21490584) and Key Research Program of Frontier Sciences of CAS (QYZDJ-SSW-JSC030).

References

1. A. Abdollahi, R. N. Sharma and A. Vatani, Fluid flow and heat transfer of liquid-liquid two phase flow in microchannels, *Int. Commun. Heat Mass.* **84**, 66-74(2017).
2. P. Dimitrakopoulos and J. T. Wang, A spectral boundary element algorithm for interfacial dynamics in two-dimensional Stokes flow based on Hermitian interfacial smoothing, *Eng. Anal. Bound. Elem.* **31**, 646-656(2007).
3. C. Yang and Z.-S. Mao, Numerical simulation of interphase mass transfer with the level set approach, *Chem. Eng. Sci.* **60**, 2643-2660(2005).



Formation of frozen waves on miscible interface

Ilya B. Simanovskii¹, Antonio Viviani²

- ⁽¹⁾ Technion – Israel Institute of Technology, 32000 Haifa, Israel
⁽²⁾ Università della Campania “Luigi Vanvitelli”, 81031 Aversa, Italy.
email: antonio.viviani@unicampania.it

It is known that two-layer liquid systems are subject to numerous instabilities. Several classes of instabilities have been found by means of the linear stability theory for purely thermocapillary (or thermal Marangoni) flows and for buoyant-thermocapillary flows. The most interesting phenomena take place if there are two independent factors creating the temperature gradient, namely external heating/cooling from the solid substrate, and the interfacial heat source/sink. The interplay of both factors significantly influences the basic temperature distribution in a two-layer system. In the absence of the heat source/sink, the temperature gradients in both layers are proportional, and their directions coincide. By means of the heat release/consumption, one can achieve arbitrary directions and absolute values of the temperature gradient in each layer. An important problem is controlling the development of instabilities, i.e., the suppression of undesired kinds of patterns or generation of a desired kind of patterns. A possible way of controlling the pattern selection is a spatial modulation of the control parameter. In the present work, we consider the nonlinear dynamics of the flows in the 47v2 silicone oil -water system with rigid heat-insulated lateral walls under the action of a spatial temperature modulation of the heat release/consumption at the interface. It is shown that the spatial modulation can change the sequence of bifurcations. Specifically, it is found that rather intensive spatial temperature modulations suppress the steady states and lead to the development of asymmetric oscillatory flows in the system.

Effect of Pool Rotation on Thermal-solutal Marangoni Convection in a Shallow Annular Pool with Radial Temperature and Concentration Gradients

Cheng-Zhi Zhu, Lan Peng, Li Ma and Jian Gao

Key Laboratory of Low-grade Energy Utilization Technologies and Systems of Ministry of Education,
College of Power Engineering, Chongqing University
No.174 Shazhengjie, Shapingba, Chongqing, 400044, China
E-mail: penglan@cqu.edu.cn

To understand the effect of pool rotation on stability and flow pattern transitions in thermal-solutal Marangoni convection, a series of three-dimensional (3D) numerical simulations of silicon-germanium melt flowing in a slow rotating shallow annular pool were conducted. The annular pool with inner radius $r_i = 20\text{mm}$, outer radius $r_o = 40\text{mm}$ and depth $d = 3\text{mm}$, rotated in the anticlockwise direction around a vertical axis at different rotation rates ranging from the Taylor number $Ta = 0$ to 1200. The bottom surface and the top surface of the annular pool were adiabatic. The radial temperature and concentration gradients were induced by temperature and solute concentration differences between the outer wall and the inner wall. The capillary ratio applied to describe the interaction between the thermal and solutal capillary effects was fixed at -1 , which means that the thermal and solutal capillary effects were equal but in opposite direction. The results indicate that when the thermal Marangoni number (Ma_T) is small, the basic flow of silicon-germanium melt in a rotating annular pool appears as an axisymmetric steady flow with two counter-rotating roll cells in R-Z plane. The clockwise roll cell and anticlockwise roll cell are driven by the solutal and thermal capillary forces respectively. When Ma_T exceeds the critical value, the basic flow becomes unstable and bifurcates into 3D oscillatory flow. All critical Marangoni numbers (Ma_{cri}) in rotating pools are larger than that in the stationary pool. This means the pool rotation stabilizes the basic axisymmetric flow of silicon-germanium melt. However, Ma_{cri} do not increase monotonically with increasing rotation rates. When pool rotates at lower rotation rate ($0 \leq Ta \leq 600$), Ma_{cri} increases with the increase of the pool rotation rate. Meanwhile, when it comes to a higher rotation rates ($600 \leq Ta \leq 1200$), Ma_{cri} decreases with the increase of the pool rotation rate. In addition, some 3D flow patterns which strongly depend on Ma_T and the rotation rate were observed in the rotating annular pool. It was found that the travel waves (TW) occur near the outer wall firstly and propagate into the same azimuthal direction as that of pool rotation at large rotation rates. Then the instabilities occur near the inner wall with the increase of Marangoni number, and the TW near the inner wall propagate into the opposite direction to the pool rotation as shown in Figure 1. The mechanisms of the flow destabilization and flow pattern formation in binary mixtures were discussed.

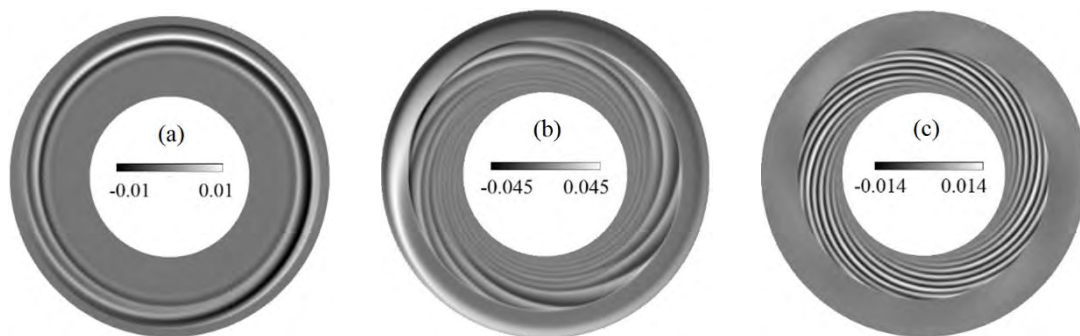


Figure 1: Snapshots of surface solute concentration fluctuation at $Ta = 1200$. (a) $Ma_T = 5000$; (b) $Ma_T = 40000$; (c) $Ma_T = 60000$.



Linear stability of thermocapillary liquid layers on an inclined plane

Chen-Yi Yan, Kai-Xin Hu

Ningbo University, School of Mechanical Engineering and Mechanics
Ningbo, Zhejiang, 315211, China
E-mail: 156001547@nbu.edu.cn

The linear stability analysis has been performed for the thermocapillary liquid layers on an inclined plane. Results are presented for Prandtl numbers (Pr) of 0.01,1 and 100. When the inclination angle is positive, the gravity effect increases the velocity and destabilizes the flow. When the inclination angle is negative, the influence of inclination on the stability depends on Pr. For high Pr, three kinds of instabilities are found: oblique wave, streamwise wave and spanwise stationary mode. For small Pr, the critical Marangoni number has a maximum when the inclination angle increases, and the prefer mode changes from spanwise stationary mode to oblique wave, meanwhile the energy mechanism of perturbation temperature field changes from convection to conduction.

Short-Wave Marangoni instability in thin films

Dipin S. Pillai, R. Narayanan

Department of Chemical Engineering, University of Florida
 1030 Center Drive, Gainesville, FL, USA 32611

dipinsp@ufl.edu

In this work, we investigate the classic problem of Marangoni instability in the context of thin films. It is well known that the Marangoni problem exhibits two modes of instability: (i) a long-wave (LW) instability associated with interface deformation that nonlinearly leads to rupture of thin films, (ii) a short-wave (SW) instability, known as the Pearson mode, associated with convection within the bulk of the liquid without significant interface deformation. The long-wave theory based on separation of length-scales, has been extensively used to derive evolution equations that capture the dynamics of interface in the case of the LW mode (Oron, 1997). In this work, we develop a mathematical model capable of predicting both LW and SW instability in thin films. The model is derived based on the long-wave theory and exploits the “mixed-Galerkin” weighted residual approach as outlined by Ruyer-Quil & Manneville (2002) and Trevelyan & Kalliadasis (2004).

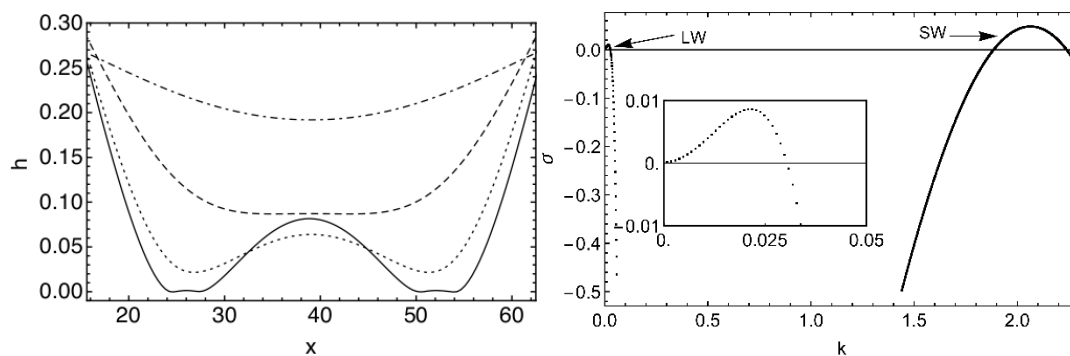


Figure 1(a): Linear stability results of our weighted residual model showing both LW and SW modes (inset shows the LW mode). (b) Time evolution of interface in LW instability of thin films showing cascade of buckling events.

We show that the linearized evolution equations are able to capture the short-wave (SW) Pearson instability mode, in addition to the LW interface deformation mode as shown in Fig 1(a). The nonlinear evolution of the system captures the well-known dynamics associated with the long-wave Marangoni instability such as interfacial rupture and cascade of buckling events as shown in Figure 1(b). In addition, the nonlinear simulation of the SW mode exhibits convective flow in the fluid domain without rupture. Additionally, interesting dynamics resulting from the interactions between the SW and LW modes are also discussed.

References

- Oron, A., Davis, S. H. & Bankoff, S. G. 1997 Long-scale evolution of thin liquid films. *Rev. Mod. Phys.* **69**, 931-980
 Ruyer-Quil, C. & Manneville, P. 2002 Further accuracy and convergence results on the modelling of flows down inclined planes by weighted-residual approximations. *Phys. Fluids* **14**, 170-183
 Trevelyan, P. M. J. & Kalliadasis, S. 2004 Wave dynamics on a thin-film falling down a heated wall. *J. Engg. Math.* **50**, 177-208



The role of physical science in material design

Dominika Zabiegaj, Nicasio Gerald

Smart Materials and Surfaces Laboratory, Faculty of Engineering and Environment, Northumbria University,
Newcastle upon Tyne, NE1 8ST, United Kingdom
E-mail dominika.zabiegaj@northumbria.ac.uk

The main motivation for the design of novel materials is based not only on the fact that properties of different components can be combined in one material but also on the multidisciplinary studies and researchers involved, coming from various fields. Where the different scientific approach, perspective and experience come into one benefit.

The good example can be porous material manufacturing, in which combination of liquid foam and/or emulsion with inorganic particles can result in a material with unique adsorptive, photocatalytic or structural properties, depending on the nature of the used precursor (particle dispersion).

The study faces the problem of porous materials tailoring, produced by solidification of liquid foams stabilized by nano sized solids coming from different origins. Furthermore, it leads to better understanding of the relation between the interfacial properties of mixed systems, containing nanoparticles at different degree of hydrophobicity, surfactants and the stability of the corresponding systems such as liquid and solid foams, or emulsions (Zabiegaj et al 2017).

The interfacial properties of the single particle-laden interfacial layer are characterized by dynamic interfacial tension, interfacial rheology and hydrodynamics measurements together with stability of the corresponding particle stabilized foams. Due to this material design can actually start on the level of single liquid-air (bubble) or liquid-liquid (drop) interface.

The porous materials obtained from these systems, according to specially developed procedure (Zabiegaj et al 2013), are then characterize in terms of porosity, cell size and structure, as well as surface chemical composition.

References

1. D. Zabiegaj et al, Activated carbon monoliths from particles stabilized foams, Microporous and Mesoporous Materials 239 (2017) 45-53
2. D. Zabiegaj et al, Nanoparticle laden interfacial layers and application to foams and solid foams, Colloids and Surfaces A: Physicochem. Eng. Aspects 438 (2013) 132-140

Elastic deformation instability in soft microfluidic configurations induced by non-uniform electro-osmotic flow

Evgeniy Boyko, Amir D. Gatand Moran Bercovici

Faculty of Mechanical Engineering, Technion –Israel Institute of Technology
3200003, Israel.

evgboyko@campus.technion.ac.il

Non-uniform electro-osmotic flow (EOF) in microfluidic configurations gives rise to internal pressure gradients, dictated by mass conservation (Stone et al. 2004). In soft devices, these internal pressures result in elastic deformation, further triggering viscous-elastic interaction (Rubinet et al. 2017; Boyko et al. 2018).

In this theoretical work, we report for the first time a deformation instability of an elastic sheet separated from a rigid plate surface by a thin liquid film and subjected to an EOF-induced attraction force. We first provide insight into the physical behavior of the system by considering a simplified 1D model, inspired by electrostatic MEMS actuators (Rebeiz 2004), in which the elastic sheet is modeled as a rigid plate connected to a linear spring, as shown in Fig. 1(a). Our linear stability analysis, validated by numerical simulations, reveals that the instability is controlled by a non-dimensional parameter representing the ratio of electro-osmotic attractive force to the elastic restoring force. Instability occurs when the gap between the deforming surface and the fixed rigid floor reduces to below $2/3$ (for constant voltage, as illustrated in Fig. 1(b)) or $3/4$ (for constant current) of its initial value, independently of the magnitude of EOF attraction. We further expand our analysis for the case for an elastic sheet that is free to deform under bending or tension conditions. We show that the elastic sheet exhibits qualitatively similar behavior to the rigid plate, and provide approximate asymptotic solutions validated by direct numerical simulations. We believe that the mechanism illustrated in this work, together with the provided analysis, may prove valuable for the implementation of instability-based actuators.

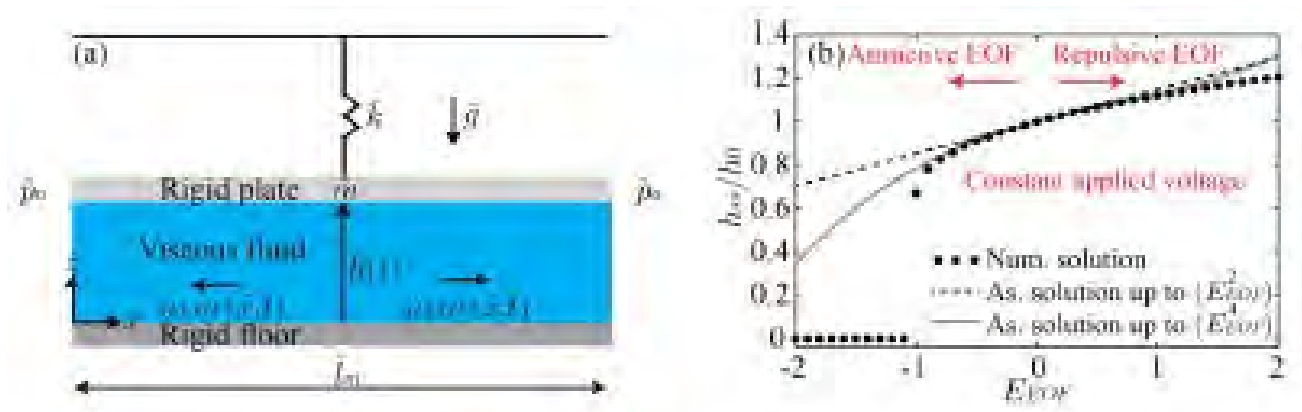


Figure 1: (a) Schematic illustration of a simplified 1D model, consisting of a rigid plate connected to a linear spring and separated from a fixed rigid floor by a thin fluid layer, subjected to non-uniform EOF. (b) The normalized steady-state height h_{ss}/h_0 as a function of the dimensionless electro-osmotic force E_{EOF} in the case of constant voltage.

References

- Boyko, E., Eshel R., Gommed K., Gat, A. D. & Bercovici, M., 2018 Elastohydrodynamics of a pre-stretched finite elastic sheet lubricated by a thin viscous film with application to microfluidic soft-actuators., under review in J. Fluid Mech.
- Rebeiz, G. M. 2004 RF MEMS: theory, design, and technology. John Wiley & Sons.
- Rubin, S., Tulchinsky, A., Gat, A. D. & Bercovici, M. 2017 Elastic deformations driven by non-uniform lubrication flows. J. Fluid Mech. 812, 841-865.
- Stone, H. A., Stroock, A. D. & Ajdari, A. 2004 Engineering flows in small devices: microfluidics toward a lab-on-a-chip. Annu. Rev. Fluid Mech. 36, 381-411.

Controlling Coffee Ring Drying from a Sessile Colloidal Droplet through Diffusion-Limited Aggregation Approach

Junheng Ren, Alexandru Crivoi, and [Fei Duan](#)

School of Mechanical and Aerospace Engineering, Nanyang Technological University
50 Nanyang Ave. Singapore, 639798

feiduan@ntu.edu.sg

Evaporation of a pinned colloidal droplet on a surface would leave a residual deposit near the contact line and coffee-ring. The effect is resulted from a capillary flow toward the pinned edge of the droplet. Many investigations have been conducted to alter the formation of the coffee-stain deposition, however, the system is complex and brings the challenge to the simulation in considering the more affecting factors. A Monte Carlo model has been set up to investigate the transition from the coffee-ring deposition to the uniform coverage and other configurations in drying pinned sessile colloidal droplets. The diffusion limited aggregation approach is applied with coupling the biased random walk to simulate the particle migration and agglomeration during the droplet drying process. The results show that the simultaneous presence of the particle adsorption, long-range attraction, and circulatory motion processes is important for the transition from the coffee ring deposit to the uniform pattern of particles after the sessile droplet is totally dried. The absence of one of the specified factors favors the coffee-ring deposition near the droplet boundary. The strong outward capillary flow on the latest evaporation stage can easily destroy the entire particle pre-ordering at the early drying stages. The formation of a robust particle structure is required to resist the outward flow and alter the coffee-ring formation. Additional quantitative comparison with the experiments can potentially shed light on the physical transition.

Numerical Study of Marangoni Effect and Buoyancy Effect in Enclosed Cavity with a Fluid Phase Change Interface

Guo-Feng Xu^{1,2} and Qiu-Sheng Liu^{1,2*}

¹Institute of Mechanics, Chinese Academy of Sciences, Beijing 100190, China

²University of Chinese Academy of Sciences, Beijing 100049, China

*liu@imech.ac.cn

Buoyancy-thermocapillary convection of the liquid layer have attracted the attention of researchers for many years. Nevertheless, most of the previous research use the one-sided model [1] and the phase change occurring at the interface is eliminated along with the latent heat absorbing or releasing on the free surface. Recently, Qin et al. [2] reported a 2-D and 3-D numerical model studying the Buoyancy-thermocapillary convection of volatile fluids under atmospheric conditions using the two-sided model.

Inspired by Qin, we propose a new two-sided numerical physical model (Fig. 1) to describe the Marangoni and buoyancy effects on both liquid phase and gas phase in a sealed cavity that is laterally heated, coupled with the phase change (evaporation and condensation) occur on the liquid-gas interface. The volatile 0.65 cSt silicone oil with $Pr = 6.83$ is chosen as the working liquid. The governing equations in both liquid and gas phases along with the boundary conditions are solved based on the finite difference method. Steady solutions are obtained when the relative variation of the primitive variables is less than 10^{-6} in a marching step. The accuracy of the calculation program is validated by comparing with the experimental results conducted by [3].

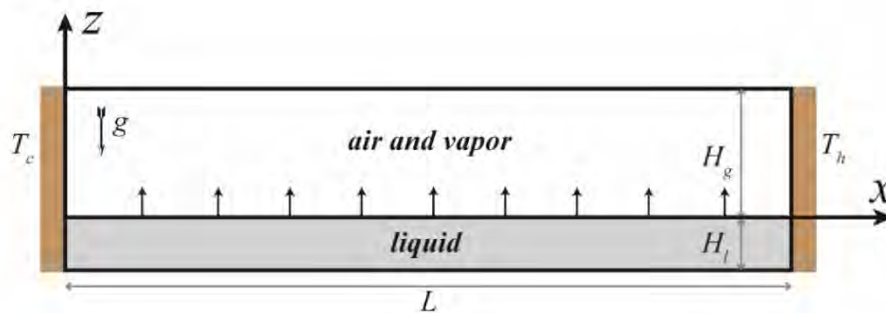
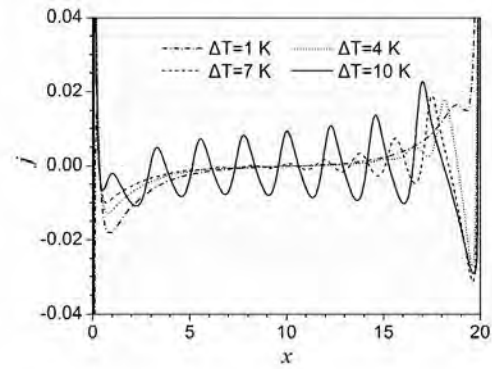
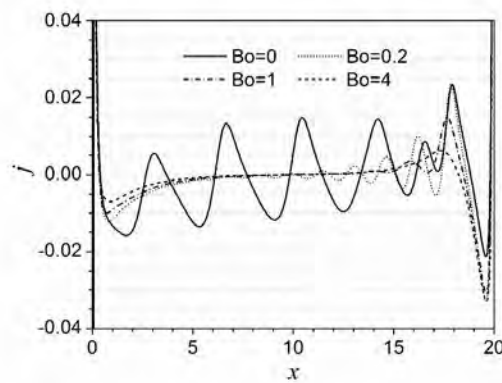


Fig. 1. Schematic of the mathematical model. White and grey regions correspond to the gas phase and liquid phase, respectively. Phase change occurs at the gas-liquid interface ($z = 0$).

With the phase change going on along the liquid-gas interface, the fluid in the closed cavity is driving by the thermocapillary force on the free interface and buoyancy force in the bulk. The basic state of return-flow in both liquid and gas phase layers show up when the temperature gradient parallel to the interface are established. With the imposed temperature difference increased, flow pattern transforms from the steady unicellular flow (SUF) to the steady multicellular flow (SMC), finally the oscillating multicellular flow (OMC). However, at a fixed Marangoni number, the flow pattern degenerates from the steady partial multicellular flow (PMC) to SUF as the dynamic Bond number increased. In addition, we will report the mass flux distribution influenced by the Marangoni number and the Bond number, respectively, shown in Fig. 2. Different regions of evaporation ($j > 0$) and condensation ($j < 0$) distribute across the interface. It is found that high value of the mass flux occurs near the rigid walls and the mass flux in the core region fluctuates with the increasing thermocapillary convection effect and the decreasing buoyancy convection effect. Finally, the flow regimes for different Bo and Ma will be given.



(a)



(b)

Fig. 2. Interfacial dimensionless mass flux distribution for different imposed temperature difference ΔT (a) at $Bo = 0.6$ and different dynamic Bond numbers (b) at $Ma = 868$: $Bo = 0 (g = 0)$.

Acknowledgements

This research was financially supported by the National Natural Science Foundation of China (Grants Nos. 11532015, U1738119) and the China's Manned Space Program (TZ-1).

References

- [1] Y. Ji, Q.-S. Liu, R. Liu, Coupling of evaporation and thermocapillary convection in a liquid layer with mass and heat exchanging interface, *Chin. Phys. Lett.* 25 (2008) 608–611
- [2] Qin T, Tuković Z, Grigoriev R O. Buoyancy-thermocapillary convection of volatile fluids under atmospheric conditions[J]. *International Journal of Heat & Mass Transfer*, 2014, 75(4):284-301.
- [3] Burguete J, Mukolobwicz N, Daviaud F, et al. Buoyant-thermocapillary instabilities in extended liquid layers subjected to a horizontal temperature gradient[J]. *Physics of Fluids*, 2001, 13(10):2773-2787.

Crystallization controlled by Marangoni Flows

Hans Riegler,¹ Stephan Eickelmann,² Bingbing Sun,³ and Junbai Li⁴

1. Max Planck Institute of Colloids and Interfaces, Science Park Golm,
 14424 Potsdam, Germany. hans.riegler@mpikg.mpg.de

2. Max Planck Institute of Colloids and Interfaces, Science Park Golm,
 14424 Potsdam, Germany. stephan.eickelmann@mpikg.mpg.de

3. Beijing National Laboratory for Molecular Sciences,
 CAS Key Laboratory of Colloid, Interface and Chemical Thermodynamics,
 Institute of Chemistry, Chinese Academy of Sciences,
 Beijing 100190, China. sunbingbing@iccas.ac.cn

4. Beijing National Laboratory for Molecular Sciences,
 CAS Key Laboratory of Colloid, Interface and Chemical Thermodynamics,
 Institute of Chemistry, Chinese Academy of Sciences,
 Beijing 100190, China. jbli@iccas.ac.cn

Marangoni flows can be initiated and regulated by the interplay of (local) evaporation conditions and the resulting concentration gradients [1]. It is proposed that such a scenario can successfully be applied to precisely regulate the local conditions for solute enrichment and crystallization. This is demonstrated in the case of the adjustment and optimization of the crystallization and growth of dipeptide fibers from ternary mixtures on planar substrates (see figure) and within small capillaries [2, 3].

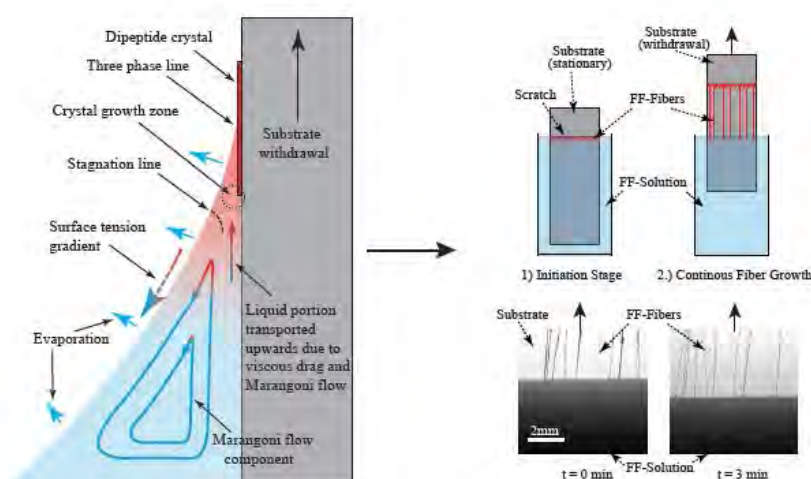


FIG. 1: Growth of dipeptide (FF) fibers controlled by Marangoni flow at the contact line in a dip-coat configuration.

[1] V. Soulie, S. Karpitschka, F. Lequien, P. Prene, T. Zemb, H. Moehwald and H. Riegler, The evaporation behavior of sessile droplets from aqueous saline solutions, *Phys. Chem. Chem. Phys.*, 17, 22296–22303 (2015).

[2] B. Sun, G. Li, H. Riegler, S. Eickelmann, L. Dai, Y. Yang, R. Perez-Garcia, Y. Jia, G. Chen, J. Fei, K. Holmberg, and J. Li, Self-Assembly of Ultralong Aligned Dipeptide Single Crystals, *ACS Nano* 11, 10489–10494 (2017).

[3] B. Sun, H. Riegler, L. Dai, S. Eickelmann, Y. Li, G. Li, Y. Yang, Q. Li, M. Fu, J. Fei, and J. Li, Directed Self-Assembly of Dipeptide Single Crystal in a Capillary, *ACS Nano* 12, 1934–1939 (2018).

Surface Ondulations of Ultrathin Liquid Films Induced by Marangoni Flows

Hans Riegler,¹ Stefan Karpitschka,² and Stephan Eickelmann³

1. Max Planck Institute of Colloids and Interfaces, Science Park Golm,
14424 Potsdam, Germany hans.riegler@mpikg.mpg.de

2. Max Planck Institute for Dynamics and Self-Organization, Science Park Golm,
14424 Potsdam, Germany stephan.eickelmann@mpikg.mpg.de

3. Max Planck Institute of Colloids and Interfaces, Am Faberg 17,
37077 Göttingen, Germany stefan.karpitschka@ds.mpg.de

The topography of thin liquid films on planar solid substrates is investigated. If the films consist of mixtures of different liquid components, the volatility and the differences of the surface tensions of the components have an influence on the film topography. The film surfaces may remain planar or, with (slightly) different composition or evaporation conditions they may undulate. Marangoni flows cause these ondulations. They may enhance/stabilize local ondulations, which start from local variations of the surface tension resulting from occasional local variations of the composition caused by evaporation. The scenario with planar films is similar to the impact of Marangoni flows on the topography of drops, where Marangoni flows can stabilize partial wetting although the components individually as well as their mixtures completely wet the surface if there is no evaporation [1].

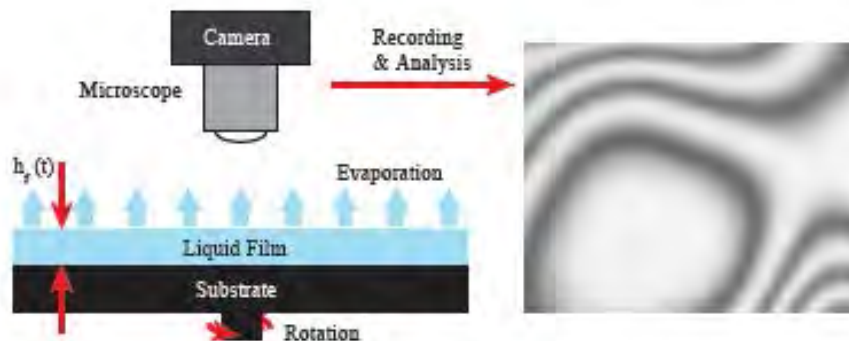


FIG. 1: Experimental setup to investigate the topography of films containing volatile components.

The experiments are performed with a unique setup. It combines a spin cast configuration with timeresolved, on-line, interference-enhanced optical reflection microscopy and image processing [2]. The spin cast mimic allows the preparation and study of liquid films within a wide range of thicknesses, extending from a few micrometers down to ultrathin films of only nanometer thickness. The optical microscopy provides images on the surface topography and also interferometric data on the local film thickness with nanometer resolution [3]. Meanwhile it is understood how the composition varies during film thinning in a spin cast configuration [4, 5]. Therefore such a setup provides information on the topography of the liquid film in relation to its (momentary) thickness and its (momentary) composition.

[1] S. Karpitschka, F. Liebig and H. Riegler, Marangoni Contraction of Evaporating Sessile Droplets of Binary Mixtures, *Langmuir* 33, 4682–4687 (2017).

[2] S. Eickelmann and H. Riegler, Rupture of ultrathin solution films on planar solid substrates induced by solute crystallization, *Journal of Colloid Interface Science*, submitted (2018).

[3] R. Köhler, P. Lazar and H. Riegler, Optical imaging of thin films with molecular depth resolution, *Applied Physics Letters* 89, 241906 (2006).

[4] S. Karpitschka, C. M. Weber and H. Riegler, Spin casting of dilute solutions: Vertical composition profile during hydrodynamic-evaporative film thinning, *Chemical Engineering Science* 129, 243–248 (2015).

[5] J. Danglad-Flores, S. Eickelmann and H. Riegler, Deposition of polymer films by spin casting: A quantitative analysis, *Chemical Engineering Science* 129, 243–248 (2015).

Effect of rotating magnetic field on the thermocapillary flow instability in a liquid bridge

Hao Liu¹, Zhong Zeng^{1,*}, Long Qiao¹

¹Chongqing University, College of Aerospace Engineering, Department of Engineering Mechanics,
 Chongqing, 400044, China
zzeng@cqu.edu.cn

Thermocapillary flow plays an important role in heat and mass transfer during floating zone crystal growth, and the instability of thermocapillary flow affect seriously the crystal quality. Due to the good electrical conductivity of semiconductor melt, the external rotating magnetic field is taken as an effective way to control the thermocapillary flow and thus improve crystal quality (Dold and Benz 1999).

To understand the effect of rotating magnetic field on thermocapillary flow instability of silicon melt (Prandtl number $Pr=0.01$), the linear stability analysis was performed by using Legendre spectral element method, a high precision numerical method. The effects from the one-pole-pair and two-pole-pair rotating magnetic field Φ_1 - Φ_2 model are compared. The results indicate that the rotating magnetic field suppresses the radial and axial flow driven by the thermocapillary force. In the absence of rotating magnetic field, the bifurcation of thermocapillary flow is stationary, but convection loses stability to become oscillating flow when a rotating magnetic field is applied. The critical Marangoni numbers (Ma_c) depend on the applied rotating magnetic field (Fig. 1). The Ma_c increases firstly, then decreases steeply to a minimum and finally increases again when the rotating magnetic field becomes stronger. Two transitions between the wavenumber $k=1$ and $k=2$ mode are observed. Moreover, the results show that the two-pole-pair rotating magnetic field has a relatively weak influence compared with the one-pole-pair rotating magnetic field.

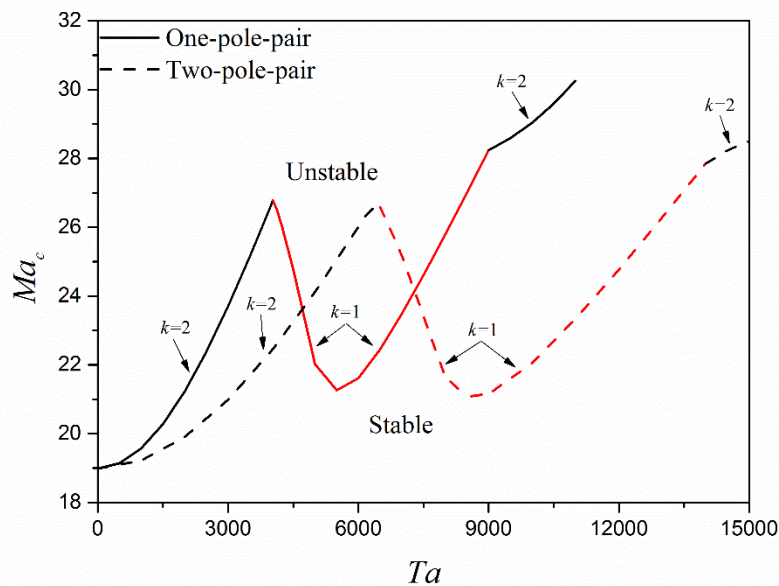


Figure 1: Dependence of the Ma_c on Ta .

References

Dold, P. and K. W. Benz (1999). "Rotating magnetic fields: Fluid flow and crystal growth applications." Progress in Crystal Growth and Characterization of Materials **38**(1): 39-58.

Surface waves in a circular channel: experiment and simulation

Ion Dan Borgia,¹ Rodica Borgia,² Michael Bestehorn,² Wenchao Xu,³ and Uwe Harlander³

1. Department of Computational Physics, Brandenburg University of Technology (BTU) Cottbus-Senftenberg,
Erich-Weinert-Straße 1 03046 Cottbus, Germany borciai@b-tu.de

2. Department of Statistical Physics and Nonlinear Dynamics, Brandenburg University of Technology (BTU) Cottbus-Senftenberg,
Erich-Weinert-Straße 1 03046 Cottbus, Germany

3. Department of Aerodynamics and Fluid Mechanics, Brandenburg University of Technology (BTU) Cottbus-Senftenberg,
Siemens-Halske-Ring 14, Cottbus, Germany

Two excitation phenomena related to different surface wave types occurring in a circular channel placed on a rotating table are studied experimentally: tidal bore generation (see Fig. 1) and horizontally excited Faraday waves. We use an experimental device that has been developed for studying rotating baroclinic or barostrat [1] flows. For the original experiment a constant rotation ratio of the tank was imposed. In the actual setup, libration of the rotation table with different frequencies and amplitudes is required. The experiment works in two parameter regimes: high libration amplitudes and small frequencies are used for the generation of traveling surface waves [2] while small amplitudes and high frequencies are necessary for studying the patterns generated by horizontally excited Faraday waves [3].

The results of the experiment are compared with simulation results [3, 4].

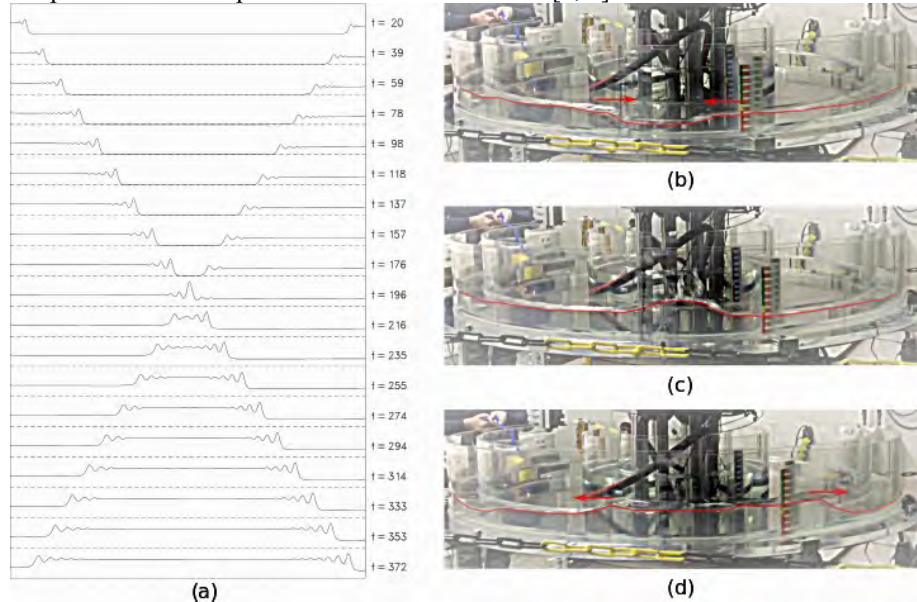


FIG. 1: Numerical simulation of the collision of two positive bores with different Froude numbers $F=0.2$ (left) and $F=0.133$ (right) from [4] (a). Bore collision from the experiment: before impact (b), during the impact (c) and after the impact (d).

[1] M. Vincze, I. Borgia, U. Harlander, and P. Le Gal, "Double-diffusive convection and baroclinic instability in a differentially heated and initially stratified rotating system: the barostrat instability," *Fluid Dynamics Research* 48, 061414 (2016).

[2] H. Chanson, "Tidal Bores, Aegir, Eagre, Mascaret, Pororoca: Theory and Observations." World Scientific (2012).

[3] M. Bestehorn, "Laterally extended thin liquid films with inertia under external vibrations", *Physics of Fluids* 25, 114106 (2013).

[4] M. Bestehorn and P. A. Tyvand, "Merging and colliding bores.", *Physics of Fluids* 21, 042107 (2009).

Bénard-Marangoni Instability Patterns in Evaporating Sessile Droplet at Constant Contact Angle Mode on a Heated Substrate

Ji-Long Zhu^a, Wan-Yuan Shi^{a, b}

^a College of Power Engineering, Chongqing University, Chongqing 400044, China

^b Key Laboratory of Low-grade Energy Utilization Technologies and Systems, Ministry of Education, Chongqing 400044, China

E-mail: shiwuy@cqu.edu.cn

In previous works (Sefiane et al 2008), the hydrothermal wave was observed in an evaporating sessile droplet of methanol at constant contact line (CCL) mode. However, there is yet lack of report on Marangoni instability patterns at another kind of evaporation mode named the constant contact angle (CCA) mode up to now. In this work, a series of experiments are thus conducted to observe the Marangoni instability of a sessile droplet of 1 cSt silicone oil evaporating at CCA mode in a wide ranges of the substrate temperatures (T_w) and the contact angles (θ). We found that when the Marangoni number ($Ma = |\gamma_T| \Delta T d_0 / \mu a$, where $\Delta T = T_w - T_s$, the substrate temperature T_w , the temperature of droplet apex T_s , the surface tension temperature coefficient γ_T , dynamic viscosity μ , thermal diffusivity a , initial droplet thickness d_0) exceeds a threshold value at a certain contact angle of droplet, a flower-like Bénard-Marangoni instability pattern occurs with uniformly distributed cells along azimuthal direction. In contrast to the classical polygonal Bénard-Marangoni cell in bottom heated flat liquid layer, the cell in droplet is intrinsically circular except for the linked boundary straight line between the cells. With the receding of the triple line, the cell decreases one by one but the flower-like pattern remains until only one cell in the droplet. When only one cell remains in the droplet, it is perfect circular. The ratio of the cell diameter to its averaged thickness when only one cell remaining in droplet has no significant discrepancy with the contact angle ranging from $\theta = 16.28^\circ$ to 24.32° . And the averaged ratio is 2.96 ± 0.56 , which is very close to the ratio of 3.0 for the classical BM hexagonal cell in flat liquid layer (Mizev et al. 2009). We thus confirm the cell patterns in the sessile droplet at CCA mode are BM cells. Moreover, the higher the substrate temperature is, the faster the growth of BM cells is and the pattern seems more irregular. Fig.1 shows the critical Marangoni number for incipience of BM cell patterns at the different contact angle of droplet. The critical Marangoni number for the incipience of the BM convection increases linearly with increasing contact angles, which means that the BM convection becomes more stable with increase of the contact angle.

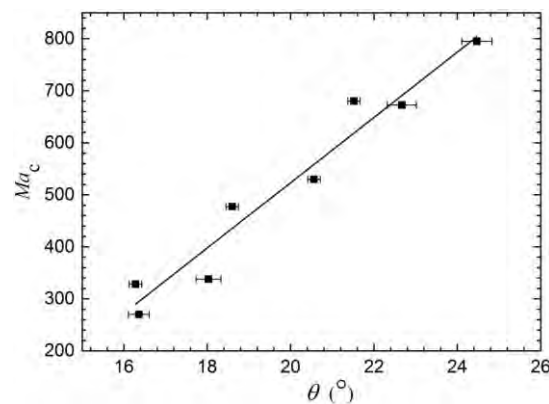


Figure 1: The critical Marangoni number for incipience of BM cell patterns at the different contact angle of droplet.

References

- [1] K. Sefiane, J. R. Moffat, O. K. Matar, R. V. Craster. Self-excited hydrothermal waves in evaporating sessile drops. *Appl. Phys. Lett.*, 2008, 93: 074103.
- [2] Mizev A I, Schwabe D. Convective instabilities in liquid layers with free upper surface under the action of an inclined temperature gradient. *Phys. Fluids*, 2009, 21(11): 112102.

Acknowledgement: This work was funded by the National Nature Science Foundation of China (No. 51676018).

Mass transfer and fluid dynamics in disperse multiphase systems: Interfacial phenomena in the presence of surfactants

Joschka M. Schulz, Lutz Böhm and Matthias Kraume

Technische Universität Berlin, Chair of Chemical and Process Engineering
Ackerstraße 76, 13355 Berlin, Germany
j.schulz@tu-berlin.de

The transport processes in multiphase systems strongly depend on the characteristics of the interface and the occurring transport phenomena. In industrial processes surfactants occur intentionally or as an impurity and change the interfacial behavior. The induced interfacial phenomena such as Marangoni convection or adsorption may lead to a change of important process parameters. Since the aforementioned transport phenomena have contrary effects on the mass transfer in multiphase systems, the prediction of their occurrence and the resulting mass transfer rates is a challenging task.

The present work focuses on the interaction between mass transfer and fluid dynamics in disperse liquid/liquid systems in the presence of surfactants. Due to the interaction between the transport processes, fluid dynamic measurements of single droplets can act as an indicator for the prediction of interfacial phenomena and mass transfer rates. For experimental purposes a single drop rising test cell as well as the experimental setup shown in Merker et al. (2017) is used, which extends the concept of the rising test cell by adding a vertical traverse system with real-time control, thus enabling the three-dimensional measurement of shape, velocity and trajectory of the particle during the ascent with high temporal and spatial resolution.

Fig. 1 (left) shows the transient drop rise velocity of single 1-octanol droplets in water for varying surfactant concentrations. Butyldiglycol is chosen as a model surfactant. With increasing surfactant concentration the terminal drop rise velocity decreases from the calculated velocity for a movable interface (Feng and Michaelides 2001) to the value for rigid spheres (Martin 1980). In case of deformation, the measured velocities can decline even further. Although the observed effect is in good agreement with the literature, the mass transfer rates show contrary behavior due to the occurrence of Marangoni convection, which can be identified by detailed consideration of the drop movement.

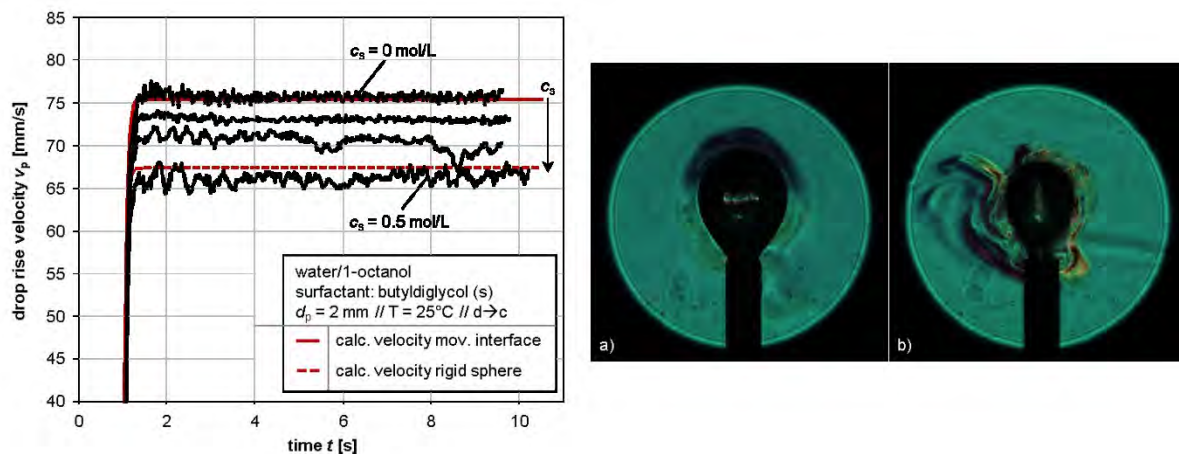


Figure 1: Left: Experimental transient drop rise velocity of 2 mm 1-octanol droplets in water for different surfactant concentrations. Right: Concentration gradient field of a surfactant around a droplet during droplet formation at a capillary visualized by CCS, a) without interfacial instabilities, b) with interfacial instabilities due to Marangoni convection.

To get a deeper insight into the mass transfer in liquid/liquid systems, an experimental setup applying the calibrated color schlieren technique (CCS) is developed in order to visualize and quantify local concentrations in multiphase-systems in situ and in real-time. The CCS method is capable of measuring the projected density gradient field directly by means of measuring the light deflection angle due to inhomogeneities from, e.g., concentration or temperature differences. Fig. 2 shows the concentration gradient field of the surfactant butyldiglycol around a stagnant 1-octanol droplet in water.

References

- D. Merker, L. Böhm, M. Oßberger, P. Klüfers, M. Kraume, Chem. Eng. Technol., 2017, 40, 1391-1399.
- H. Martin, Chem. Ing. Techn., 1980, 52, 199-200.
- Z.-G. Feng, E. E. Michaelides, J. Fluids. Eng., 2001, 123, 841-849.

Linear stability of thermocapillary liquid layers of non-Newtonian fluids

Kai-Xin Hu, Chen-Yi Yan

Ningbo University, School of Mechanical Engineering and Mechanics
Ningbo, Zhejiang, 315211, China
E-mail: hukaixin@nbu.edu.cn

The thermocapillary flows of polymer liquids appear in many practical applications, such as film coating, inkjet printing and polymer processing in microgravity. We study the linear stability of thermocapillary liquid layers for polymer liquids. There are three kinds of instabilities, which includes oblique wave, streamwise wave and spanwise stationary mode. In viscoelastic fluids, the flow is stabilized by the elasticity for the first mode; the second has several fluctuations in vertical direction; the last becomes the preferred mode when the elasticity is high enough. In shear-thinning fluids, the shear-thinning effect is destabilizing for small and moderate Prandtl numbers (Pr) but increases the stability slightly for large Pr for linear flow. For return flow, the perturbation kinetic energy concentrates near the surface. In viscoplastic fluids, there is a plug region in the flow, which divides the yielded flow into two regions. When the flow is subjected to a small perturbation, the velocity perturbation below the upper surface of plug region is negligible. These results are valuable for the flow control of polymer fluid layer in microgravity conditions.

Electrohydrodynamic Instabilities in Microchannels for non-Newtonian Liquids

Seymen İlke Kaykanat, Berkay Keklik and Kerem Uguz

Bogazici University, Department of Chemical Engineering
Bebek, Istanbul, 34342, Turkey
Kerem.uguz@boun.edu.tr

The interface between two immiscible liquids that flow in a microchannel is flat due to small Reynolds number. This interface may become unstable, i.e. lose its flatness in the presence of an electric field. The discontinuities in the electrical properties of the liquids cause this instability, known as electrohydrodynamic (EHD) instability (Thaokar and Kumaran, 2005). The electric field may be applied either parallel or normal to this flat interface. In this work, we present both experimental and numerical results when two immiscible non-Newtonian liquids flow in a microchannel and compare them with the Newtonian case (Eribol and Uguz, 2015; Ozan and Uguz, 2017). The electric field may destabilize the interface depending on the electrical properties of the liquids (Uguz et al., 2008). If the field has a destabilizing effect, then, at some critical voltage the interface starts deflecting and may reach one of the walls of the channel, leading to its rupture. Between the two hits of the interface, some volume of one liquid is encapsulated by the other one, which transforms into a slug or a droplet. Various parameters, including the concentration of the solute will be investigated. In the numerical part, the liquids will be considered as leaky dielectric and the linear stability analysis results will be presented.

References

- Eribol, P. and Uguz, A.K 2015 Experimental investigation of electrohydrodynamic instabilities in micro channels European Physical Journal - Special Topics 224, 423-432
- Ozan, S. C. and Uguz, A.K 2017 Nonlinear evolution of the interface between immiscible fluids in a micro channel subjected to an electric field European Physical Journal - Special Topics 226, 1207-1218
- Thaokar, R.M. and Kumaran, V. 2005 Electrohydrodynamic instability of the interface between two fluids confined in a channel Physics of Fluids 17, 084104
- Uguz, A.K., Ozen, O., and Aubry, N. 2008 Electric field effect on a two-fluid interface instability in channel flow for fast electric times Physics of Fluids 20, 031702

Surface Heat Dissipation Dependence of Thermocapillary Convection in Shallow Annular Pool

Li Zhang, You-Rong Li and Chun-Mei Wu

Key Laboratory of Low-grade Energy Utilization Technologies and Systems of Ministry of Education,
 College of Power Engineering, Chongqing University
 No.174 Shazhengjie, Shapingba, Chongqing, 400044, China
 E-mail: liyourn@cqu.edu.cn

In the past few decades, thermocapillary convection has received much attention from both fundamental and industrial aspects. Many scholars have been focused on thermocapillary convection in the liquid pool with an adiabatic free surface. However, due to the non-equilibrium effect on the free surface, surface heat dissipation is inevitable and is also a common thermal process in engineering fields, which has significantly influenced on thermocapillary convection in the liquid layer. Surface heat dissipation is bound to change the temperature distribution along the free surface and impacts on the flow patterns and the critical condition of the flow bifurcation. There are many kinds of surface heat dissipation, such as convective and radiative heat transfer, and the evaporative cooling etc. In order to understand the effect of surface heat dissipation on thermocapillary convection in a shallow annular pool, a series of three-dimensional numerical simulations were carried out by using the finite volume method. The radius ratio of the annular pool is fixed at $R=0.5$ and the aspect ratio is $H=0.1$. Biot (Bi) numbers are limited in $0 \leq Bi \leq 3$ and $0 \leq Bi \leq 50$ for the working fluids with Prandtl (Pr) number of 0.011 and 6.7, respectively. Results indicate that with the increase of surface heat dissipation, the thermocapillary convection intensity increases at first, and then decreases slightly; furthermore, the center of the thermocapillary convective cell in the meridian plane gradually moves to the hot outer wall. With the increase of Marangoni (Ma) number, the stable axisymmetric flow bifurcates to the three-dimensional steady or oscillatory flow, depending on surface heat dissipation rate and Prandtl number of the working fluids. After thermocapillary convection destabilizes, the hydrothermal waves and the longitudinal rolls appear at different surface heat dissipation rate, as shown in Figure 1. The flow pattern transition is always accompanied by the variations of the temperature fluctuation amplitude, the oscillatory frequency and the wave number.

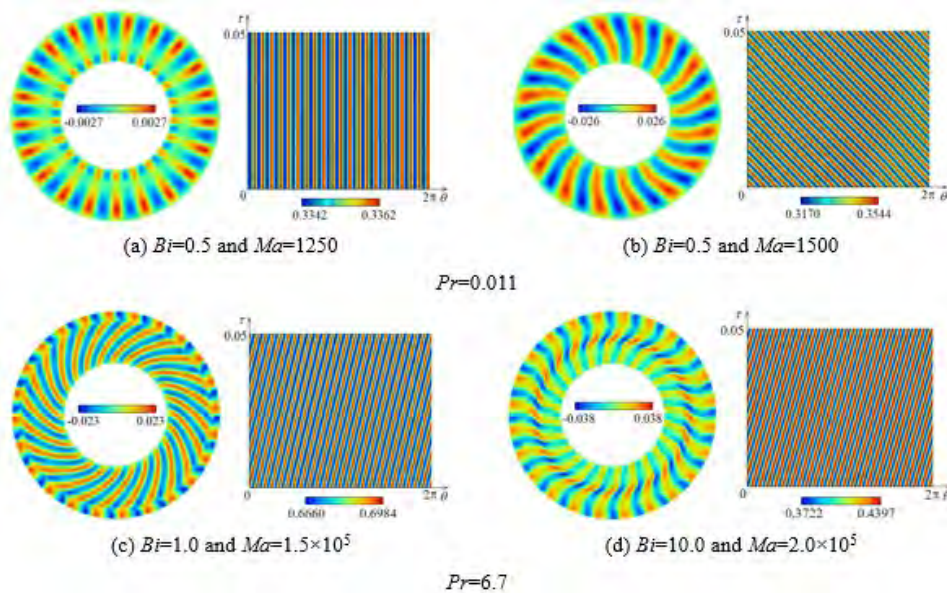


Figure1: Temperature fluctuation (left) and space-time diagram (right) at $R=1.5$ on the free surface at different Marangoni number, Biot number and Prandtl number.

Experimental Study of Thermocapillary Convection of Liquid Layer with an Evaporating Interface

Li-Li Qiao^{1,2}, Qiu-Sheng Liu^{1,2*} and Zhi-Qiang Zhu¹

¹ Institute of Mechanics, Chinese Academy of Sciences, Beijing 100190, China

² University of Chinese Academy of Sciences, Beijing 100049, China

*liu@imech.ac.cn

As a basic problem of evaporative cooling, thermocapillary convection of a volatile liquid subjected to a horizontal temperature gradient has become an important direction in cooling technology. Many experimental and theoretical works have been performed to study the coupling mechanism of evaporation and thermocapillary convection. Yaofa Li(2016) studied experimentally the Buoyancy-Marangoni convection of a volatile binary fluids. Phase change plays an important role in thermal instabilities of the liquid layer (Pedro J. S'aeza 2015). WanYuan Shi(2017) studied the marangoni convection induced by evaporation.

This work details an experimental study of thermocapillary convection of a ~2mm deep layer of 0.65cSt silicon oil confined in an open rectangular pool. And the evaporation rate and the thermal field of interface were examined by the laser co-focal displacement meter and the infrared thermography.

According to its instability to hydrothermal waves and a steady multicellular, the evaporation processes are divided into three stages. Thermal instabilities at the evaporation interface are shown in Figure 1 for three different stages. Evaporation process of liquid layers is shown in Figure 2. Compared with Figure 1, the thermal instability has little effect on evaporation rate.

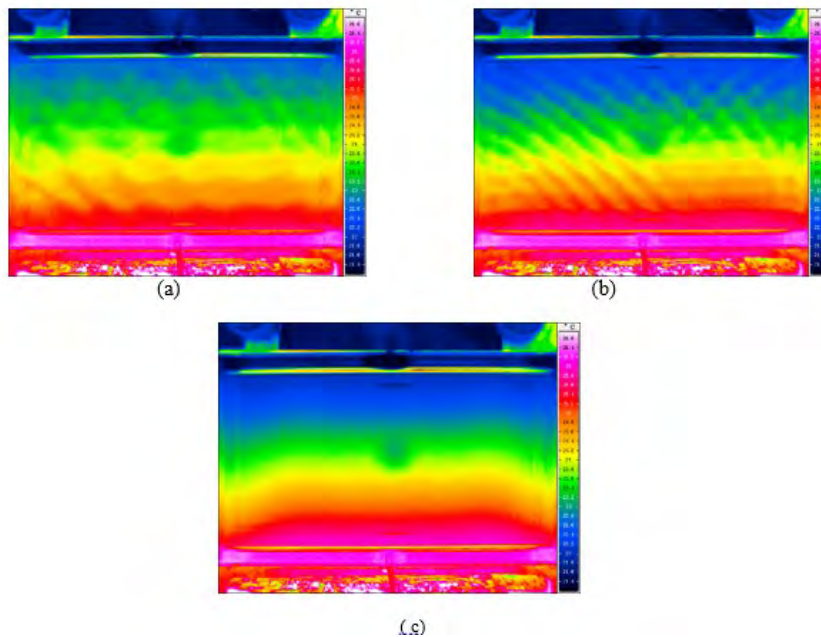


Figure 1: Thermal field of three different stages: (a) oscillatory multicellular; (b) hydrothermal waves; (c) static thermal convection

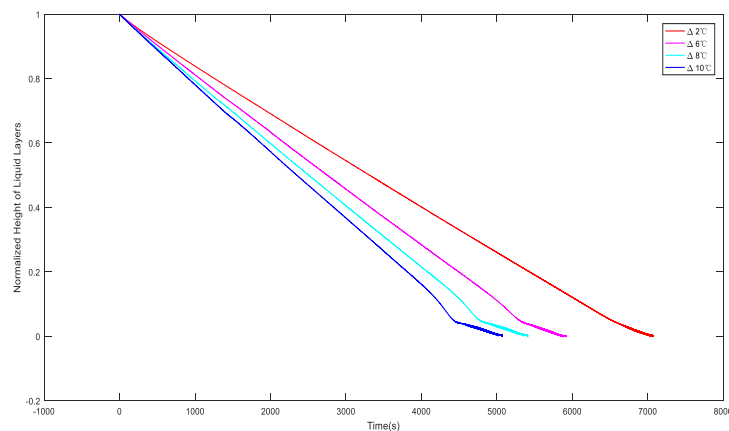


Figure 2: Evaporation process of the liquid layers under different temperature difference

Acknowledgements

This research was financially supported by the National Natural Science Foundation of China (Grants Nos. 11532015, U1738119), and the China's Manned Space Program (TZ-1).

Reference

- [1] Yaofa Li, Minami Yoda, International Journal of Heat and Mass Transfer 102 (2016) 369–380
- [2] Pedro J. S'aeenza, Prashant Valluria, Khellil Sefiane, Omar K. Matarb, Procedia IUTAM 15 (2015) 116 – 123
- [3] Wan-Yuan Shi, Shang-Ming Rong, Lin Feng, Microgravity Sci. Technol. (2017) 29:91–96

Thermocapillary Flow at the Evaporating Interface of a Liquid Pool Powered by an Interfacial Line Heater

Lu Qiu¹, Fei Duan^{2*}

¹ School of Energy and Power Engineering, Beihang University, Beijing, 100191, P. R. China.

E-mail: luqiu@buaa.edu.cn

² School of Mechanical and Aerospace Engineering, Nanyang Technological University, 50 Nanyang Avenue, 639798, Singapore.

E-mail: feiduan@ntu.edu.sg (* Corresponding author)

The temperature gradient at the interface of a liquid pool could generate a thermocapillary flow along the interface due to the temperature dependent liquid surface tension. Once the evaporation at the interface is significant, the evaporation required energy must be supplied either from the direction perpendicular to the interface, or from the direction parallel to the interface. The latter one is normally accompanied with a marangoni flow. In the current work, we investigated the evaporation induced marangoni flow at the interface of an ethanol liquid pool and the associated wavy temperature patterns with a high-resolution infrared camera. In order to eliminate the aforementioned perpendicular component, a line heater (thin heating wire) was placed exactly at the interface in order to supply the evaporation required energy, as shown in Figure 1(a, b). The evaporated ethanol was compensated by the liquid supply at the bottom of the liquid tank. The flow rate of the liquid supply was carefully controlled with a syringe pump in order to maintain a stable liquid level in the tank. The evaporating ethanol pool was encapsulated in a chamber in order to control the system pressure at 800 ± 5 mbar with a vacuum pump. An equilibrium state was reached while the liquid supply rate equaled to the evaporation rate, and the heating power of the line heater was balanced by the evaporation latent heat. It was observed that increasing the heating power of the line heater generated a stronger marangoni flow and required a higher liquid compensation rate. Moreover, the temperature pattern was dependent on the strength of marangoni flow, which was also proportional to the evaporation rate. A series of two-dimensional temperature oscillation pattern could be identified at different levels of marangoni flow.

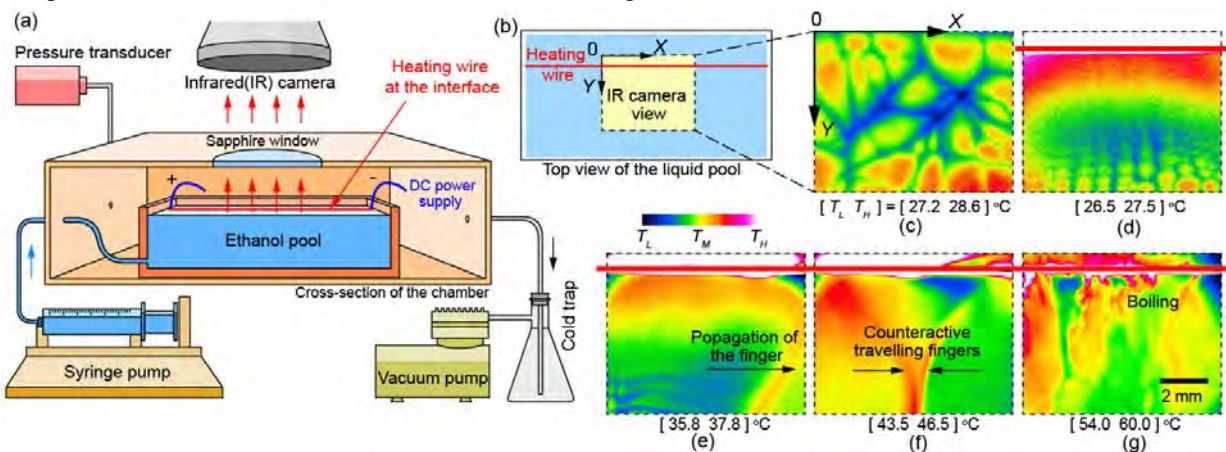


Figure 1: (a) The configuration of the test section. (b) The top view of the evaporating interface of the ethanol pool. (c-g) The infrared camera captured temperature profiles at different levels of heating power: (c) non-heating power, random cells are observed, (d) low heating power, structure micro-cells are transporting away from the heater, (e) medium heating power, uni-directional travelling wave was generated, (f) high heating power, counteractive travelling waves were captured, (g) ultra-high heating power, boiling occurred.

As shown in Figure 1 (c-g), five different interfacial temperature patterns could be observed. Without the heating power of the line heater, the equilibrium state could not be reached due to the cooling effects of the evaporation, therefore, a vertical temperature gradient was anticipated. Once a temperature gradient was generated in the direction perpendicular to the interface, the Bernard cells were observed in Figure 1(c). At a low heating power, the structured micro-cell lattice was observed, which were travelling away from the heater (see Figure 1(d)). Increasing the heating power resulted in a uni-directional travelling fingering wave (see Figure 1(e)). The oscillation of the temperature was getting significant. At a higher heating power, as shown in Figure 1(f), the counteractive travelling waves could be observed. Finally, the boiling of the ethanol was initiated on the heater and the chaotic temperature pattern was captured in Figure 1(g).

Effect of using mixed working fluid on the performance of open pulsating heat pipe (OLPHP)

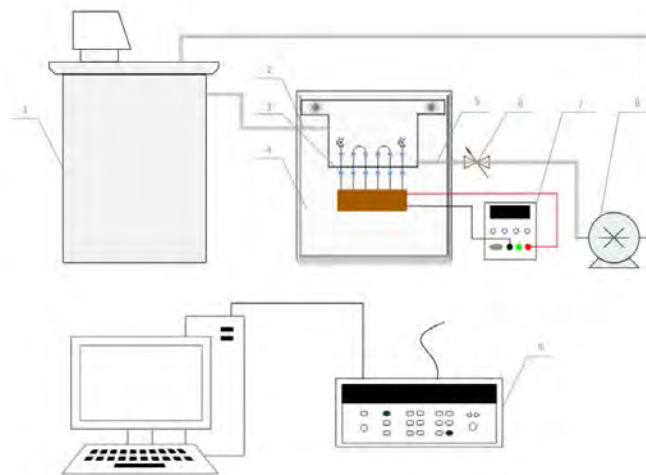
Meilan Zhou, Caihang Liang*

Guilin University of Electronic Technology, School of Mechanical and Electrical Engineering, Mechanical Engineering, Jinji road, Guilin, 541004, China

E-mail: lianghang@guet.edu.cn

Pulsating heat pipe (PHP) has great application prospects in the cooling of electronic components due to its excellent heat transfer characteristics. The objective of this experiment is to observe the performance OLPHP using two fluids mixed together at different working power, inclination angle and loops number. The PHP is a copper capillary tube of 2mm inner and 4mm outer diameter. The open loop pulsating heat pipe (OLPHP) has a total length of 150mm, in which the evaporation section and condensation section of pulsating heat pipe are 50mm. The evaporation section is heated by electric heating band and the condensation section is cooled by water. The results show that the greater the input power, the smaller thermal resistance. When the filling rate is 50%, the heating power is 100W, the angle is 90 degrees, the performance of the OLPHP is best. In a certain range, the more loops the worse the performance of OLPHP.

The pulsating heat pipe has been considered as one of the most effective methods to meet the challenges of higher heat fluxes. The concept of heat pipes is proposed by Gaugler[1]. However, its processing technology is tedious and has not been well applied. Then, Akachi[2] proposed and patented the pulsating heat pipe. Md. Lutfor Rahman[3-6] et al focused on the potential of OLPHP with acetone and water at different filling ratios. It can be summarized that at 70% and 50% filling ratio acetone and water performs best respectively. And they investigated on heat transfer characteristics of an open loop pulsating heat pipe with fin. In the experiment, the finned structure shows best performance at 45° inclined position whereas at 30° inclined position shows worst. At the same time, they compared the performance of the open loop and closed loop heat pipes, in the experiment for both close and open loop but from them close loop exhibits better heat transfer characteristics than open loop. RR Riehl[7] presented a preliminary investigation on the potential of using nanofluid in an OLPHP for passive thermal control. Experiment indicated that, the film evaporation effect is more predominant than nucleate boiling at low heat loads, which becomes more evident at higher heat loads. RR Riehl[8] also tested the OLPHP characteristics with different working fluids which are water, methanol, acetone, isopropyl alcohol and ethanol in vertical and horizontal directions. M Saha[9] et al studied the OLPHP of 0.9mm inner diameter. Water, methanol, 2-propanol and acetone has been studied as working fluids with 50% filling ratio. ML rahman [10] researched the effect of using acetone and distilled water on the performance of OLPHP with different filling ratios. Researchers have conducted a lot of researches on the pulsating heat pipes with single working fluid such as ethanol, acetone, and distilled water. However, there are few studies on pulsating heat pipes with mixed working fluids. Therefore, it is of great significance to study on them. The working fluid used in this experiment was a mixture of anhydrous ethanol and acetone, and the mixing ratio was 1:1.



1.Constant temperature water tank 2.Inlet 3.Temperature measuring points 4. Support structure
 5.Outlet 6. Water regulating valve cover 7. DC power supply 8. Circulating pump 9. Data acquisition system
 Fig.1 Schematic diagram of experimental setup

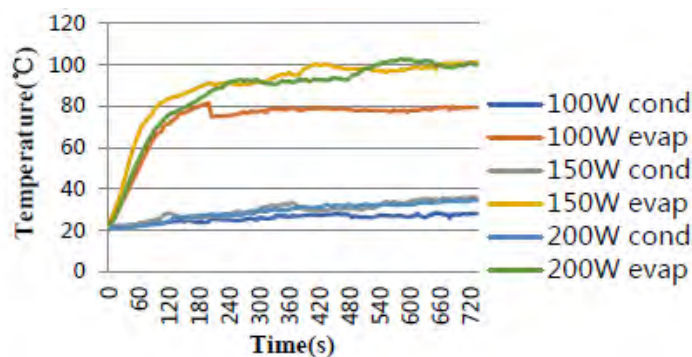


Fig.2 Variation of temperature with time for OLPHP at 90 degrees inclination & different input

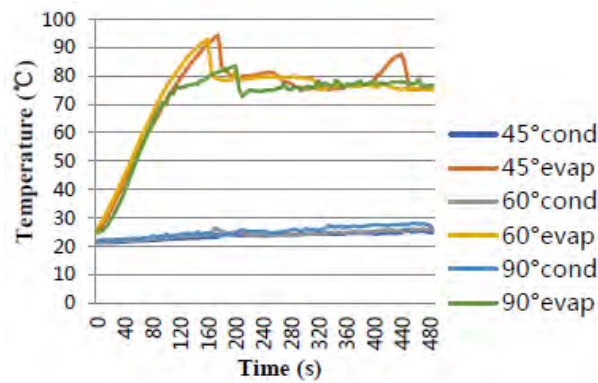


Fig.3 Variation of temperature with time for OLPHP at 100W input & different degree inclination

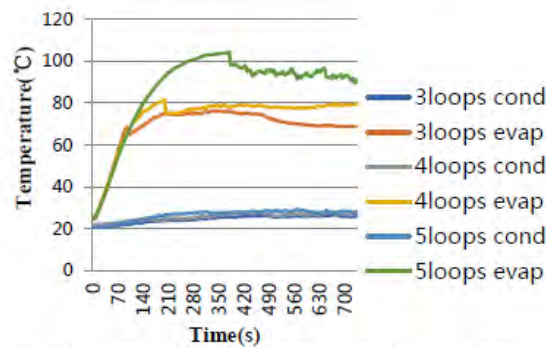


Fig.4 Variation of temperature with time for OLPHP at 90 degrees inclination ,100W input & different OLPHP

Fig.4 Variation of temperature with time for OLPHP at 90 degrees inclination ,100W input & different OLPHP

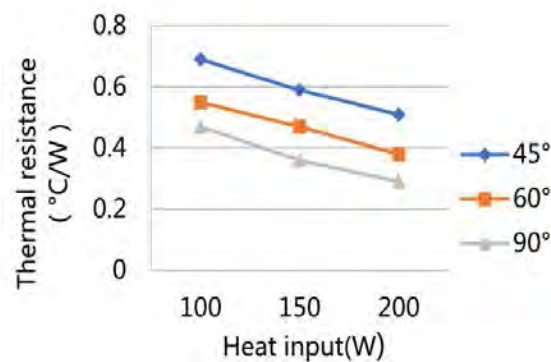


Fig.5 Effect of heat input and tilt angle on thermal resistance of 4 loops PHP

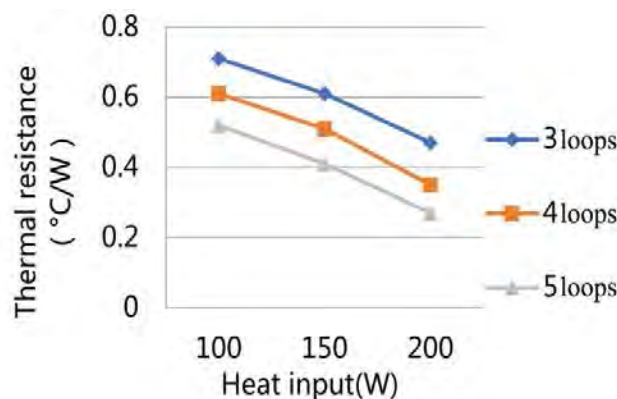


Fig.6 Effect of loops number on thermal resistance of PHP

The experimental setup is shown in Fig.1, the setup contains heating system, cooling system, OLPHP and data collection system. The heating system is mainly composed of electric heating film (The film made of silicone rubber, 1.8mm thickness, and its operating temperature range is 10 ~ 150°C) and power supply (Switch type DC regulator with input voltage 220V and output power 150W). Electrical heating film is wrapped around a layer of insulation material to reduce heat loss in the evaporation

section. At the same time, the adiabatic section is also insulated by polyurethane foam material. For cooling system, forced convection is used by cold water. The inlet of the cooling water tank is connected to the outlet of the constant temperature water tank. The water in the cooling tank flows out of the outlet passes through the circulating water pump and flows back into the constant temperature water tank. Thus, a complete water cooling system was formed. This cycle allows the thermostatic water tank to reduce the water temperature to the set temperature in a short time to ensure the water with a constant temperature in the cooling water tank. The pulsating heat pipe is connected to the power supply, thermocouples and other components.

In order to improve the accuracy of the experiment data, these measurement devices (Electronic balance, thermocouple etc) were strictly calibrated before the experiment. Install all the devices and adjust the temperature of the constant temperature water tank to 20 degrees centigrade. All experimental tests are performed on a 50% filling ratio basis. In the first set of experiments, tested the heat pipe with 4 loops under different power. In order to observe the influence of different angles on the heat pipe more clearly, chose the high power (100w,150w,200w) to provide heat in the evaporation section In the second groups of experiments. The aim of the last set of experimental tests is to evaluate the behavior of heat pipe related to the number of loops. These heat pipes are all under the thermal load of 100W and in the vertical direction The temperature vs. time curves shows a similar pattern for all the experimental conditions. So a typical curve is shown in Fig.2, 3and 4. The thermal resistance along the different number loops of OLPHP at different heat powers and in different degrees have been exhibited from Figs. 5and 6.

The conclusions that could be taken from this investigation are as follows:

It could be verified that, for tests at 100W input, the OLPHP presented higher values when compared with other heat loads. Although it takes a little longer to start it has the lowest temperature when the heat pipe is stable.

It could be observed that 90 degrees presented the best performance, it starts fastest and runs stable after startup.

At vertical orientation tests, the 5 loops OLPHP need more time to start-up and its temperature is the highest.

45 degrees inclination shows highest thermal resistance at all heat loads and lowest at 90 degrees inclination.

It is found from the experiment that when the heat load is same, thermal resistance decreases with increasing loops amount of pipe.

Acknowledgments: This project was jointly supported by The National Natural Science Foundation of China, No. 51566002.

References

- [1] Gaugler, R. S US patent 2350348. Appl. 21 Dec, 1972. Published 6 June 1944.
- [2] H. Akachi, "Structure of a Heat Pipe," US Patent 4921041, 1990.
- [3] Zhang Y, Faghri A. Heat transfer in a pulsating heat pipe with open end[J]. International Journal of Heat & Mass Transfer, 2002, 45(4):755-764.
- [4] Rahman M L, Afrose T, Tahmina H K, et al. Effect of using acetone and distilled water on the performance of open loop pulsating heat pipe (OLPHP) with different filling ratios[C]// International Conference on Mechanical Engineering: International Conference on Mechanical Engineering. AIP Publishing LLC, 2016:755-764.
- [5] Rahman M L, Saha P K, Mir F, et al. Experimental Investigation on Heat Transfer Characteristics of an Open Loop Pulsating Heat Pipe(OLPHP) with Fin ☆[J]. Procedia Engineering, 2015, 105:113-120.
- [6] Rahman M L, Nawrin S, Sultan R A, et al. Effect of Fin and Insert on the Performance Characteristics of Close Loop Pulsating Heat Pipe (CLPHP) ☆[J]. Procedia Engineering, 2015, 105(2015):129-136.
- [7] Riehl R R, Santos N D. Water-copper nanofluid application in an open loop pulsating heat pipe[J]. Applied Thermal Engineering, 2012, 42(3):6-10.
- [8] Riehl R R. Characteristics of an Open Loop Pulsating Heat Pipe[J]. Environment, 2004.
- [9] Saha M, Feroz C M, Ahmed F, et al. Thermal performance of an open loop closed end pulsating heat pipe[J]. Heat & Mass Transfer, 2012, 48(2):259-265.
- [10] Rahman M L, Afrose T, Tahmina H K, et al. Effect of using acetone and distilled water on the performance of open loop pulsating heat pipe (OLPHP) with different filling ratios[C]// International Conference on Mechanical Engineering: International Conference on Mechanical Engineering. AIP Publishing LLC, 2016:755-764.

Dimension-Reduced Model for DeepWater Waves

Michael Bestehorn¹ and Peder A. Tyvand²

1. Brandenburg University of Technology, 03044 Cottbus, Germany, bestehorn@b-tu.de

2. Norwegian University of Life Sciences, 1432 As, Norway

Starting from the 2D Euler equations for an incompressible potential flow, a dimension-reduced model describing deep-water surface waves is derived [1]. Similar to the Shallow-Water case, the z-dependence of the fluid's velocity and surface elevation is found explicitly from the Laplace equation and a set of two one-dimensional nonlinear partial differential equations (PDE) for the dependent variables remains.

As applications of the model we present some numerical solutions for several initial conditions. The side-band instability of Stokes waves and stable envelope solitons known from the nonlinear Schrödinger equation are obtained in agreement with other work. The conservation of the total energy is checked.

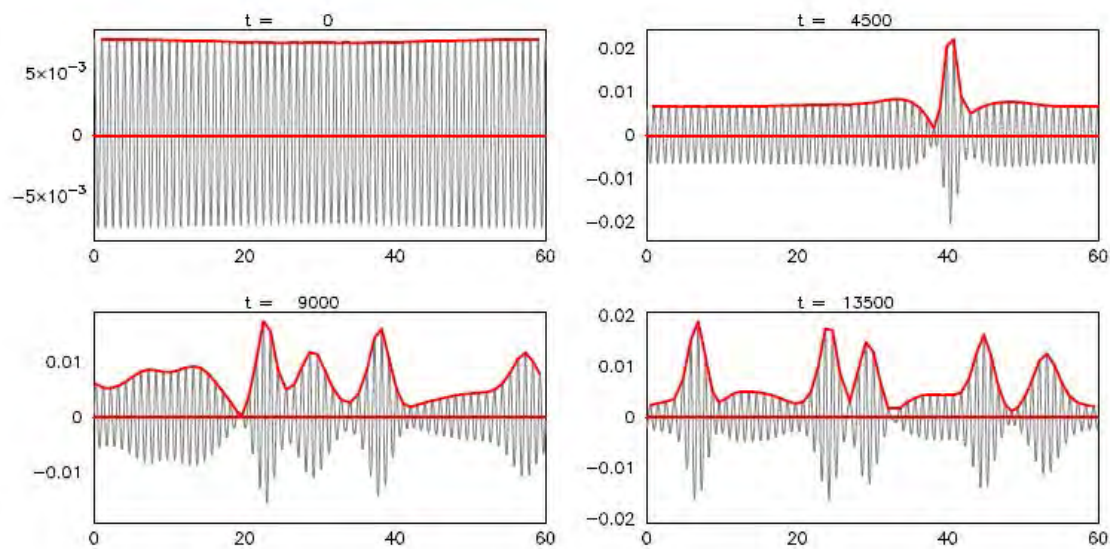


FIG. 1: Benjamin-Feir instability of a slightly disturbed monochromatic wave.

From the numerical side, the great advantage of the present model is its relatively straightforward and effective numerical realization. Due to the dimension reduction, CPU-times of the performed runs are in the range of hours on a standard PC or Laptop. Our system can be extended both to higher order nonlinearities as well as to three-dimensional potential flows, resulting in a reduced 2D PDE set. Thus, the numerical examination of ocean rogue waves [2] or of 3D envelope solitons should become feasible.

[1] M. Bestehorn, P. A. Tyvand, T. Michelitsch, *subm. to Physics of Fluids*, February 2018.

[2] C. Kharif, E. Pelinovsky, A. Slunyaev, *Rogue Waves in the Ocean*, Springer (2009).

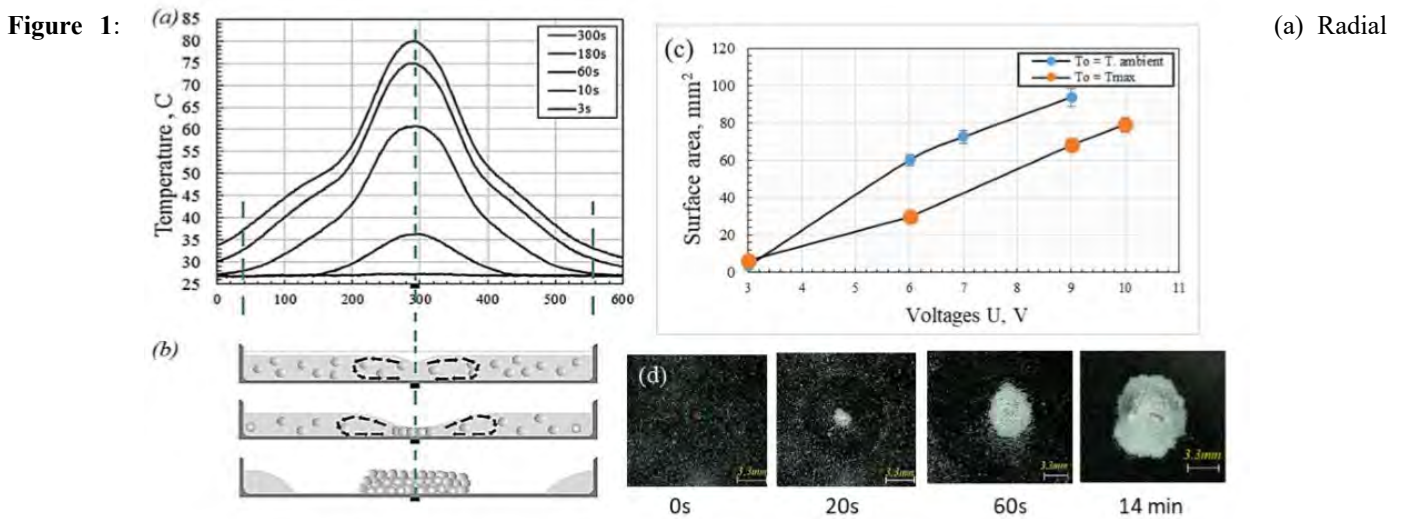
Thermal Marangoni convection for particle assembling in colloidal films

Mohammed Al-Muzaiqer, Victor Fliagin, Natalia Ivanova

Tyumen State University, Photonics and Microfluidics Laboratory 6 Volodarskogo st., Tyumen, 625003, Russia
n.ivanova@utmn.ru

Development of methods for controlling the particle assembling in colloidal films is a topical issue of modern fundamental theory and applied sciences (Harris and Lewis, 2008; Varanakkottu et al., 2016). The research of the different factors of self-assembly and construction of physical and computer models of processes allows us to work out the principles of development of new materials with the given properties, creation of photonic crystals and novel coatings, metalized ceramic layers.

In the present work, we report experimental results on the particles assembling in colloidal films using the thermally induced Marangoni convection. A thin layer of a suspension of polyethylene particles (average particle size is 150 μm) in n-butanol was locally heated with an electrical heater embedded in the bottom of a dish. Time evolution of the radial distribution of temperature in the suspension layer is shown in Fig. 1(a).



temperature distribution (applied voltage 9V); (b) schematic illustration of thermally induced Marangoni convection for the assembly of particles; (c) the surface area covered with assembled particles ($T_0 = 25$ and $T_0 = 80^\circ\text{C}$); (d) series of top-view images of the particle assembling process caused by thermal Marangoni flows.

At the beginning, particles move in a toroidal Marangoni vortex above the heating center, until the thickness of the suspension layer due to thermocapillary deformation becomes comparable to the size of particles, Fig. 1(b and d). Then the particles begin to attach to the substrate by capillary forces and serve as a trapping site for surrounding particles. Further heating results in an accumulation (assembling) of particles at the heating spot and increasing the area covered with particles, Fig 1(d). With increasing the heating temperature, the area of substrate covered with assembling particles increases resulting in segregation of all particles from the bearing liquid. The experiments were done in two different ways. In the first case, the suspension layer on the substrate was heated from T_0 to T_{max} . In the second case, the suspension was placed on the initially heated for up T_{max} substrate. As shown in Fig. 1(c), the surface area on which the particles assembled in the first case is larger than the one in the second case.

References

- D.J. Harris, J.A. Lewis, Marangoni Effects on Evaporative Lithographic Patterning of Colloidal Films. *Langmuir*, 24, 3681-3685 (2008).
- S.N. Varanakkottu, M. Anyfantakis, M. Morel, S. Rudiuk, D. Baigl. Light-Directed Particle Patterning by Evaporative Optical Marangoni Assembly. *Nano Lett.* 16, 644-650 (2016).

Thermocapillary deformation of a pinned sessile droplet caused by a laser beam

Sergey Semenov¹, Alexander Malyuk² and Natalia Ivanova²

¹Aix-Marseille University, IUSTI UMR 7343 CNRS, 13453 Marseille, France ²Tyumen State University, Photonics and Microfluidics Lab, Volodarskogo 6, Tyumen, 625003, Russia
n.ivanova@utmn.ru

Controlling the shape of a sessile liquid droplet on a solid surface is of great importance in digital microfluidics, lab-on-chips (Choi et. al., 2012), optofluidics (Krupenkin et. al., 2003; Shahini et. al., 2016). In present work, we study deformation of a sessile droplet caused by the laser-induced thermal Marangoni forces. Different shapes of the droplet, which may be obtained by changing the power of laser beam, are shown in Fig. 1(a). When the laser is turned-off, the droplet on the substrate has a hemispherical shape with the radius of curvature $R_0 > 0$. When the laser beam starts to heat the center of the droplet, then the radially outward thermal Marangoni flows transfer liquid from the hot area of the droplet to the area of a lower temperature resulting in an increase in the curvature radius $R > R_0$. At a certain power of the laser beam, the droplet surface takes a flat shape. Further power increase leads to the formation of a thermocapillary dimple in the central part of the droplet with $R < 0$. Fig. 1(b) shows the radius of curvature versus the power of laser beam for 0.3 and 0.6 μL droplets of Ethylene Glycol colored to absorb the laser beam.

The time-dependent problem of the laser-induced deformation of the sessile droplet-air interface has been approached numerically using COMSOL Multiphysics[®] software, which is based on the Finite Element Method. Second- and third-order shape functions has been used for the spatial discretization of the simulation domain. Generalized alpha method is used to integrate incompressible Navier-Stokes and heat transfer equations in time. Moving mesh with Arbitrary Lagrangian-Eulerian (ALE) formulation of equations is used to follow the deforming droplet geometry. The computer model includes laser beam absorption in the droplet; loss of the energy input due to direct reflection of the laser beam from interfaces; heat transfer in solids (conductive) and fluids (conductive and convective); simplified radiative heat exchange with the ambient environment; hydrodynamics of air below and above the substrate; thermocapillary convection in the droplet; free deformation of the droplet surface; droplet evaporation and corresponding heat consumption at the droplet-air interface; evaporation-induced Stefan flow in the air phase; buoyancy force in the air phase due to non-uniform temperature and composition. Viscosity, thermal conductivity and density of air are considered as functions of temperature. Liquid viscosity is considered to be strongly dependent on the local temperature. The assumptions of problem's axial symmetry and of pinned contact line are adopted for this computer simulation.

Preliminary numerical results, presented in Fig. 1(c) and (d), has been obtained for the Ethylene Glycol droplet ($V = 0.45 \mu\text{L}$, contact radius of 1.2 mm, the initial contact angle of 18.5°). The power of laser beam is 125 mW, with Gaussian energy distribution and diameter of 1.19 mm. Fig. 1(d) shows a reasonable agreement between experimental and numerical time evolutions of the droplet's apex temperature.

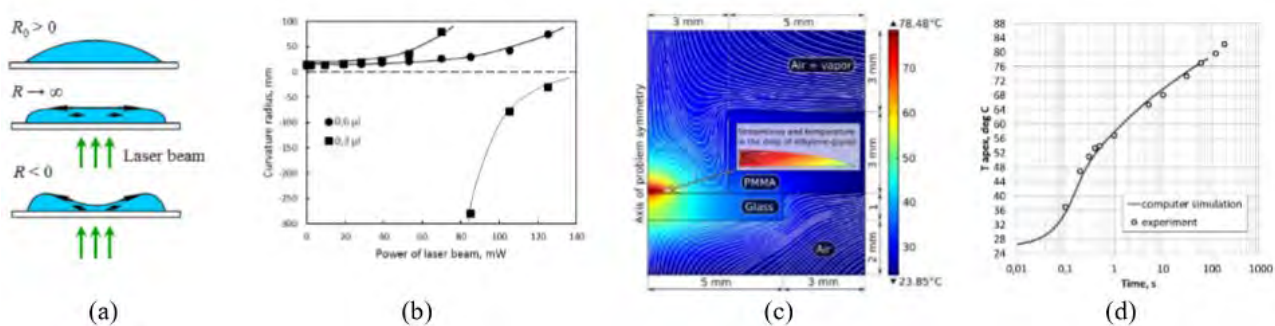


Figure 1: (a) Schematic illustration of the droplet deformation by thermal Marangoni forces. (b) The curvature radius variation in response to the power of laser beam for the droplets of Ethylene glycol (0.3 and 0.6 μL). (c) Geometry of the problem, streamline and temperature in the droplet of ethylene glycol. (d) Evolution of temperature of the droplet apex (solid line - numerical simulation, symbols – experimental data).

References

- Choi K., Ng A.N.C., Fobel R., Wheeler A.R. Digital microfluidics. *Annu. Rev. Anal. Chem.*, 5, 413-440 (2012). Krupenkin T., Yang S., Mach P. Tunable liquid microlens. *Appl. Phys. Lett.*, 82, 316 (2003). Shahini A., Xia J., Zhou Z., Zhao Y., Cheng M.M-Ch. Versatile miniature tunable liquid lenses using transparent graphene electrodes. *Langmuir*, 32, 1658-1665 (2016).

Laser-induced thermocapillary rupture of a thin liquid layer laying on a liquid substrate

Natalia Ivanova, Denis Klyuev, Victor Fliagin

Tyumen State University, Photonics and Microfluidics Lab
 Volodarskogo 6, Tyumen, 625003, Russia
 n.ivanova@utmn.ru

The study of the mechanism of a rupture of thin liquid films laying on liquid surfaces is of great interest for various technological applications such as coating and painting, as well as in wetting and spreading science (Bonn et al., 2009; Bratukhin et al., 2009; Kupershtokh et al., 2015). Generally the instability and the rupture of the upper liquid layer is generated by dropping a small amount of a surfactant solution from above (Bratukhin et al., 2009) or by applying magnetic field on a layer of a ferromagnetic liquid (Bushueva et al. 2010).

In this paper, we report experimental results on thermocapillary rupture of a thin liquid layer on a liquid substrate caused by heating with a laser beam. We studied two liquid-liquid systems: (1) Silicone oil/Ethylene glycol* and (2) Silicone oil/Glycerol*. Laser irradiation was absorbed by the liquid substrate (*) near the liquid-liquid interface.

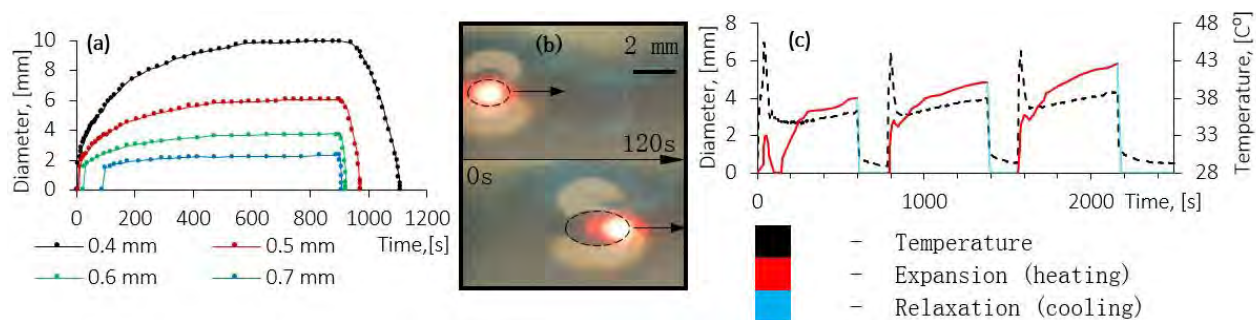


Figure 1:(a) The evolution of the diameter

(b) The movement of the rupture after the laser beam; (c) The dependency of temperature and the diameter on time during three cycles of evolution/relaxation of the thermocapillary rupture.

It was found out that time of the rupture diameter growth and its relaxation, after the laser beam is switched-off, decreases with an increase in the top layer thickness, whereas time required for the rupture formation increases, Fig. 1(a). Moreover, the thinner the top layer the larger the thermocapillary rupture diameter, Fig. 1(a). A comparison of the growth rates of the rupture for Ethylene Glycol and Glycerol substrates shows that on Ethylene Glycol it grows faster, but more deformable in the course of motion due to the influence of the added mass (as a convective flow) of liquid substrate. Conversely, the circular rupture of top layer on Glycerol has insignificant distortions at the same rates of motion (50–60 μm/s for 0.8–0.6 mm top layer height range) because of high viscosity of Glycerol, Fig. 1(b). Interestingly to note, that a thermocapillary splash in the top layer in the Silicone oil/Ethylene Glycol system takes place, Fig. 1(c).

Such systems have a great potential in optical applications (optical tunable diaphragms) or in environmental science for removal of contaminants on liquid interfaces.

Acknowledgements: The research was supported by the RFBR (Grant no. 17-08-00291).

References

- Bonn D., Eggers J., Indekeu J., Meunier J., Rolley E. Wetting and spreading. *Rev. Mod. Phys.*, 1, 739-805 (2009).
- Bratukhin Yu.K., Zuev A.L., Kostarev K.G., Shmyrov A.V. Stability of a Steady-State Discontinuity of a Fluid Layer on the Surface of an Immiscible Fluid. *Fluid. Dyn.*, 44(3), 340-350 (2009).
- Kupershtokh A.L., Ermanyuk E.V., Gavrilov N.V. The Rupture of Thin Liquid Films Placed on Solid and Liquid Substrates in Gravity Body. *Commun. Compt. Phys.*, 17(5), 1301-1319 (2015).
- Bushueva C.A., Kostarev K.G., Lebedev A.V. Deformation of a layer of ferrofluid, lying on a liquid substrate, subjected to the action of the magnetic field. *Physics Procedia* 9, 205-209 (2010).

Humidity-induced breath of droplets: Marangoni-driven against sorption-driven mechanisms

Nikolay Kubochkin, Natalia Ivanova

Tyumen State University, Photonics and Microfluidics Lab, Volodarskogo 6, Tyumen, 625003, Russia

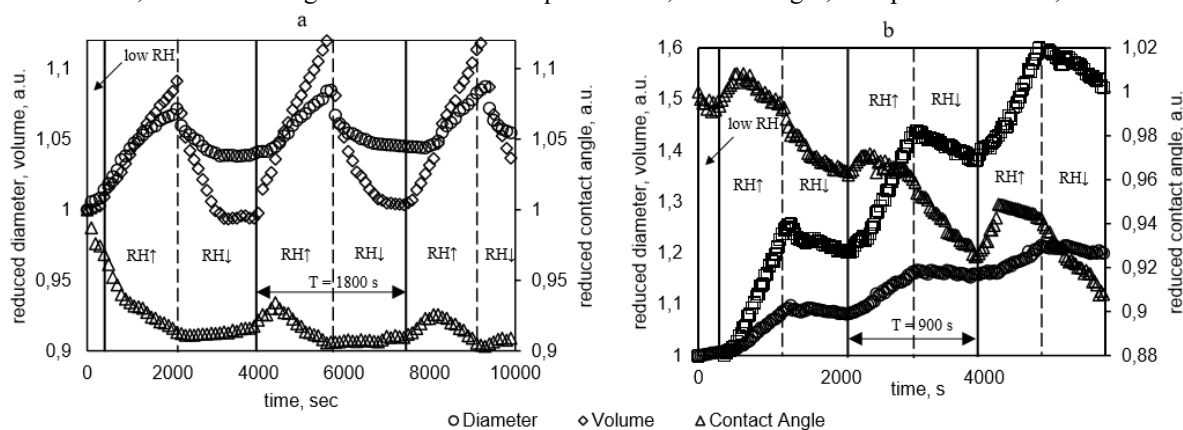
nikolaykubochkin@gmail.com, n.ivanova@utmn.ru

Wetting and spreading phenomena are ubiquitous and are investigated intensively in last decades from both theoretical and experimental points of view (Venzmer 2007). Despite there are a number of works focusing on spreading of simple and complex liquids over different substrates, information about humidity influence on spreading kinetics of sessile droplets is still obscure. Recently, we showed that increasing humidity leads to spreading of pure surfactants droplets from quasi-equilibrium state (Ivanova et al. 2017).

In this paper, we present the experimental results on cyclically changing humidity influence on spreading kinetics of pure liquids and their water solutions on hydrophobic substrates. Pure surfactants and hygroscopic liquids were under the investigation. We found out that periodically changing humidity causes «breath» of droplet: increasing and decreasing of diameter, contact angle and volume with respect to the current humidity level (Fig. 1, a-b). Besides, it was revealed that different mechanisms are responsible for such effect in case of different liquids.

We assume that spreading of pure surfactants is caused by Marangoni forces: due to water adsorption onto the substrate, at increasing humidity precursor layer with higher surface tension is forming in close vicinity to the droplet edge. In turn, reverse wetting behavior, i.e. droplet contraction, is governed solely by evaporation, which triggers the retracting shear stress. «Breathing» of hygroscopic liquid droplets occurs probably due to water sorption from the surrounding air: when humidity is increasing, droplet accumulates moisture and changes its configuration (diameter and contact angle), whilst in a time span when humidity is diminishing, evaporation begins to force a droplet reach a steady state. Thus, we propose that the role of precursor film for hygroscopic liquids is negligible even at high relative humidities.

Moreover, it is interesting to notice that for liquids tested, for all stages, except the first one, critical advancing



contact angle, which corresponds to critical humidity, is required to continue spreading (expansion).

Figure 1: Wetting behavior of Silwet L-77 (a) and glycerol (b) on PTFE at periodically changing relative humidity (RH).

References

J. Venzmer: Superspreading – 20 years of physicochemical research, *Curr. Opin. Colloid Interface Sci*, 16 (4), 335–343, 2011.

N.A. Ivanova; N.S. Kubochkin; V.M. Starov: Wetting of hydrophobic substrates by pure surfactants at continuously increasing humidity, *Colloids Surf A Physicochem Eng Asp*, 08, 2016.

Radiative heat transfer from the surface of thermocapillary liquid bridges of high-Prandtl-number fluids in microgravity

Nobuhiro Shitomi, Taishi Yano and Koichi Nishino

Department of Mechanical Engineering, Yokohama National University

79-5 Tokiwadai, Hodogaya-ku, Yokohama, Kanagawa 240-8501, Japan

shitomi-nobuhiro-nk@ynu.jp, yano-taishi-gh@ynu.ac.jp, nishino-koichi-fy@ynu.ac.jp

Heat transfer at the liquid-gas interface can strongly affect the instability of thermocapillary convection in liquid bridges (LBs) of high-Prandtl-number fluids [1]. Some recent studies (e.g., [2]) show that the radiative heat transfer can be more important than the convective one in microgravity (μg) where no buoyant flows exist. The present study aims at clarifying the combined effect of radiative and convective heat transfers on the steady thermocapillary convection in LBs by using the commercial CFD solver (STAR-CCM+) and by making detailed comparison with the experimental data taken in space experiments.

The computation assumes the presence of steady axisymmetric temperature and flow fields and hence considers a cylindrical sector whose central angle is 20° as shown in Figure 1 (a). The computational domain includes the LB of silicone oil, the heated/cooled disks, the ambient gas and the chamber. The surfaces of the LB, the disks and the chamber are assumed to be gray surfaces to consider only surface radiation and diffuse reflection. Isothermal conditions are given to the heated/cooled disk surfaces and the chamber wall (T_H , T_C , and T_W , respectively) and the adiabatic condition is given to the top and bottom wall surfaces. The periodic boundary condition is imposed on the side surfaces of the cylindrical sector. The computation of temperature and flow fields in both LB and ambient gas provide the direct effect of the radiative heat transfer on the thermocapillary convection in the LB.

Figure 1 (b) shows the flow visualization and the IR image of a long LB formed in μg experiments conducted in the Japanese experiment module on ISS. Although the LB is suspended between T_H and T_C , a temperature minimum region ($T_{min} < T_C$) appears near the cooled disk and the surface flow goes toward this region from both heated and cooled disk sides. Such a unique feature is reproduced well by the present computation considering the radiative heat transfer as shown in Figure 1 (c) while such a feature is not predicted by the computation without radiative heat transfer. It is demonstrated from a series of the present computations that the effect of radiative heat transfer can be of significant in μg even in room-temperature conditions.

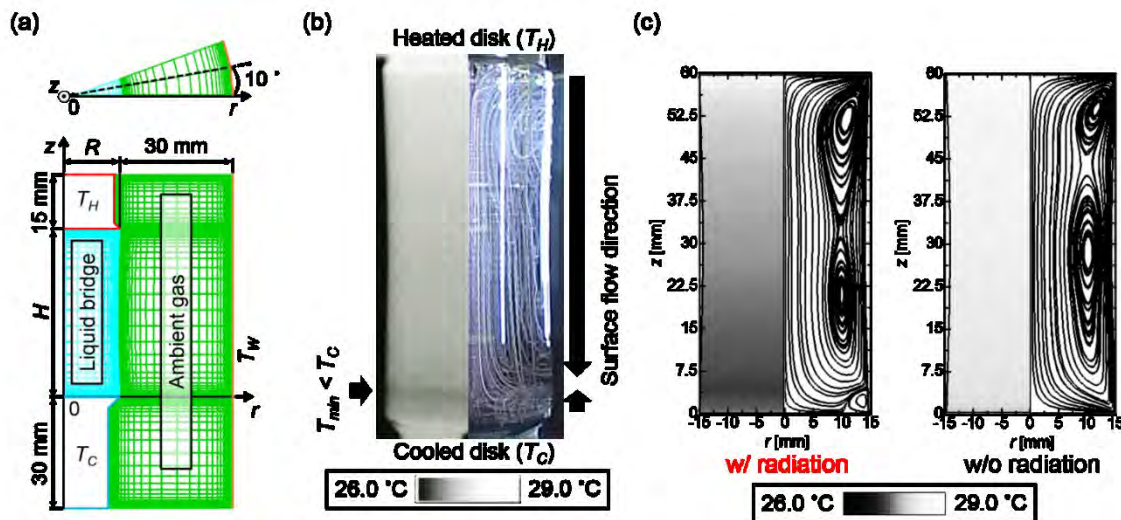


Figure 1: (a) computational domain, (b) surface temperature distribution and flow structure in LBs for $T_C = 27.5^\circ\text{C}$, $T_H = 28.9^\circ\text{C}$, and $T_W = 25^\circ\text{C}$ in (b) experiment and (c) CFD

References

- [1] Y. Kamotani, L. Wang, S. Hatta, A. Wang, and S. Yoda, "Free surface heat loss effect on oscillatory thermocapillary flow in liquid bridges of high Prandtl number fluids," *Int. J. Heat Mass Transfer* 46(17), 3211 (2003).
- [2] D. E. Melnikov, V. Shevtsova, T. Yano, and K. Nishino, "Modeling of the experiments on the Marangoni convection in liquid bridges in weightlessness for a wide range of aspect ratio," *Int. J. Heat Mass Transfer* 87, 119 (2015).

Thermocapillary flow instability in low Pr fluid pool: Effects of Pr and pool geometry

Nobuyuki Imaishi¹, M.K. Ermakov² and W.Y. Shi³

¹ Kyushu University, Kasuga 816-8580, Japan, imaishi@cm.kyushu-u.ac.jp

² Ishlinsky Institute for Problems in Mechanics of RAS, Moscow, 117526, Russia, ermakov@ipmnet.ru

³ College of Power Engineering, Chongqing University, Chongqing 400044, China, shivy@cqu.edu.cn

We apply a linear stability analysis over a wide range of the Prandtl number, $Pr \in [10^{-5}, 10^2]$ to investigate how Prandtl number and curvature affect the stability boundary of axisymmetric steady thermocapillary flow in shallow annular pools with an aspect ratio $\Gamma = (R_o - R_i)/d = 20$ and two radius ratios $\Gamma_R = R_i/R_o = 0.50$ and 0.98039 , where d , R_o , and R_i are the liquid depth and the radii of the heated outer wall and the cooled inner wall, respectively. [Some results for $\Gamma_R = 0.50$ were reported earlier.¹⁾] The results, some part of which are shown in Fig. 1 for $Pr \in [10^{-3}, 1.0]$, elucidate that the steady axisymmetric thermocapillary flows in these annular pools become unstable against any of the oscillatory instabilities OSC1, OSC2, and hydrothermal wave instability (HTW1). The critical mode for $Pr \leq Pr_1^*$ is OSC2, which is characterized by its large wave number, high frequency, and almost constant Re_c throughout the range of Pr. The critical mode for $Pr_1^* \leq Pr \leq Pr_2^*$ is OSC1 with smaller wave number and lower frequency, and Re_c decreases with increasing Pr. In addition to these critical modes, we find in both pools two neutral stability curves for three-dimensional steady flows 3DSF1 and 3DSF2 for $Pr < Pr_2^*$. For $Pr \geq Pr_2^*$, the hydrothermal wave HTW1 is the critical mode and a neutral stability curve for hydrothermal wave HTW2 appears for $Pr_2^* < Pr < 77$ for $\Gamma_R = 0.50$. There is no stability curve for HTW2 for $\Gamma_R = 0.98036$. The values of (Pr_1^*, Pr_2^*) are $(0.00953, 0.03054)$ for $\Gamma_R = 0.50$ and $(0.01919, 0.01946)$ for $\Gamma_R = 0.98039$. Energy-budget analyses reveal that the four instabilities in low-Pr range are caused primarily by instabilities in the steady toroidal vortex (or vortices) near the cold wall. Present results indicate that hydrothermal wave instability of Smith and Davis²⁾ is not responsible for the instability in low-Pr range. Present results also indicate that two types of HTW are caused by the two different periphery-lengths in the smaller annular pools and only one HTW appears in large annular pool because the difference in the periphery-lengths becomes small.

Effects of (liquid depth) and the buoyancy on the stability limits will be presented at the venue.

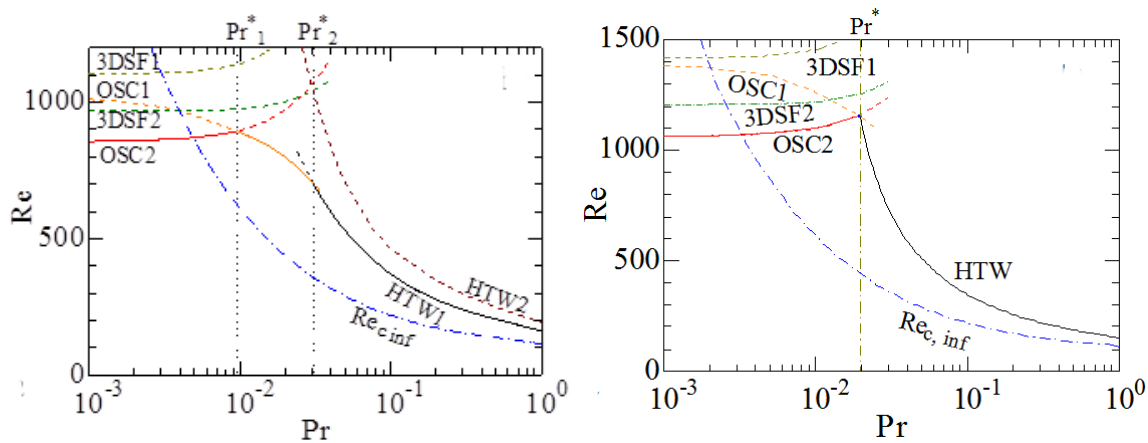


Figure 1: Critical Reynolds number as a function of Pr for small and large annular pools with $\Gamma = 20$, under microgravity condition. For small annular pool with $\Gamma_R = 0.50$ at left, and for large annular pool with $\Gamma_R = 0.98036$ at right. $Re_{c,inf}$ is the critical Reynolds number for the onset of hydrothermal wave in infinite return flow given by Smith and Davis²⁾.

Reference

- 1) N. Imaishi, M.K. Ermakov, W.Y. Shi, Y.R. Li and L. Peng, presented at IMA-7 (2014).
- 2) M. K. Smith and S. H. Davis, J. Fluid Mech., **132**, 119 (1983).

Structures of film flow with phase transitions

Oxana A. Frolovskaya^{1,2} and Vladislav V. Pukhnachev^{1,2}

¹Lavrentyev Institute of Hydrodynamics of SB RAS, Lavrentyev Prospect 15, Novosibirsk, 630090, Russia

²Novosibirsk State University, Pirogova Street 2, Novosibirsk, 630090, Russia

oksana@hydro.nsc.ru, pukhnachev@gmail.com

A mathematical model proposed by Nakoryakov, Ostapenko and Bartashevich (2012) is used to describe the motion of a thin layer along a vertical wall with condensation or evaporation. It reduces to a single equation for the film thickness $h(x, t)$, which satisfies equation in dimensionless variables

$$\frac{\partial h}{\partial t} + \frac{\partial}{\partial x} \left[\frac{h^3}{3} \left(1 + \alpha \frac{\partial^3 h}{\partial x^3} \right) \right] = \frac{\beta}{h}. \quad (1)$$

The model contains two similarity criteria α and β , are proportional to surface tension coefficient and difference between the wall temperature and saturation temperature, respectively. In addition, both parameters α and β were supposed to be constant. Case $\beta > 0$ corresponds the condensation process while case $\beta < 0$ corresponds to the evaporation one. Typical values of these parameters are $\alpha = 5 \cdot 10^{-5}$, $|\beta| = 1$. Limiting transition $\alpha \rightarrow 0$ transforms equation (1) into first-order quasi-linear hyperbolic equation that can be converted into the classical Hopf equation, $u_t + uu_x = 0$, via change of variables $x = z + 2 \int_0^t (t-s)\beta(s)ds$, $h^2(x, t) = u(z, t) + 2 \int_0^t \beta(s)ds$. Here it is not assumed that $\beta = const$ (it means that the wall temperature can be an arbitrary function of time but is does not depend on x). In the series of publications of the authors (2012, 2015), and also speakers (2016), the solutions of the equation (1) under zero surface tension are investigated. Their characteristic feature is the presence of strong and weak discontinuities in the thickness of the layer. In this paper, the regularizing effect of surface tension on the structure of film flow in the presence of phase transitions is studied. Numerical and asymptotic analysis of emerging structures is performed. We also consider the case when the wall temperature is an arbitrary function on time and give the examples of solutions with strong and weak discontinuities at $\alpha = 0$, as well as the results of a numerical solution of the Cauchy problem for small values of the parameter α . Figure 1 presents structure of a strong discontinuity in the condensation process in the new variables, $H(y, t) = h(x, t)$, $y = (\alpha/3)^{-1/3}(x - L(t))$, where $x = L(t)$ is a strong discontinuity line. Figure 2 displays the regularization of a weak discontinuity in the evaporation process.

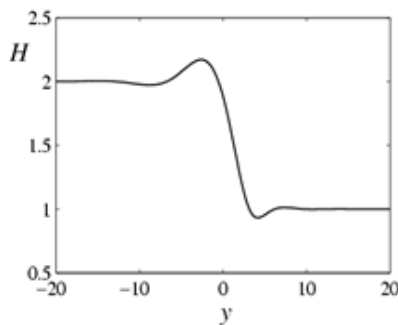


Figure 1: Structure of strong discontinuity (condensation process).

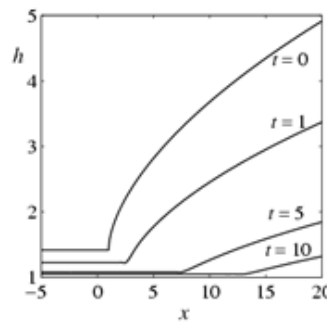
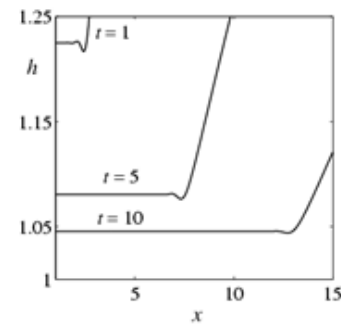


Figure 2: Regularization of weak discontinuity (evaporation process).



References

- [1] V.E. Nakoryakov, V.V. Ostapenko and M.V. Bartashevich, Heat and mass transfer in the liquid film on a vertical wall in roll-wave regime, *Int. J. Heat Mass Transfer*, **55** (23-24), 6514-6518 (2012).
- [2] V.E. Nakoryakov, V.V. Ostapenko and M.V. Bartashevich, Rolling waves on the surface of a thin layer of viscous liquid at phase transition, *Int. J. Heat Mass Transfer*, **89**, 846-855 (2015).
- [3] O.A. Frolovskaya and V.V. Pukhnachev, Traveling waves and structures in the Nakoryakov-Ostapenko-Bartashevich model of film flow with phase transitions. In: *Abstracts of International Symposium and School for Young Scientists "Interfacial Phenomena and Heat Transfer"*, Novosibirsk, Russia, p. 69 (2016).

Mathematical Models of Polymer Solutions Motion

Oxana A. Frolovskaya^{1,2} and Vladislav V. Pukhnachev^{1,2}

¹Lavrentyev Institute of Hydrodynamics of SB RAS, Lavrentyev Prospect 15, Novosibirsk, 630090, Russia

²Novosibirsk State University, Pirogova Street 2, Novosibirsk, 630090, Russia

oksana@hydro.nsc.ru, pukhnachev@gmail.com

Studies of recent decades initiated by Toms (1948) have shown that the addition of a small amount of polymers in water significantly changes the rheological properties of the resulting solution. Experiments showed that the presence of even small amount of a soluble polymer gives relaxation properties to the liquid. Voitkunsii, Amfilokhiev and Pavlovskii (1970) have suggested the model describing motion of aqueous polymer solutions considering relaxation properties of the medium. Unknown functions in this model are the liquid velocity and pressure fields. The model also contains two empirical parameters, relaxation time θ and relaxation viscosity κ . Authors started from one variant of the hereditary Maxwell-type model of viscoelastic fluid with the rheological constitutive law

$$P = -pI + 2\mu D + 2\frac{\kappa}{\theta} \int_{-\infty}^t \exp\left\{-\frac{s-t}{\theta}\right\} \frac{d}{ds} D(s) ds.$$

Here P is the stress tensor, I is the unit tensor, D is the strain tensor of velocity field v , p is the pressure, μ is dynamic coefficient of viscosity, d/dt denotes convective derivative in time. The initial model includes the integro-differential equation with Volterra operator. Pavlovskii (1971) has carried out asymptotic simplification of model using smallness of the parameter θ .

In work the mathematical properties of model of the motion of aqueous polymers solutions (Voytkunsii, Amfilokhiev, Pavlovskii, 1970) and her modifications in a limit case of small relaxation times (Pavlovskii, 1971) are investigated. The plane non-stationary layered motions in both models are studied. It is found that Pavlovskii's model has solutions with weak discontinuities of the velocity field (Fig. 1). The initial model does not allow such solutions because the weak discontinuities which are available at the initial time instantly are smoothed out. The family of the exact solutions describing the stationary and non-stationary plane motion near a critical point is found. The problem on the stationary motion of aqueous polymers solutions in a cylindrical pipe under the influence of a longitudinal gradient of pressure is also considered. Here the flow with linear trajectories is implemented.

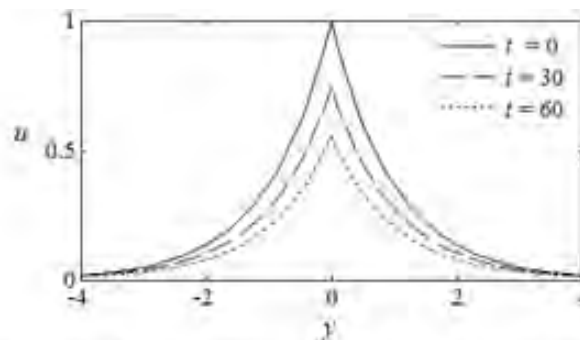


Figure 1: Evolution of weak discontinuity in layered motion (Pavlovskii's model).

The research was supported by RFBR (project No. 16-01-00127).

References

- [1] B.A. Toms, Some observations on the flow of linear polymer solutions through straight tubes at large Reynolds number, In: Proceedings of the 1st Intern. Congress on Rheology. **2**, 135-141 (1948). Amsterdam. The Netherlands.
- [2] Ya.I. Voitkunsii, V.B. Amfilokhiev, and V.A. Pavlovskii, Equations of a fluid motion with taking into account its relaxation properties, Trudy Leningrad Korablestr. Inst. **69**, 19-27 (1970). [in Russian]
- [3] V.A. Pavlovskii, To the question about theoretical description of weak aqueous polymers solutions, Dokl. Acad. Nauk. **200** (4), 809-812 (1971). [in Russian]

Two- and three-dimensional numerical simulations of sessile droplets

Paul G. Chen^{1,a}, Jalil Ouazzani² and Qiusheng Liu^{3,4}

1 Aix Marseille Univ, CNRS, Centrale Marseille, M2P2, 13451 Marseille, France

2 Arcofluid Consulting LLC, 309 N Orange Ave, Orlando, FL 32801, USA

3 Chinese Academy of Sciences, Institute of Mechanics, Beijing, 100190, China

4 University of Chinese Academy of Sciences, Beijing, 100049, China

p.g.chen@univ-amu.fr

It cannot be expected that two-dimensional (2D) numerical results give an accurate representation of the three-dimensional (3D) physics of sessile drop evaporation when surface-tension-induced (Marangoni) flow is not symmetric. Also, a 2D model only considers the components of interface curvature lying in the computational plane, whereas the out-of-plane components are neglected. This means that surface-tension-driven hydrodynamic instabilities can usually not be captured in a realistic way. Developing a high resolution numerical method for the simulation of two-phase heat and mass transfer is a viable way of getting deeper insights into such phenomena, and as consequence to better understand them. A reliable and flexible numerical method is developed in the present paper in order to achieve this goal. The method is applied to the simulation of sessile drop evaporation phenomena. Within this framework, a numerical model is developed using the PHOENICS Computational Fluid Dynamics software, which permits a high flexibility and sustainability of the model. The Finite Volume discretization method is used to solve the governing equations of the problem. The method is developed in two- and three-dimension. A mass-conservative Volume-of-Fluid (VOF) interface tracking method is adopted to capture the position of the two-phase interface and its influence on the fluids flow. For the latter two VOF methods have been developed the CICSAM and the THINC-WLIC methods. Marangoni, capillary forces, static contact angles and evaporation are also developed and included in the model. The developed model is applied to the evaporation of well-defined sessile drop where experimental data are available. We investigate the coupled physical mechanism during the evaporation of a pinned drop that partially wets on a heated substrate. The model accounts for mass transport in surrounding air, Marangoni and gravitational convection inside the drop and heat conduction in the substrate as well as moving interface. We show that under some specific circumstances we have transition from 2D axisymmetric to 3D patterns.

Cohesion of natural cave sediments in the presence of thin liquid films

Perrine Freydier¹, Frédéric Doumenc^{1,2}, Jérôme Martin¹, Béatrice Guerrier¹, Pierre-Yves Jeannin³

¹ Lab. FAST, Université Paris-Sud, CNRS, Université Paris-Saclay,
Bâtiment 502, Campus Universitaire, F-91405, Orsay France

perrine.freydier@u-psud.fr

² Sorbonne Universités, UPMC Univ. Paris 06, UFR919F-75005, Paris, France

³ Swiss Institute for Speleology and Karstology (SISKA), La Chaux-de-Fonds, CH-2301, Switzerland

Vermiculations are small aggregates (a few centimetres long typically) made of particles (clay, calcite, minerals, organic matter, prehistoric paintings...) present at the surface of cave walls. When particles agglomerate, due to mechanisms that we seek to understand, pigments of prehistoric paintings may be dragged with them, deteriorating irremediably these remains of the past (see Figure 1). Vermiculations have been observed in caves by speleologist community for 60 years. The related literature mainly reports descriptive studies based on field observations (Bini et al. 1978). Most authors mention the presence of thin liquid films at the walls, originating from percolation or condensation water, which can lead to mobilization, displacement and aggregation of particles forming vermiculations.

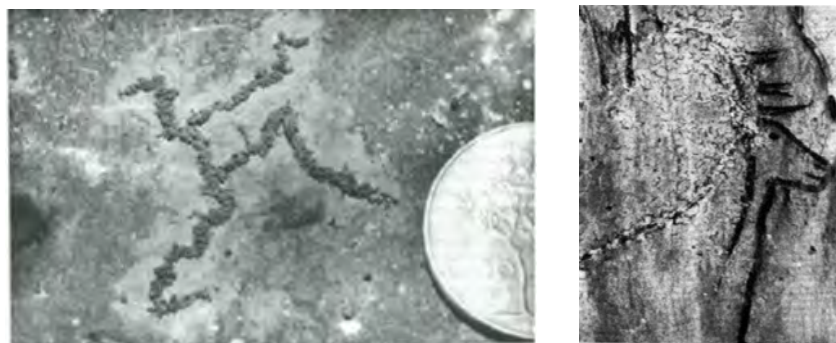


Figure 1: Example of vermiculations. Left: “Ramified vermiculation” (Bini et al. 1978); Right: Degradation of wall paintings in the cave of Niaux (Clottes, 1981).

To further assess and prevent the degradation of paintings due to vermiculations, a better insight into their mechanisms of formation is now needed. To date, no controlled experimental study tackled this issue. The aim of the present study is to find out the conditions required to mobilize sediments and form vermiculations, through experimental investigations coupled with field observations.

For our experiments, we use typical natural sediments collected in caves. Rheometrical analyses, performed with a rough-plate rheometer, show that these wet sediments exhibit a stress threshold, called yield stress, above which they flow as viscous fluids and below which they present a solid-like behavior. As a decrease of the yield stress of these sediments will lead to an easier mobilization by external forces (gravity, viscous friction due to water flow...), we believe that such a yield stress decrease is needed to form vermiculations. Our experiments consist in measuring the evolution of yield stress of typical cave sediments depending on conditions that sediments are expected to encounter in a cave environment. Sediments are immersed from 20 min to several weeks in pure water representing the condensation water, calcium carbonate saturated water representing the percolating water, or different chemical composition to test the influence of the ions in solution. Carbon dioxide partial pressure ($p\text{CO}_2$) is varied from 300 ppm to 10%, as in cave conditions, to study the influence of pH and dissolution of calcium carbonate on sediment cohesion. In a second experiment, a continuous and controlled flow of water is applied over the sediment. It aims at evaluating the cohesion decrease induced by the water renewal and at characterizing the effect of an additional hydrodynamic stress to the mobilization. These experiments provide an interesting dataset highlighting the evolution of cohesion of natural sediments through different water composition and $p\text{CO}_2$. Furthermore, the reproduction of vermiculations in laboratory is awaited to help qualifying degradation factors of cave paintings.

References

- Bini A., Cavalli Gori M., Gori S. A critical review of the hypotheses on the origin of vermiculations. *International Journal of Speleology* 10 (1978), 11-33.
Clottes, J. *Midi-Pyrénées. Gallia préhistoire* 24 (1981), 525-570.

Velocity profiles in the front of viscoplastic surges: experimental-theoretical comparisons

Perrine Freydier^{1,2}, Guillaume Chambon¹

¹ Grenoble Alpes University, Irstea, Snow Avalanche and Torrent Control Research Unit
 Saint Martin d'Hères, 38402, France

² *Current position:* Lab. FAST, Université Paris-Sud, CNRS, Université Paris-Saclay,
 Bâtiment 502, Campus Universitaire, F-91405, Orsay, France
perrine.freydier@u-psud.fr

Free-surface flow characterized by a complex rheology of viscoplastic type are encountered in various geophysical situations (mudflows, debris flows, avalanches, etc) or industrial processes (civil engineering, food-processing industry, etc). The materials involved in these flows are characterized by the existence of a yield stress, i.e. a stress threshold, below which they behave as solids and above which they flow as viscous fluids. These flow are thus characterized by the presence of solid or quasi-solid zones (plug) that tend to develop close to the free-surface, where the shear stress is low (Balmforth and Craster, 1999). The coexistence of solid and liquid zones renders the modelling of these free-surface flows particularly problematic. In particular, in thin-layer models, velocity profile shape in non-uniform zones is assumed identical to that of the steady uniform flow. However, this approximation is not consistent and velocity profile corrections should be taken into account to express the deviation from the steady uniform profile (Ruyer-Quil and Manneville, 2000).

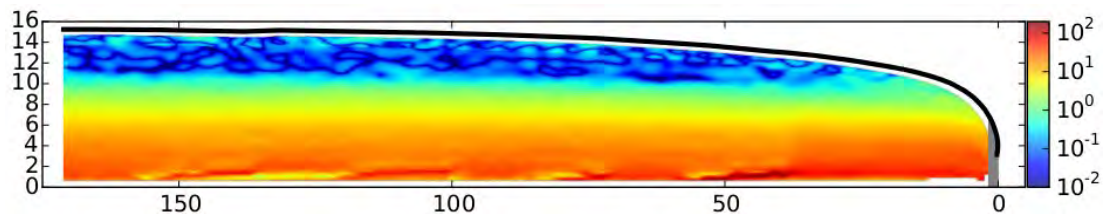


Figure 1: Experimentally-determined shear rate (in s-1) inside a free-surface viscoplastic surge (axes x and y are in mm). The blueish zone at the top of the flow (shear rate less than 10^{-1} s-1 typically) corresponds to the unsheared plug, (Freydier et al. 2017).

In that context, the aim of this study is to characterize the evolution of the velocity profile shape in the front of viscoplastic free-surface flows, experimentally and theoretically. Our experimental works documents the internal dynamics (velocity profiles, shear rate, etc.) of free-surface flows made of a model viscoplastic material (Carbopol). The experiments were performed in a conveyor-belt channel in which gravity-driven surges remain stationary in the laboratory reference frame. Through advanced velocimetry techniques, the velocity field and position of the plug interface in the vicinity of the front could be measured with a high accuracy. Results show, in particular, that velocity profiles become sheared across the whole flow depth when approaching the front, resulting in a disappearance of the plug (see Figure 1). These experimental data were compared to theoretical predictions based on asymptotic developments of the primitive equations. This theoretical approach follows, and extends, that of Fernandez-Nieto et al. (2010). The zeroth-order approximation, which is equivalent to the lubrication model, appears to satisfactorily capture the dynamics of the flow except in the tip of the surge front. Considering order-1 corrective terms for the velocity profile, the model ensures better predictions for the velocity profiles in the front and remarkably captures the shape of the solid-fluid interface in this strongly non-uniform zone. In particular, corrective terms arising from the existence of plastic normal stresses, which are specific to viscoplasticity, appear to play an important role. Such comparisons between experiments and theoretical predictions provide relevant results to further develop consistent thin-layer models well-suited to complex fluid flows.

References

- Balmforth N.J. and Craster R.V. A consistent thin-layer theory for Bingham plastics, *J. Non-Newton. Fluid Mech.* 84 (1999), 65-81.
 Fernandez-Nieto E. D., Noble P., Vila J.P. Shallow Water equations for Non-Newtonian fluids. *J. Non-Newton. Fluid Mech.* 165 (2010), 712-732.
 Freydier P., Chambon G., Naaim M. Experimental characterization of velocity fields within the front of viscoplastic surges down an incline. *J. Non-Newton. Fluid Mech.* 240 (2017), 56-69.
 Ruyer-Quil Ch. and Manneville P. Improved modeling of flows down inclined planes. *Eur. Phys. J. B* 15 (2000), 357-369.

Image super resolution reconstruction based on deep parallel convolution neural network

Qiang Yu¹, Liu Xiaoke^{1,2}

1 National Space Science Center, Chinese Academy of Sciences,

2 School of Computer and Control Engineering, University of Chinese Academy of Sciences,

Beijing 100190, China

E-mail: yuqiang@nssc.ac.cn

Using electrostatic levitation and drop tube to study the intrinsic characteristics of materials under the condition of microgravity without container is an important means to study metastable new materials. The droplet of the sample drops freely from the height of 50 meters. The changes of density, specific heat and surface tension can be calculated by the temperature sensor and the image sensor. When the droplet reaches the bottom, the image pixels obtained by the image sensor are extremely low. Super-resolution image reconstruction is an algorithm that provides finer details than the sampling grid of a given imaging device by increasing the number of pixels per unit area in the image. We present an image super resolution reconstruction algorithm based on deep parallel convolution neural network. Image super-resolution (SR) aims to reconstruct high-resolution (HR) image from low-resolution (LR) input image. The super resolution reconstruction is based on convolution consists of three steps. The first step is the extraction and representation of the image blocks, which are represented as vectors of high latitude. The second step is nonlinear mapping, and maps every high-dimensional vector to another high-dimensional vector. The third step is to reconstruct the image and reconstruct all the high-resolution vectors in the second step to generate the final high-resolution images. On this basis, aiming at feature extraction and reconstruction, some convolution kernels are directly applied to low resolution images, and local and global features are obtained. Then connect these characteristic maps, draw lessons from the idea of parallel network, and use parallel CNN network to reconstruct images. The proposed CNN model focuses on learning the residuals between bicubic interpolations of LR images and HR original images. This algorithm overcomes the block effect and edge blur caused by image patch splicing and can be applied to address low-resolution images which are achieved by a high-speed camera (10^6 fps).

Study on combined buoyancy-Marangoni convection heat and mass transfer of nanofluids in porous media

Y.J. Zhuang, Q.Y. Zhu*

School of Engineering, Sun Yat-sen University

mcszqy@mail.sysu.edu.cn

In this paper, the combined buoyancy-Marangoni convection of non-Newtonian power-law nanofluids in a 3D porous fibrous media is investigated with the compact high order finite volume method. Special attentions are given to detect the effects of pore size distribution, Marangoni number, thermal Rayleigh number, buoyancy ratio and nanoparticle volume fraction on the fluid flow as well as on rates of heat and mass transfer. On the other hand, the effect of the surface tension on the heat and mass transfer intensity becomes insignificant when the buoyancy force is strengthened. Further, the average Nusselt and Sherwood numbers increase as the Marangoni number and thermal Rayleigh number increase due to the combined effects of buoyancy and surface tension. The augmentation of the buoyancy ratio causes convection heat and mass transfer to increase for the thermal dominated flow while decrease in buoyancy ratio also augments it for the solutal dominated flow. The heat transfer (mass transfer) rate is found to increase (decrease) with increasing the nanoparticle volume fraction. Moreover, for all above studied parameters, an intensification of the flow and an increase in average Nusselt and Sherwood numbers occur with the decrease in power-law index.

Effect of rod-rotating on stability of thermocapillary flows under microgravity conditions

Q.-S. Chen^{1*}, P. Zhu¹, M. He¹, K.-X. Hu²

¹Key Laboratory of Microgravity,
Institute of Mechanics, Chinese Academy of Sciences,
15 Bei Si Huan Xi Road, Beijing 100190, China

²School of Mechanical Engineering and Mechanics, Ningbo University, Ningbo 315211, China

*Corresponding author: qschen@imech.ac.cn

Instabilities of thermocapillary flows between counter-rotating disks under microgravity conditions are investigated by linear stability analysis. The basic-state and perturbation equations are solved using the Chebyshev-collocation method. The critical capillary Reynolds number is a function of Prandtl number, Coriolis number and aspect ratio [1-3].

Energy analysis shows that the perturbation energy consists of the viscous dissipation, the work done by surface tension and the interaction between the perturbation flow and the basic flow, respectively. For large Prandtl number liquids ($Pr \geq 0.1$), the work by surface tension becomes more important, which shows that the thermocapillary effects are important for onset of instabilities.

In some cases, the interaction between the perturbation and the basic flow in the azimuthal direction is positive when a moderate rotation is applied on the disks ($Pr \geq 0.1$). So, the moderate rotation can have destabilizing effect on the thermocapillary flows for large Prandtl number liquids (Fig. 1).

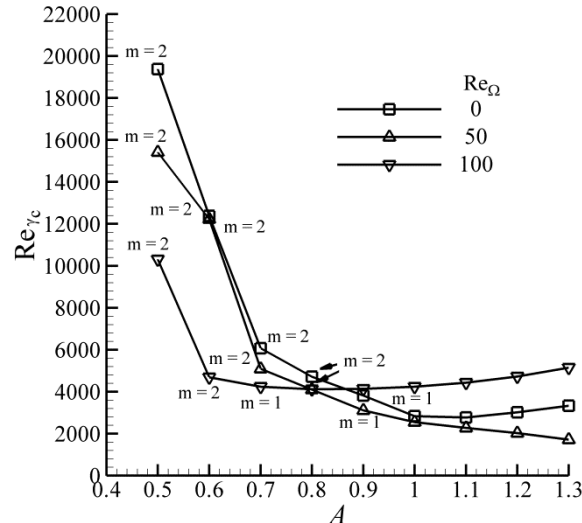


Figure 1: Dependence of the critical capillary Reynolds number on the aspect ratio for $Pr = 0.1$.

References

1. M. Lappa, R. Savino, and R. Monti, "Three-dimensional numerical simulation of Marangoni instabilities in non-cylindrical liquid bridges in microgravity," *Int. J. Heat and Mass Transfer* 44, 1983 (2001).
2. Q. S. Chen, and Y. N. Jiang, "Instabilities of vortex rings generated by surface-tension gradients between co-axial disks," *Int. Commun. Heat Mass Transf.* 39, 1542(2012).
3. Qi-Sheng Chen, Meng He, Peng Zhu, Kai-Xin Hu, Instabilities of thermocapillary flows between counter-rotating disks under microgravity conditions, *International Journal of Heat and Mass Transfer* 117, 183-187, 2018.

Phase-Changed Interfacial Formation of Evaporation and Condensation under Microgravity Condition onboard Space Platforms TZ-1

Qiusheng Liu^{1,2*}, Zhiqiang Zhu¹, Wenjun Liu^{1,2}, Zhengzhi Zhang^{1,2}, Guofeng Xu^{1,2}, Jingchang Xie¹

¹Institute of Mechanics, Chinese Academy of Sciences, 100190, Beijing, China

²University of Chinese Academy of Sciences, 100049, Beijing, China

*liu@imech.ac.cn

The evaporation and condensation process in space have recently attracted more scientific interests owing to engineering applications as efficient ways of heat management. In space, the phase change coupling with typical interfacial phenomena of heat and mass transfer will play main role in the process of evaporation and condensation, while which are still absent of comprehensive understanding in space where the influence of gravity (i.e. natural convection, buoyancy) can be minimized. In present paper, the preliminary experimental results of both the evaporation and the condensation in microgravity condition will be presented. These results are obtained in recent two space flight missions of Chinese 1st Cargo Spacecraft TZ-1 launched in 2017. Experiments were performed successfully during the total 234 hours' working time in orbit. (1) The comprehensive experimental investigations of phase change during evaporation and condensation were firstly carried out, which is helpful to understand the influence of gravity effects on the heat and mass transfers of during phase change process. Specifically, evaporation of liquid layer and drop, condensation of the liquid vapor were observed experimentally in a closed test cell of space facility established with controlling parameters (substrate temperature, volume of injecting working medium and inner pressure), subsequently, scientific data, including typical temperature, heat flux and vapor pressure are measured during the process of phase change. Synchronously, the feature evolution (liquid layer and drop evolution for evaporation, formation of liquid film for condensation) and the vapor-liquid interfacial temperature field are captured by a CCD camera and an infra camera, respectively. Obviously, the interfacial-tension maintained the larger size of evaporation droplet and condensation film in microgravity condition of space. With special structure on the evaporation test plate, the flat liquid films of 2mm thickness are created at the beginning of the film evaporation. Comparisons of the space experimental results with these on ground show that both evaporation rate and condensation rate in space are lower than those on the ground.. Quantitative investigations of evaporating evolution of liquid drops and liquid layers were achieved on a substrate. We obtained the Drop and Film Evaporation Rate "Map" in space, which provide the basic dates of space evaporation heat transfer coefficients. It was found that the gravity effect had distinct influence on the phase change heat and mass transfer, with obvious different convective cells in the thermal fields. Due to the absent of buoyancy convection in space, formation of the "vapor-clouds" of evaporating liquid FC72 and its diffusion near the interface are observed by IR camera in microgravity condition. The thickness variation of condensation film formed on the cooling plate with minimum temperature at -5°C are recorded by CCD camera from side view for different condensation environment conditions inside the closed test cell. The onset of condensation was successfully recognized by thermal measurements and optical investigations. It was found the heat transfer efficiency induced by condensation worsen than ground, owing to the condensate liquid film stabilized by surface tension in space.

Acknowledgements

This research was financially supported by the China's Manned Space Program (TZ-1) and the National Natural Science Foundation of China (Grants No. 11532015).



Electrostatically Forced Interfacial Instability

Ranga Narayanan¹,Nevin Brosius*¹, Kevin Ward¹, Dipin Pillai¹, and Satoshi Matsumoto²

¹University of Florida, Department of Chemical Engineering, Gainesville, Florida 32611, USA

²Japan Aerospace Exploration Agency, Human Spaceflight Technology Directorate, Tsukuba, Ibaraki 305-8505, Japan

*nbb5056@ufl.edu

This work utilizes the electrostatic analogue of the Faraday instability, where the interface(s) of a stacked multi-fluid system are subjected to an oscillating external forcing that may resonate with the natural frequency of the system and form standing or breaking interfacial waves. We discuss the instability and also apply this idea to electrostatically excited movement of a levitated spherical liquid drop such that the periodic forcing frequency equals to one of its natural frequencies, yielding resonant structures. The natural frequencies of a liquid sphere directly depend on the modal structure, the mass of the liquid, and the surface tension. Comparisons and contrasts between experiments and theory are explained.

Liquid pumping induced by transverse forced vibrations of an elastic beam: A lubrication approach

Rodica Borcia and Michael Bestehorn

Brandenburg University of Technology Cottbus-Senftenberg, Chair of Statistical Physics and Nonlinear Dynamics, Cottbus, Germany

E-mail: borciar@b-tu.de

Sebastian Uhlig^{1,2}, Matthieu Gaudet^{1,2}, and Harald Schenk^{1,2}

¹Brandenburg University of Technology Cottbus-Senftenberg, Chair Micro- and Nanosystems, Cottbus, Germany

²Fraunhofer Institute for Photonic Microsystems, ISS, Cottbus, Germany

The behavior of liquid thin films is of great importance for technological applications such as oil recover, ink-jet printing, emulsion stability or control in micro- and nanofluidics, actuators and micropumps with a large range of potential use in micro-electro-mechanical systems (MEMS), especially in biological, chemical and medical fields.

Two liquid pumps are theoretically/numerically investigated: a single thin liquid layer actuated by a periodical force at an elastic beam (Fig. 1-a) and a two-layer geometry actuated by an elastic beam (Fig. 1-b). For the second geometry, the beam actuates the liquid from both sides. For both pumps, the liquid film thickness is small compared to the lateral characteristic length of the system. A lubrication theory is developed. The Euler-Bernoulli equation for transverse deformations of an elastic beam is coupled to the fundamental hydrodynamic equations: Navier-Stokes equation and continuity equation in long-wave approximation. In this way, one connects the transverse displacement of the beam with the hydrodynamic quantities (pressure, velocity fields, flow rates). Appropriate boundary conditions incorporate the function of the valves. The derivation of the theoretical model is followed by numerical simulations. We estimate flow rates (in two and three spatial dimensions) for different system parameters and we compute the efficiency of a well-designed liquid pump.

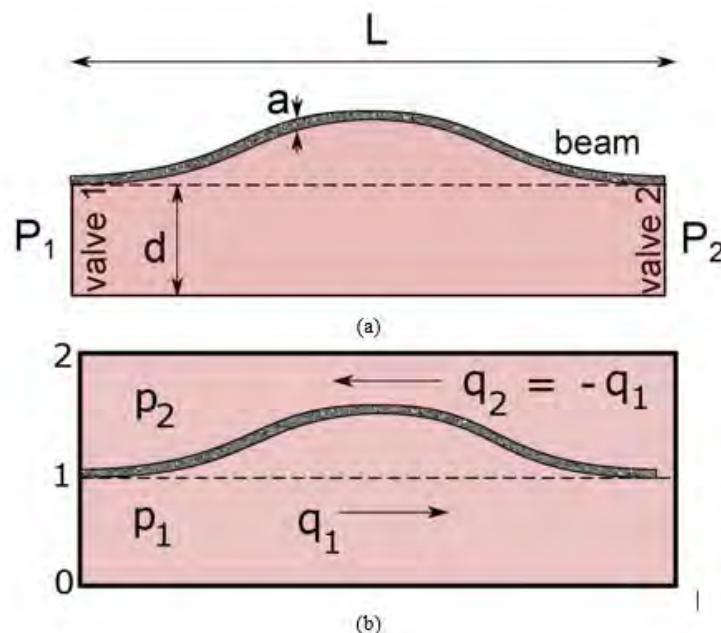


Figure 1: Liquid pumps actuated by an elastic beam: (a) one-layer system; (b) two-layer system.



Breath Figures on ice films

Ruddy Urbina¹ and Wenceslao González-Viñas²

Universidad de Navarra, Complex Systems group and PHYSMED group, Pamplona, Spain

¹rurbina@alumni.unav.es, ²wens@unav.es

Breath Figures are patterns that water droplets form onto a surface where a condensation process takes place (Rayleigh 1911). Those patterns depend on different parameters such as temperature and environmental humidity. At surface temperatures below the freezing point a Breath Figure can evolve via condensation frosting, passing through supercooled condensation, inter-droplet ice bridging (Guadarrama-Cetina et al. 2013), percolation clusters and frost densification (Nath et al. 2017). At lower temperatures, the phase transition could be given by direct deposition.

We perform an experimental study of water condensation on ice films. We first make an ice film, at controlled temperature within a condensation chamber. Afterwards, we promote the condensation process by constant humid air flux. At these conditions, we can have condensation of supercooled water droplets on the ice film and, simultaneously, direct deposition. From our observations, it is distinguishable between the formation of small features and predominant edges. The edges get thicker due to deposition, and a lateral growth of their boundaries is visible. Meanwhile, we notice a surface tension-mediated migration of smaller spots towards clusters of the aforementioned features, to be finally integrated as part of them. We also report the enlargement of edges and features with time, as a measure of the condensation rate on the ice surface.

References

Guadarrama-Cetina, J. et al. (2013). EPL, 101(1), 16009.

Nath, S. et al. (2017). Nanoscale and Microscale Thermophysical Engineering, 21 (2), 81-101.

Rayleigh, L. (1911). Nature, 86 (2169), 416-417

Melting Dynamics of Phase Change Materials under Thermocapillarity

Santiago Madruga

Universidad Politécnica de Madrid, Aerospace Engineering School,
 Plaza Cardenal Cisneros 3, Madrid, 28040, Spain
santiago.madruga@upm.es

The Phase Change Materials (PCM) allow to use the large latent heat of the solid/liquid phase change to store large amounts of thermal energy during melting, the charging phase, and release it to the environment during solidification, the discharging phase. These materials allow more compact and efficient thermal management units than traditional materials based on sensible heat. Because of that, they can be used to increase the thermal energy storage capacity of construction elements in light structures, in solar power plants to offset the shift between energy production and consumption, cooling of electronic components, thermal management of space crafts in microgravity conditions, etc [1].

In addition to ground applications, the usual cycles of operation of devices on-board spacecrafts suits well with the the heat storage and discharge phases of PCMs. Thus thermal control using PCMs in microgravity has been widely used in space systems for low and high temperature applications to avoid temperature peaks from electronic devices, electrical power components, control battery temperature in lunar and Mars rovers, or even to refrigerate food and biological waste samples in manned spacecrafts [2]. However, a major issue in thermal regulation with these materials is their low conductivity. This leads to very long times during the heat storage and discharge phases, reducing their usability and performance on heat control.

Thermocapillary effects are a mechanism to enhance the heat transfer on PCMs in microgravity, without increasing the mass and volume [3,4]. We model the PCM using an enthalpy-porosity formulation and show the effect of the thermocapillarity on their melting dynamics, improvement of heat transport and scaling laws relating the Nusselt number with the strength of the convective motions [5]. In addition, we discuss the effect of dispersed metallic nanoparticles on the Prandtl and Marangoni numbers and their influence on heat transfer performance in microgravity [6].

References

1. Zhang, H., Baeyens, J., Cáceres, G., Degève, J., Lv, Y., 2016. Thermal energy storage: Recent developments and practical aspects. *Prog. Energy Combust. Sci.* 53, 1–40.
2. Swanson, T. D., Birur, G. C., 2003. NASA thermal control technologies for robotic spacecraft. In: *Appl. Therm. Eng.* Vol. 23. pp. 1055–1065.
3. Enhancement of heat transfer rate on phase change materials with thermocapillary flows. S. Madruga and C. Mendoza. *European Physical Journal Special Topics.* 226, 1169-1176 (2017).
4. Heat transfer performance and melting dynamic of a phase change material subjected to thermocapillary effects. S. Madruga and C. Mendoza. *International Journal of Heat and Mass Transfer.* 109, 501-510 (2017).
5. Dynamic of plumes and scaling during the melting of a Phase Change Material heated from below. S. Madruga and J. Curbelo. <https://arxiv.org/abs/1711.07744>
6. Melting dynamics of a phase change material (PCM) with dispersed metallic nanoparticles using transport coefficients from empirical and mean field models. S. Madruga and G.S. Mischlich. *Applied Thermal Engineering.* 124, 1123-1133 (2017).

Direct Numerical Simulation of the Navier-Stokes equations

Sebastian Richter and Michael Bestehorn

BTU Cottbus-Senftenberg, Department of Theoretical Physics, Erich-Weinert-
Straße. 2, Cottbus, 03044, Germany
Sebastian.richter@b-tu.de

We investigate the spatiotemporal evolution of a two-dimensional thin liquid film located on a horizontal and completely wettable substrate. The system is subjected to an external time-periodic gravitational field in normal direction or tangential to the surface. Periodic lateral boundary conditions are applied in order to obtain a horizontally homogeneous base flow in the latter case. Based on the nonlinear transformation

$$z = h(x, t) \cdot \tilde{z}$$

of the vertical coordinate, we develop a staggered-grid finite-differences method for the exact problem which avoids surface tracking and reduces the necessary interpolations to a minimum. The pressure field is directly calculated from the mass conservation and the Navier-Stokes equations. Combining both equations, a sparse matrix system for the pressure is received whose solution fulfills momentum and mass conservation. Thus, we refrain from using pressure correction techniques. Vertical excitations lead to the formation of harmonically (driver's frequency) and subharmonically (half of the driver's frequency) oscillating Faraday patterns. Lateral excitations yield coarsening droplets and no rupture (Fig. 1). Our results show good agreement with the lubrication-approximation-based model discussed in [1] and [2].

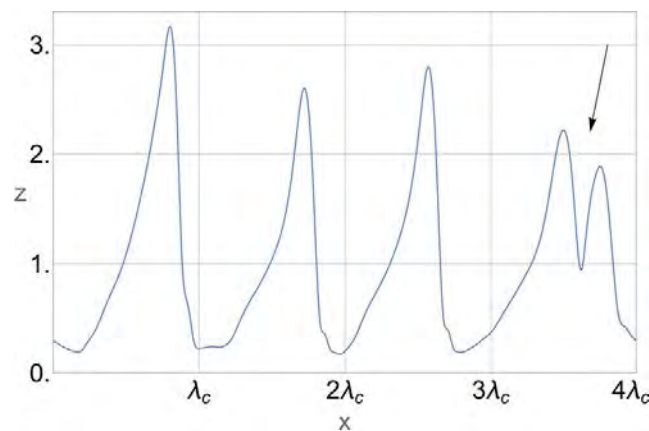


Figure 1: Coarsening of vibration-induced waves on a laterally oscillating thin liquid layer. Arrow: Two droplets just before they merge together.

References

- [1] M. Bestehorn, Laterally extended thin liquid films with inertia under external vibrations, *Phys. Fluids* 25, 114106 (2013).
- [2] S. Richter and M. Bestehorn, Thin-Film Faraday patterns in three dimensions, *Eur. Phys. J. Special Topics* 226, 1253-1261 (2017).

Experimental investigation of thermocapillary deformation of thin liquid films on heated structured substrates

Iman Nejadi, Cihat Ates, Timm Schröder, Peter Stephan and Tatiana Gambaryan-Roisman

Chair of Technical Thermodynamics, Technical University of Darmstadt

Alarich-Weiss-Straße 10, 64287 Darmstadt, Germany

nejati@ttd.tu-darmstadt.de

Thin liquid films are present in numerous technological applications including thermal management of electronic chips, ink-jet printing and separation techniques. The variation of the temperature along the liquid-gas interface leads to variation of surface tension. This mechanism is responsible for the appearance of thermocapillary-induced shear stress and consequently for the motion in fluid layers subjected to temperature gradients (Schatz et al. 1995, Nejadi et al. 2015, 2016). The fluid motion gives rise to film deformation which can lead to spontaneous film rupture and a strong deterioration of heat and mass transfer in the system. Using structured substrates is one of the methods used to influence the thermocapillary convection in thin liquid films (Alexeev et al. 2005, Fath et al. 2015). Theoretical and numerical works predict a strong influence of substrate topography on deformation of liquid-gas interface and film stability (Kabova et al. 2006). However, these predictions have not yet been verified by direct experimental investigations.

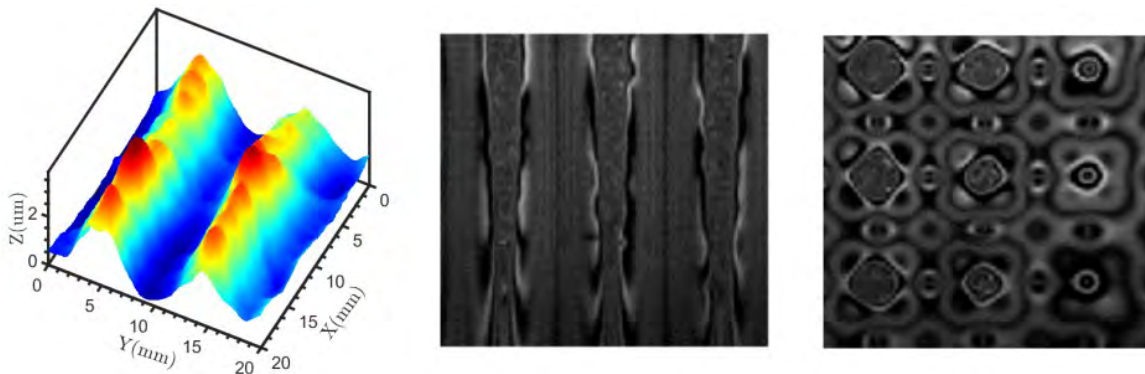


Figure 1: Silicone oil film on structured heated substrates. Left: Liquid/gas interface topography reconstructed using the Phase-Shifting Schlieren method. Schlieren images of film break-up on substrates with single and double sinusoidal topography are shown in the middle and right images, respectively.

Within this context an experimental analysis of thin liquid films on heated structured substrates has been performed. For the experiments, silicone oil is used, whereas two types of substrate with single and double sinusoidal topography are utilized. Temperature of the copper substrates is controlled using an embedded heater on the lower side, while the initial film thickness is measured using a chromatic confocal sensor. During the experiments, the interfacial deformation of the liquid films has been visualized and measured using a Phase-Shifting Schlieren method (see Fig. 1). For the initial thicknesses below $200\mu\text{m}$, the film rupture occurs in the first minutes, while no break-up has been observed for the films thicker than this value. The influence of the substrate topography and temperature as well as the effect of film thickness on the occurrence of film rupture and amplitudes of the interfacial deformations are presented and discussed.

References

- Alexeev, T. Gambaryan-Roisman and P. Stephan, Marangoni convection and heat transfer in thin liquid films on heated walls with topography: Experiments and numerical study, *Phys. Fluids* **17**, 062106-1 – 062106-13 (2005).
- A. Fath, T. Horn, T. Gambaryan-Roisman, P. Stephan and D. Bothe, Numerical and experimental analysis of short-scale Marangoni convection on heated structured surfaces, *Int. J. Heat Mass Trans.* **86**, 764–779 (2015).
- Y. Kabova, A. Alexeev, T. Gambaryan-Roisman and P. Stephan, Marangoni-induced deformation and rupture of a liquid film on a heated microstructured wall, *Phys. Fluids* **18**, 012104-1–012104-15 (2006).
- I. Nejadi, M. Dietzel and S. Hardt, Conjugated liquid layers driven by the short-wavelength Bénard-Marangoni instability: experiment and numerical simulation, *J. Fluid Mech.* **783**, 46–71 (2015).
- I. Nejadi, M. Dietzel and S. Hardt, Exploiting cellular convection in a thick liquid layer to pattern a thin polymer film, *Appl. Phys. Lett.* **108**, 051604 (2016).
- M. F. Schatz, S. J. VanHook, W. D. McCormick, J. B. Swift and H. L. Swinney, Onset of surface-tension-driven Bénard convection. *Phys. Rev. Lett.* **75**, 1938–1941 (1995).

Marangoni-induced isothermal levitation of n-butanol droplet above n-butanol-silicone oil solutions

Natalia Ivanova, Tair Esenbaev and Denis Klyuev

Tyumen State University, Photonics and Microfluidics Laboratory 6 Volodarskogo st., Tyumen, 625003, Russia

n.ivanova@utmn.ru, t.e.esenbaev@utmn.ru, kludis_938@mail.ru

Droplet levitation has been extensively studied in recent years. This phenomenon has a promising prospect to be used for transportation of very small liquid volumes, for example in lab-on-a-chip devices as discussed by Nagy and Neitzel (2008). Literature review on droplet levitation has highlighted several approaches for control of non-coalescence. There are magnetic (Liu et al., 2010) and acoustic (Priego-Capote & de Castro, 2006) levitation methods, that allow studying a droplet in zero-gravity conditions but require a source of strong magnetic field or standing acoustic wave, respectively. Another approach proposed by Bush et al. (2017) is to use gradients in temperature between a droplet and a liquid substrate; however, this leads only to the order of 10^4 ms lifetime of a droplet.

In the present work we observe stable and long ($\sim 10^3$ s) isothermal levitation of n-butanol droplet above a surface of different n-butanol-silicone oil solutions with no external stimuli applied (fig. 1, c). The experiments were performed for different concentrations of n-butanol in the liquid substrate. The evaporation process of n-butanol droplet was studied, and the result was that the droplet evaporates slower with an increase in n-butanol concentration in the liquid substrate (fig. 1, a). However, this tendency appears only for up to 40% concentrations of n-butanol in the liquid substrate and then the trend remains similar for concentrations of 50% and 60% corresponding to the longest droplet lifetimes of up to 1617 s. Further increase in n-butanol concentration lead to fast coalescence of the droplet with the liquid substrate. The conclusion was that as the concentration of nbutanol in the liquid substrate increases, evaporation of the liquid substrate is enhanced, thus, vapors of n-butanol lift and slow down evaporation of the droplet until some equilibrium state is reached when the evaporation rate of droplet does not change.

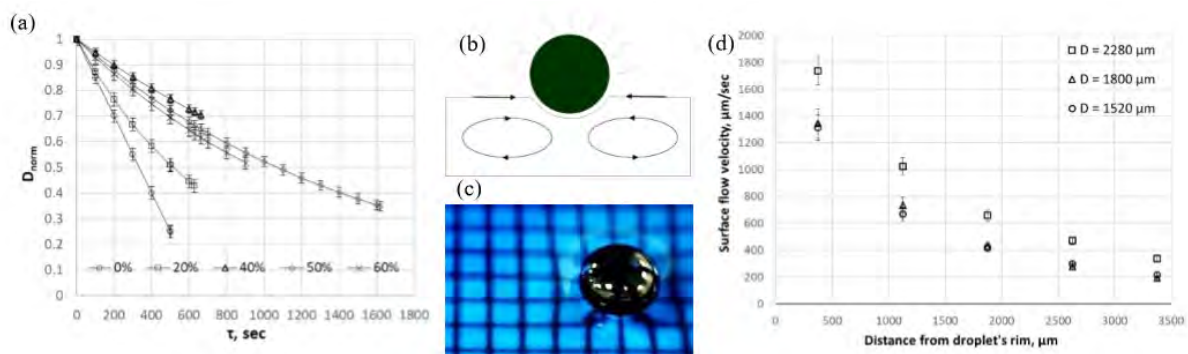


Figure 1: (a) The normalized diameter of the levitating n-butanol droplet vs. time for different concentrations of n-butanol in the liquid substrate; (b) Schematic of the levitating droplet and Marangoni flows; (c) Image of the levitating n-butanol droplet; (d) Surface flow velocity distribution for different droplet diameters.

The evaporation process of the levitating droplet was also studied using IR camera: the difference in temperature between the droplet and the liquid substrate was less than 1°C . Since pure n-butanol and its 30% solution in silicone oil were both at the room temperature initially, this temperature difference clearly arises from the difference in evaporation rate between pure nbutanol and its solution in silicone oil. This negligible difference in temperature shows that the observed levitation is isothermal. Since there is a surface tension gradient between n-butanol and silicone oil, the levitation is induced by Marangoni stresses and maintained by a recirculating air flow between the droplet and the liquid substrate. We also observed using polyethylene particles that Marangoni flow is directed on the liquid surface towards the droplet (fig. 1, b) as shown by Bush et al. (2017). The surface flow velocity was measured, fig.1 (d), in four different circular regions around the droplet. Figure 1(d) shows that as the droplet evaporates (and its diameter reduces), the surface flow velocity decreases. The measurements of the surface tension for n-butanol-silicone oil solutions showed that there is a sharp increase for concentrations above 70% of n-butanol. This reduces Marangoni stresses and, thus, might lead to coalescence as was observed.

References

- Geri, M., Keshavarz, B., McKinley, G. H., Bush, J. W. M., (2017). Thermal delay of drop coalescence. *Journal of Fluid Mechanics*, 833, 1–12. Liu, Y., Zhu, D. M., Strayer, D. M., Israelsson, U. E. (2010). Magnetic levitation of large water droplets and mice. *Adv. Space Res.*, 45(1), 208–213. Nagy, P.T., Neitzel, G.P., (2008). Optical levitation and transport of microdroplets: Proof of concept. *Physics of Fluids*, 20(10), 1–5. Priego-Capote, F., de Castro, L. (2006). Ultrasound-assisted levitation: Labon-a-drop. *Trends in Analytical Chemistry*, 25(9), 856–867.

Thermocapillary Convection in High-Prandtl-Number Liquid Bridges with Free Surface Cooling/Heating by Ambient Gas Flow

Taishi Yano, Makoto Hirotsu and Koichi Nishino

Yokohama National University, Department of Mechanical Engineering

79-5 Tokiwadai, Hodogaya-ku, Yokohama, 240-8501, Japan

yano-taishi-gh@ynu.ac.jp

Thermocapillary flow is caused by the temperature gradient along the liquid-gas interface as well as the resultant surface tension difference, and therefore the thermal boundary condition at the liquid-gas interface is an important subject for understanding of this phenomenon. The attention of the present study is focused on the relation between the interfacial heat transfer and the thermocapillary convection in liquid bridges of high-Prandtl-number fluids, say $Pr = 12.6-42.8$. The liquid bridge of 2 cSt silicone oil is suspended between the parallel disks separated by a gap $H = 1.5-2.5$ mm, where the diameter of the disks is $D = 5.0$ mm and the resultant aspect ratio is $AR (= H/D) = 0.30-0.50$. Since the upper disk temperature is always higher than the lower one, the upper and lower disks are hereafter referred to as the heated and cooled disks, respectively. The temperature difference between those disks $\Delta T = T_H - T_C$ drives the flow along the liquid bridge surface, and the pressure gradient imposed by this surface flow drives the return flow, consequently forming toroidal thermocapillary convection. The axisymmetry of the thermocapillary convection in high- Pr liquid bridges is retained for small ΔT while it is broken for large ΔT due to the hydrothermal wave instability. The ΔT at the instability threshold is called the critical temperature difference ΔT_c . The thermocapillary convection instability is sensitive to the experimental conditions, especially several researchers reported the important role of the heat transfer at the liquid bridge free surface (e.g., Kamotani et al. 2003, Shevtsova et al. 2005).

In this study, the data for instability were collected experimentally with various temperature conditions. Figure 1 (left) shows the plot of ΔT_c as a function of the temperature difference between the cooled disk and the ambient gas ($T_C - T_a$) for $AR = 0.50$. We note that the heat loss from the liquid bridge free surface increases with increasing $(T_C - T_a)$ and vice versa, where the interfacial heat transfer is mainly undertaken by the natural convection in the ambient gas. The results indicate that the interfacial heat transfer strongly affects the thermocapillary convection instability, and that the instability curves can be categorized into three groups by the combinations of T_H , T_C , and T_a : (I) $T_a > T_H > T_C$, (II) $T_H > T_a > T_C$, and (III) $T_H > T_C > T_a$. Figure 1 (right) shows the streamlines and the temperature contours in the steady thermocapillary convection for Condition (I), (II), and (III), which are obtained from the numerical simulation. A single roll can be recognized near the liquid bridge surface for Condition (I). The center of this roll moves toward the hot corner, and the roll is separated to two rolls for Condition (III). The heat transfer ratio Q_{LB}/Q_{HD} is evaluated to discuss the effect of interfacial heat transfer, where Q_{LB} and Q_{HD} are the heat transfer rates at the liquid bridge surface and at the heated disk surface, respectively. It is found that the instability data and the basic flow and temperature patterns in the present study are correlated well with Q_{LB}/Q_{HD} .

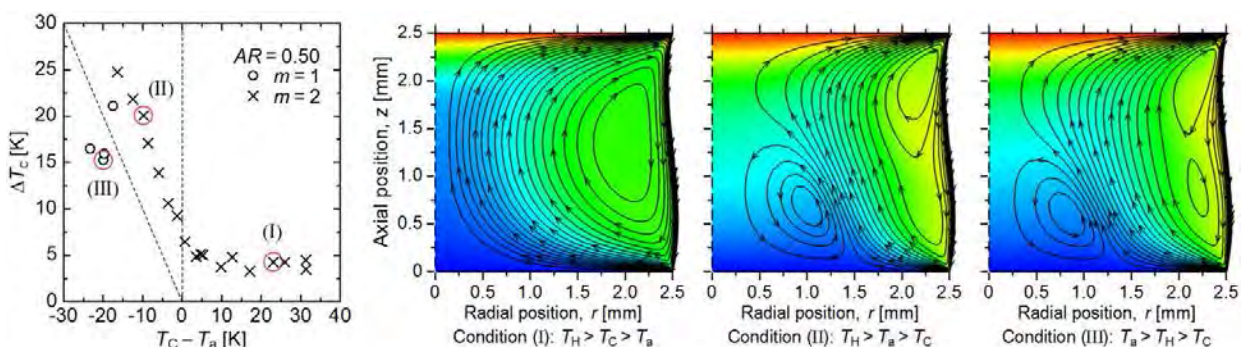


Figure 1: Left: Plot of critical temperature difference ΔT_c as a function of temperature difference between the cooled disk and the ambient gas ($T_C - T_a$). Right: Streamlines and temperature contours inside the liquid bridges with different temperature boundary conditions: (I) $T_H > T_C > T_a$, (II) $T_H > T_a > T_C$, and (III) $T_a > T_H > T_C$.

References

- Kamotani, Y., Wang, L., Hatta, S., Wang, A., Yoda, S.: Free surface heat loss effect on oscillatory thermocapillary flow in liquid bridges of high Prandtl number fluids. *Int. J. Heat Mass Transf.* 46(17), 3211-3220 (2003)
- Shevtsova, V. M., Mialdun, A., Mojahed, M.: A study of heat transfer in liquid bridges near onset of instability. *J. Non-Equilib. Thermodyn.* 30(3), 261-281 (2005)

Rayleigh-Benard-Marangoni instability in a system of two superposed horizontal layers of immiscible fluids with deformable interface

Tatyana Lyubimova^{1,2}, Yanina Parshakova¹

¹ Institute of Continuous Media Mechanics UB RAS, Koroleva Str 1., 614013 Perm, Russia, lyubimova@psu.ru

² Perm State University, Bukireva Str. 15, 614990 Perm, Russia

It is known that the consideration of interface deformations in the framework of conventional Boussinesq approximation can lead to physically incorrect results. At the same time, in many situations, the approximation of non-deformable interface is not sufficient. For example, if difference in densities is of the same order of magnitude as density heterogeneities caused by nonisothermality, then the gravity is not able to keep the interface flat at finite Grashof numbers. In this case the interface deformations can be considerable and should be taken into account. The generalized Boussinesq approximation allowing correct accounting for the interface deformations in such situations was formulated in [1]. In the present paper, within the framework of this approximation, we study the onset of the Rayleigh-Benard-Marangoni instability in a system of two superposed horizontal layers of immiscible fluids of close densities. External boundaries of the system are assumed to be rigid and perfectly conductive, the thicknesses of layers equal to each other. The system is subject to homogeneous vertical temperature gradient. This problem was studied earlier in [1] neglecting thermocapillary effect; new deformational long-wave instability mode was found. Investigation of the contribution of thermocapillary effect is carried out in the present work. Longwave instability is studied analytically by means of series expansion with respect to the wave number. It is shown that thermocapillary effect leads to the lowering of the longwave instability threshold, besides, with the increase of Marangoni number the instability boundary $Ra(Ga)$ is shifted as a whole to the range of negative values of the Galileo number. The instability of the conductive state to finite-wavelength perturbations is studied numerically by differential sweep method. The calculations are performed for the case of formic acid - transformer oil system. It is found that in the presence of thermocapillary effect the oscillatory instability mode disappears. The threshold of convection decreases with the increase of Marangoni number besides the most dangerous perturbations are the longwave monotonic perturbations.

We also investigated the effect of high frequency vertical vibrations on the Rayleigh-Benard-Marangoni instability. It is found that the longwave instability of the conductive state is not affected by such vibrations. The calculations carried out for finite wave numbers have shown that in the absence of thermocapillary effect (Fig.1a), vibrations make stabilizing effect on monotonic finite-wavelength perturbations. At some value of the vibrational Rayleigh number Ra_v , these perturbations become less dangerous than the longwave ones. With further growth of Ra_v finite-wavelength monotonic instability mode disappears. In the presence of thermocapillary effect (Figs.1b, 1c), vibrations make destabilizing effect on finite-wavelength monotonic perturbations and these perturbations become more dangerous than the longwave ones. With respect to oscillatory finite-wavelength instability, vibrations play stabilizing role.

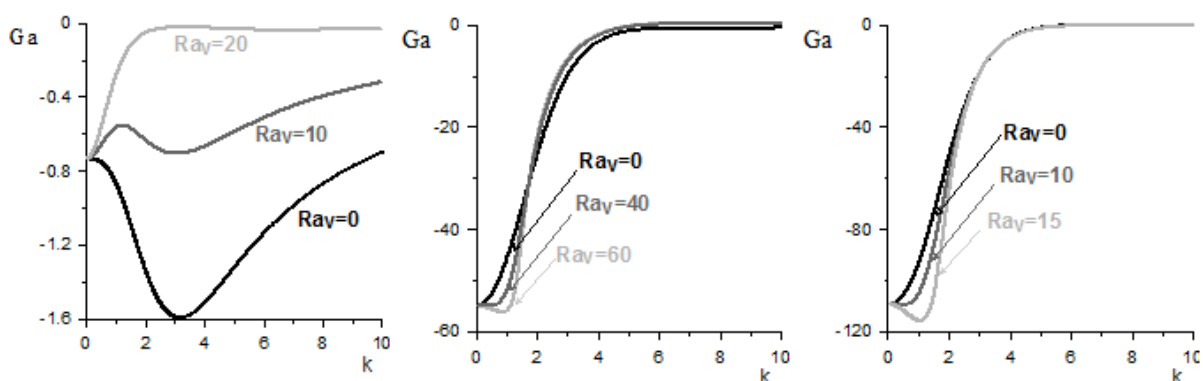


Figure 1: Neutral curves for $Ra=50$: left - $Ma=0$, middle - $Ma=-50$, right - $Ma=-100$. Instability domains are above the curves.

The work was supported by Russian Science Foundation (grant No. 14-21-00090).

References

1. Lobov N.I., Lyubimov D.V., Lyubimova T.P. Convective instability of a system of horizontal layers of immiscible liquids with a deformable interface. Fluid Dynamics. 31 (2), 86-192 (1996).

Rayleigh-Taylor and Kelvin-Helmholtz Instabilities of a Miscible Interfaces

Tatyana Lyubimova^{1,2}, Anatoly Vorobev³, Sergei Prokopev¹ and Andrey Ivantsov¹

¹Institute of Continuous Media Mechanics UB RAS, Koroleva Str. 1, 614013 Perm, Russia,

²Perm State University, Bukireva Str. 15, 614990 Perm, Russia

³University of Southampton, SO17 1BJ, UK

lyubimova@psu.ru

We study the diffusive and convective evolution of a binary mixture of two slowly miscible liquids on the basis of the phase-field approach. We assume that at the initial time moment two miscible liquids are brought into contact, which makes the system thermodynamically unstable. Additionally, for the Rayleigh-Taylor instability, we assume that the heavier liquid is placed on top of the lighter one that makes the system also gravitationally unstable. For the Kelvin-Helmholtz instability, we consider the configuration with the heavier liquid placed underneath, but with the external hydrodynamic flow imposed along the interface.

Our numerical results demonstrate that the classical growth rates for these two instabilities may be retrieved in the limit of the higher Peclet numbers (weaker diffusion) and thinner interfaces. On the longer time scale we also observe the approach of the system to the state of thermodynamic equilibrium. In addition, we found two novel effects. First, it is commonly accepted that the interface between the miscible liquids slowly smears in time due to diffusion. We however found when the binary system is subject to hydrodynamic transformations the interface boundary stretches so its thickness changes (the interface becomes thinner) on a much faster convective time scale. The thickness of the interface is inversely proportional to the surface tension, and the stronger surface tension limits the development of the Rayleigh-Taylor instability. Second, it is commonly accepted that convective flows enhance the mixing of the liquids by transporting the fresher material to the interface. We however found that the mixing is enhanced because the convective flows penetrate through the miscible boundaries, simultaneously re-arranging the liquid phases and transporting the molecules across the interfaces.

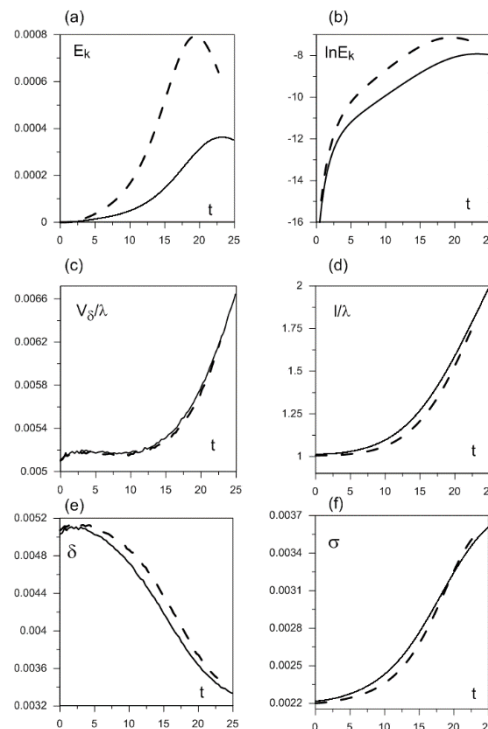


Figure 1: Rayleigh-Taylor instability. (a,b) The total kinetic energy, (c) the volume of the transition zone between the phases (interface), (d) the length of the interface, (e) the thickness of the interface, and (f) the surface tension coefficient vs. time for two different wavenumbers 4.83 (solid line), and 3.39 (dashed line).

The work was supported by Russian Science Foundation (grant No. 14-21-00090).

The effect of axial vibrations of finite frequency and amplitude on thermocapillary flow in a liquid zone

Tatyana Lyubimova^{1,2}, Yanina Parshakova¹, Robert Skuridyn¹

¹ Institute of Continuous Media Mechanics UB RAS, Koroleva Str 1., 614013 Perm, Russia, lyubimova@psu.ru

² Perm State University, Bukireva Str. 15, 614990 Perm, Russia

Meniscus deformations and flows in a liquid zone subjected to axial vibrations of finite frequency and amplitude in zero gravity conditions are studied numerically. The case where both rods perform synchronous vibrations with the same phase is considered. The calculations are performed in the framework of full (non-average) axisymmetric approach. The values of the fluid properties and geometrical parameters correspond to the silicon growth by floating zone technique. Numerical data on the instantaneous and average velocity fields and instantaneous and average meniscus deformations are obtained for different vibration amplitudes and frequencies (average fields were obtained by averaging of instantaneous fields over vibration period). The calculations performed in the absence of heating have shown that in this case vibrations generate the average flow near rigid rods in the form of two toroidal vortices with the direction of the fluid motion near the rods from the free surface to the zone axis (Schlichting mechanism of average flow generation). Additionally, vibrations induce the waves on the free surface. These waves propagate from oscillating rods to the zone center and also induce the average flow. The direction of the surface-wave-induced average flow is such that the fluid moves near free surface from oscillating rods to the zone center. With the increase of vibration frequency the contribution of the Schlichting mechanism of average flow generation decreases and that of the surface-wave mechanism grows. During crystal growth by floating zone method with the ring heater located at the zone center, there arises the thermocapillary flow in the form of two toroidal vortices with the flow direction near free surface from the heated center to the cold rods. Thus, the direction of average flow induced by surface-wave mechanism is opposite to that of thermocapillary flow. This makes promising the use of axial vibrations for the improvement of crystal quality by the suppression of thermocapillary flow. Numerical modeling of flows in a liquid zone heated with the help of ring heater located in the central part of the zone/ confirms this prediction. Indeed, in the presence of vibrations substantial decrease of the resulting flow intensity is observed (Figure 1).

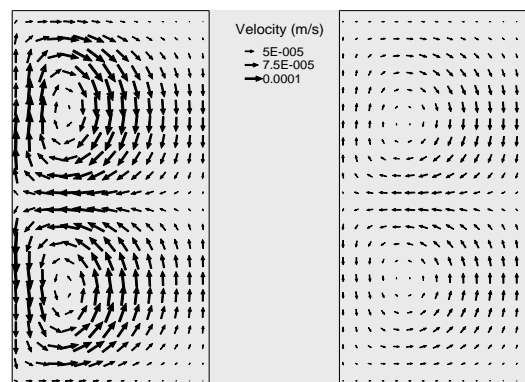


Figure 1: Average flows in a heated liquid zone in the absence of vibrations (left) and in the presence of vibrations with frequency 10 Hz and amplitude 0.15 mm.

The work was supported by Russian Foundation for Basic Research (grant No. 15-01-09069).

Thermocapillary dipole in a Hele-Shaw cell

Valeri Frumkin and Moran Bercovici

Department of Mechanical Engineering,

Technion – Israel Institute of Technology, Haifa, 32000, Israel

valeri@technion.ac.il, mberco@technion.ac.il

We present a theoretical and experimental study of thermocapillary flow in a Hele-Shaw cell containing a circular opening in the upper surface, and subjected to a linear temperature gradient. Under the assumption of shallowness (i.e. the depth of the reservoir is much smaller than its radius) we obtain a solution corresponding to a doublet flow (dipole) in the Hele-Shaw cell, providing good qualitative agreement with experimental results. We demonstrate how a superposition of dipoles can be applied for two-dimensional flow patterning, and how a confined dipole can act as a thermocapillary motor for driving liquids in microfluidic circuits. In addition, we show how the principles behind the thermocapillary dipole can be applied in order to drive thermocapillary surface swimmers on fluid-liquid interfaces.

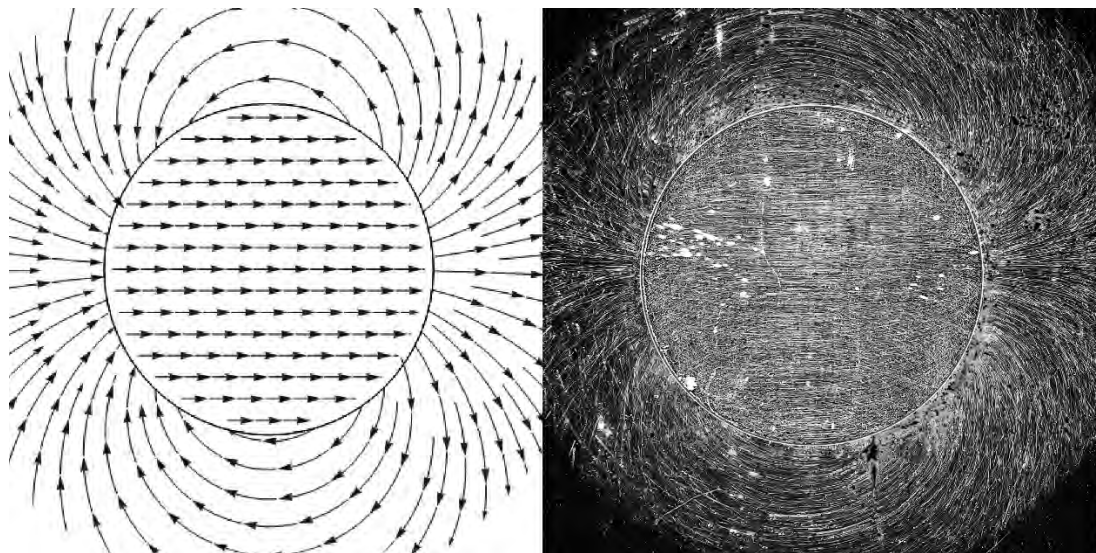


Figure 1: Left: Theoretically predicted streamlines for a thermocapillary dipole in a Hele-Shaw cell. Right: An experimental measurement of a doublet flow obtained by stacking multiple images taken with one second interval between each two images. The diameter of the circular reservoir is 5 mm, the depth is 0.5 mm, and the temperature difference between the hot and the cold sides of the reservoir is 0.5 degrees Celsius.

Formation of frozen waves on miscible interface

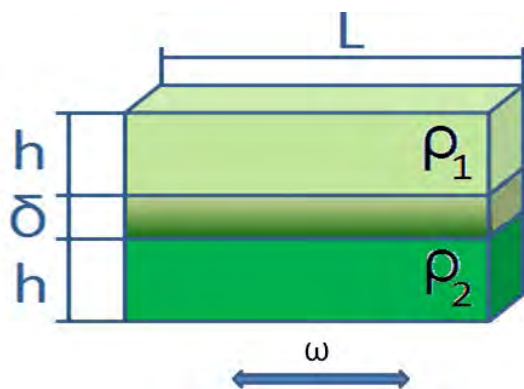
Valentina Shevtsova, Aliaksandr Mialdun and Yuri Gaponenko

Microgravity Research Center, Université Libre de Bruxelles,

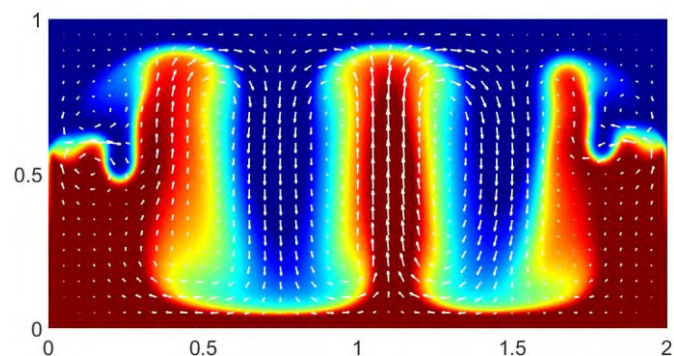
CP-165/62, Av. F.D.Roosevelt, 50, B-1050

ygonenko@ulb.ac.be, vshev@ulb.ac.be

The application of periodic vibrations to a fluid system with a density gradient can lead to a wide variety of patterns. Vibrations applied to a cell with two superimposed liquids in the direction parallel to the interface generate a horizontal pressure gradient that induces oscillatory shear flows. Here we narrow our focus to an isothermal case and two-fluid system without surface tension, in particular, miscible liquids. Instability in miscible systems caused by horizontal vibrations is noticeably different from immiscible ones because of its transient nature. In a miscible system once the mean flow sets in, the gradients begin to weaken as a result of convective mixing. In other words the miscible layer problem is necessarily transient and can never attain a periodic steady state unlike its immiscible counterpart. During laboratory and microgravity experiments it was noted that the onset of instability and the interfacial pattern depend on the width of the diffusive interface (Gaponenko et al., 2015, Shevtsova et al., 2015), i.e., on the steepness of the density gradient. A lack of clear and detailed knowledge of this phenomenon has motivated the current investigation.



a) Geometry of the numerical problem



b) Example of computed concentration field with superimposed velocity vectors of the mean flow.

Figure 1: Results of calculations which will be compared with the experimental observations in course of presentation

This study includes parabolic flight experiments in two-layer miscible liquids and extensive non-linear numerical simulations, which are aimed at the understanding of the experimental findings. We consider two layers of binary mixtures of the same constituents (water—*isopropanol*) mixtures of different percentage. The cell was fixed to a linear motor, which performs translational oscillations in the horizontal direction. In the parabolic flight experiments the cell was refilled after several parabolas. Consequently, for a series of experiments, the interface became wider with each subsequent parabola, and the initial distribution of density (concentration) tended to be linear after several parabolas. Numerical simulations were performed in the system mimicking the experimental geometry which is shown in Fig. 1a. The key parameters varied in this study include vibrational velocity, which is the product of amplitude and frequency, and width of the interface between two miscible liquids. The typical pattern in terms of concentration field is shown in Fig. 1b by colors and the velocity vectors are superimposed to highlight the mean flow structure. This figure corresponds to the case when the width of the interface corresponds half of the cell height. For the thinner interface the column structure is sharpened and, for the thicker interface, the decay of columns obser

References

- Y. Gaponenko, M. Torregrosa, V. Yasnou, A. Mialdun and V. Shevtsova, Interfacial pattern selection in miscible liquids under vibration, *Soft Matter* **11**, 8221 (2015)
- V. Shevtsova, Y. A. Gaponenko, V. Yasnou, A. Mialdun and A. Nepomnyashchy, Two-scale wave patterns on a periodically excited miscible liquid-liquid interface, *J. Fluid Mech.* **784**, 342-372 (2015).

Influence of internal energy of the interface on a stationary flow and its stability

Victor Andreev and Victoria Bekezhanova

Institute of Computational Modelling SB RAS, Department of Differential Equations Mechanics,
 Akademgorodok 50/44, Krasnoyarsk, 660036, Russia

andr@icm.krasn.ru

vbek@icm.krasn.ru

Flows of non-isothermal fluids with the interface Γ are investigated. Under study we take into account, that in general case a non-zero difference of heat fluxes at the interface arises (Andreev et al. 2000):

$$k_2 \frac{\partial \theta_2}{\partial n} - k_1 \frac{\partial \theta_1}{\partial n} = \sigma_T \theta \nabla_\Gamma \cdot \mathbf{u}. \quad (1)$$

Here k_j is the heat conductivity coefficient of j -th fluid, θ_j is the temperature of j -th fluid, θ is the common value of temperatures on the interface, ∇_Γ is the vector differential operator $\nabla_\Gamma = \nabla - \mathbf{n}(\mathbf{n} \cdot \nabla)$ which denotes the surface gradient, \mathbf{u} is the value of the velocity vector of both media at Γ . Relation (1) is valid, if the surface tension is the linear function of temperature θ along Γ : $\sigma(\theta) = \sigma_0 - \sigma_T(\theta - \theta_0)$ with constant σ_0, σ_T . There is parameter $E = \sigma_T \theta / \mu_2 k_2$ that defines a contribution of the heat defect (see the right-hand side of (1)) to the development of convective flow near the interface. For usual liquid E is quite small and variations of the convection velocity due to changes of the interface energy are insignificant. But for cryogenic and low-viscosity liquids the right-hand term in (1) should be taken into account, since $E = O(1)$.

In the present report a two-layer stationary thermocapillary flow with horizontal interface Γ in a plane channel is considered. Relation (1) is used as the energy condition together with other boundary conditions at the interface. Velocity fields in the layers are similar to the Hiemenz's one. Temperature at some point on the channel walls has an extreme value. It is proved, that linear problem (with the linear equations of energy and motion) with condition (1) can have two or one solution, or any solution does not exist. These three case are realized depending on values of temperature on the channel walls, thermophysical parameters of the fluids and thicknesses of the layers. The fact is directly related to the nonlinearity of full energy condition (1) at the interface. If the heat defect is equal to zero, then there is only stationary regime regardless of input data of the problem.

Stability of the stationary two-dimensional solution is investigated. The solution describes the joint flow of liquid and gas in a minichannel. Local heat load is applied on the bottom wall, and the upper boundary is the thermally insulated wall. Influence of the internal energy variations of the interface on character of its deformations and on the perturbation structure is studied. Appearing deformations are generated by presence of the local heat source, which provides formation of a horizontal temperature gradient at Γ and liquid thermocapillary spreading along the interface. Amplitude of the deformations grows with decreasing of the liquid layer thickness. Taking into account of the internal energy variations of the interface leads to the substantial alteration of the hydrodynamic perturbation pattern. Arising vortexes are the typical thermocapillary structures. Upon that, zones with the maximal temperature are formed where liquid thickness is minimal. Thinning of the liquid layer leads to larger deformation of the vortex structures, complication of the vortex form and intensification of the thermocapillary motion. Thus, variations of internal energy of the interface have destabilizing effect.

The work was supported by the Russian Foundation of Basic Research (project 17-01-00229).

References

Andreev, V.K., Zakhvataev, V.E., Ryabitskii, E.A. (2000) Thermocapillary instability. Moscow, Nauka, 2000. 280 p.



Thermocapillary convection in a liquid layer induced by local heating

Victoria Bekezhanova and Alla Ovcharova

Institute of Computational Modelling SB RAS, Department of Differential Equations Mechanics,
 Akademgorodok 50/44, Krasnoyarsk, 660036, Russia, vbek@icm.krasn.ru
 Lavrentyev Institute of Hydrodynamics SB RAS, Laboratory of Applied and Computational Hydrodynamics,
 Ac. Lavrentieva ave 15, Novosibirsk, 630090, Russia, ovcharova@hydro.nsc.ru

Study of thermal convection patterns in liquid layered systems is of interest both in terms of their possible applications in different technologies and as fundamental scientific problem. One of the effective ways to modify/improve fluidic technology, using multilayer liquid media with the interfaces, is preliminary analysis of features and regimes of the thermocapillary convection with the help of mathematical modeling methods. Estimates and characteristics of the basic parameters of the system (distributions of velocity and temperature, position of the interface and etc.), obtained on the theoretical stage, allows one to develop of the thermocapillary convection intensification methods or vice versa to define conditions of convection suppression by means of selection of system geometry, thermophysical parameters of the working media and relation of control actions (thermal load, liquid flow rate and etc.). Two-phase liquid-gas system in a horizontal channel is considered. The quiescent viscous heat-conducting fluids are in the gravity field and contact along the thermocapillary interface. A local thermal load is applied on one of the external immovable solid boundaries of the channel. Features of the thermocapillary motion induced by action of the point heat sources in the two-layer system are studied in the framework of the Oberbeck-Boussinesq model of convection. Structure of the temperature (Fig.1(a), (c)) and velocity (Fig.1(b), (d)) fields is calculated with the help of the original numerical method (Ovcharova 2017). Significant differences in thermophysical properties of the working media make additional difficulties.

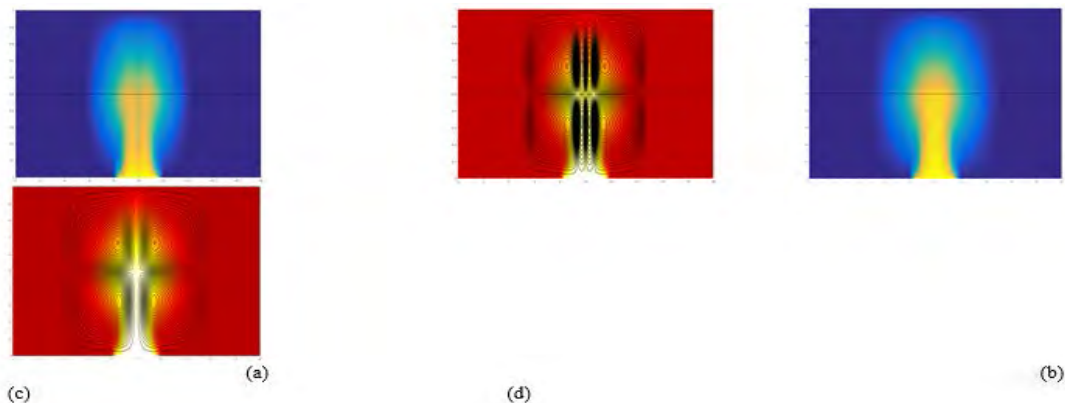


Figure 1: Dynamics of the thermal (a, c) and convective (b, d) patterns with time in the two-phase system “ethanol - nitrogen” with one local thermal source on the bottom wall.

Character of the interface deformations is investigated depending on the number of the heat sources and their sizes. Form of deformations is analyzed for the case thermal loads located on the upper wall or on the lower boundary. Local heat action leads to thermocapillary spreading of the liquid and to appearance of the typical convective patterns. Influence of the gravitational and thermocapillary effects is described.

Location and scale of the structures depend on localization of the heat sources and their sizes entirely. Evolution of arising perturbations is analyzed. With time the decay of four-vortex patterns (Fig.1(b)) occurs and transition to symmetrical double-vortex (Fig.1(d)) structures is observed in both layers. Oscillations of the interface damp and steady shape of the interface deformation is established.

The work of first author was supported by the Russian Foundation of Basic Research (project 17-08-0029117).

References

Ovcharova, A.S. (2017) Multilayer system of films heated from above. *Int. J. Heat Mass Transf.*, V. 78, P. 992–1000.

Critical characteristics of the two-layer convective flows with evaporation in a 3D channel

Victoria Bekezhanova¹ and Olga Goncharova^{2,3}

¹Institute of Computational Modeling SB RAS, Department of Differential Equations of Mechanics,
Academgorodok, 50/44, 660036, Krasnoyarsk, Russia,

²Institute of Thermophysics SB RAS,

Ac. Lavrentyev ave., 1, 630090, Novosibirsk, Russia

³Altai State University, Department of Differential Equations,

Lenin ave., 61, 656049, Barnaul, Russia,

bekezhanova@mail.ru, gon@math.asu.ru

In present work the character and structure of the joint flows of evaporating liquid and co-current laminar gas flux are investigated on the basis of a solution of special type of the Boussinesq approximation of the Navier – Stokes equations. The effects of thermodiffusion and diffusive thermal conductivity in the gas – vapor phase are taken into consideration. The constructed solution satisfies all the governing equations, interface and boundary conditions, and has the group nature (Bekezhanova and Goncharova 2017). This property is especially important because the invariant and partially invariant solutions imply the natural properties of space-time symmetry and symmetry of spatial fluid motion. Exact (invariant) solutions ensure physical plausibility of results obtained in studies of the fundamental and secondary features of physical processes, which are described by the convection equations.

Modeling of the 3D fluid flows in an infinite channel of a rectangular cross section is performed. The solution under consideration allows one to describe a formation of the thermocapillary rolls and multi-vortex structures in the layers. Influence of gravity and evaporation on the dynamic and thermal phenomena in the fluids is studied. Numerical investigations are performed for the liquid-gas system like ethanol – nitrogen, HFE-7100 – nitrogen, FC-72 – nitrogen under conditions of normal and low gravity. The fluid flow patterns are determined by various thermal, mechanical and structural effects. Alteration of topology and character of the flows takes place with change of intensity of the applied thermal loads, thermophysical properties of working media and gravity action (see figure 1 for comparison of the flow patterns under low gravity for different values of the longitudinal temperature gradient A created along the thermocapillary interface).

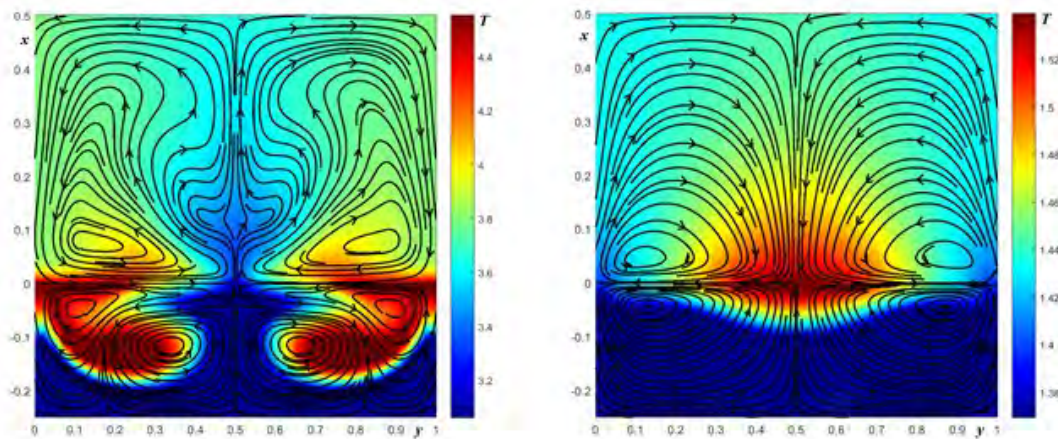


Figure 1: Temperature distribution and stream line projections in a channel cross – section in the ethanol – nitrogen system at $g = 10^{-2} g_0$ m/s²; $A=300$ K/m (left), $A=100$ K/m (right).

The critical flow characteristics, the qualitative and quantitative differences in the flow topology of various working systems, comparison of the theoretical and experimental results are presented. The investigations allowed one to develop a hierarchy of the flow regimes, to analyze the evaporation effect on the flow structures and to define possibilities to control convective flows with phase transition.

References

Bekezhanova V.B. and Goncharova O.N. (2017) Three-dimensional thermocapillary flow regimes with evaporation. J. of Phys.: Conf. Series, V. 894, P. 012023.

Measurement of the thermocapillary deformations of liquid layers using the laser-scanning method

Viktor M. Fliagin, Natalia A. Ivanova, Vasily V. Vostrikov

Tyumen State University, Photonics and Microfluidics Laboratory Volodarskogo, 6, Tyumen, 625003, Russia v.m.flyagin@utmn.ru

The shape of surface deformation of thin liquid layers, induced by Marangoni convection, is the key parameter that determines the thermocapillary signal used for qualitative analysis of properties of liquids and solid samples (Zykov and Ivanova, 2017; Bezuglyi and Flyagin, 2007). Here we present a modified laser-sheet method for direct measurement of the local thickness change of the liquid layer locally disturbed by thermal Marangoni convection, fig.1. Beam of a laser diode (1) is focused with a spherical lens (2) on the liquid layer surface (3) in an absorbing laser irradiation cuvette (4), and then is transformed into three flat laser beams with a cylindrical lens (5) and a diaphragm (6). The central beam is projected onto the deformed surface, while the side beams - on undisturbed flat surface. These beams, reflected from the liquid surface, are projected onto a screen (7) on which their images are recorded with CCD camera (8). The surface slope is calculated using a displacement of the central beam relative to the side beams on obtained image. Marangoni convection in the liquid layer is induced by a laser diode (9).

The dependence of the surface slope $\text{tg}(\alpha)$ versus a horizontal coordinate x , fig. 2(a), can be obtained by a linear shifting of the optical scheme. Then, applying the cubic spline interpolation for the calculated surface slopes, and integrating the polynomials, we obtain the piecewise-defined function of surface profile. Silicone oil (5 cSt) was deposited in the ebonite cuvette. The thickness of the liquid layer was varied in the range 320 ... 1730 μm . The power of inducing laser was 15.3 mW, and the laser beam diameter was about 3 mm. The surface profiles of the layers are shown in fig. 2(b). At the thickness of the layer of 320 μm the thermocapillary rupture of the layer takes place. Due to the very large value of the slope, it was not possible to obtain the entire surface profile; however, knowing the diameter of the dry spot allows us to get an approximate profile (shown by dashed line) of the surface in the rupture region. The maximal depth of the thermocapillary dimple increases with the decrease in the layer thickness as $\Delta h = h^{-2.3}$, fig. 2 (c).

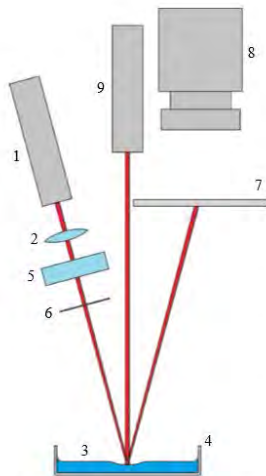


Figure 1: Experiment schematic.

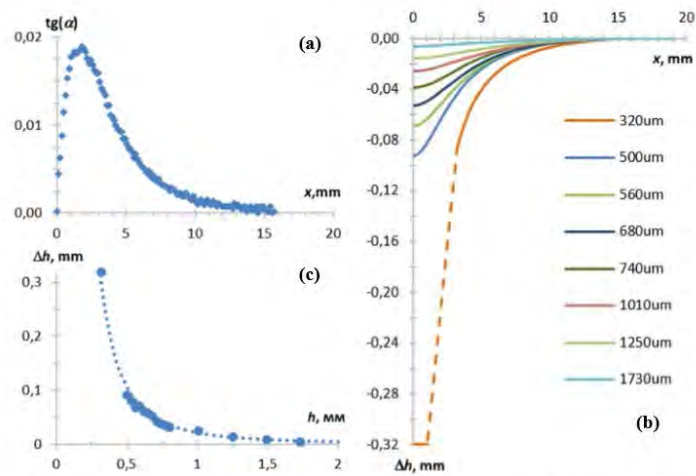


Figure 2: Surface slope (a), profiles (b), and dimple depth vs layer thickness (c).

References

- Zykov A.Yu., Ivanova N.A. Laser-induced thermocapillary convection in thin liquid layers: effect of thermal conductivity of substrate. *Appl. Phys. B.*, 123, 235 (2017).
- Bezuglyi B.A., Flyagin V.M. Thermocapillary convection in a liquid layer with a quasi-point heat source in the substrate. *Fluid Dyn.*, 42, 978-986 (2007).

Numerical Study of the Diffusion of Two Gases Equally Diluted by Third Component

Vladimir Kossov¹, Olga Fedorenko², Dauren Zhakebayev³ and Asylzhan Kizbaev³

¹Abai Kazakh National Pedagogical University, Dostyk Ave.13, 050010 Almaty, Republic of Kazakhstan. kosov_vlad_nik@list.ru

²Institute of Experimental and Theoretical Physics, Al-Farabi Kazakh National University, al-Farabi Ave. 71, 050040 Almaty, Republic of Kazakhstan. fedor23.04@mail.ru

³Al-Farabi Kazakh National University, al-Farabi Ave. 71, 050040 Almaty, Republic of Kazakhstan. dauren.zhakebayev@gmail.com

A special case that is often considered when solving practical problems in multicomponent mass transfer is the diffusion of two or more gases through a layer of diluent gas (ballast gas). A very interesting problem is the case when different diluent gases with different properties are used in the diffusion process, which, apparently, makes it possible to control the nature of the flow of mass-exchange processes, for example, in chemical reactions. If ballast gas is used as an indicator, then it is possible to estimate the actual molecular transfer of components and describe the features of multicomponent diffusion (Duncan et al. 1962, Dil'man et al. 2010, Toor 1957).

Diffusion studies in multicomponent gas mixtures with ballast gas have shown that the role of hydrodynamic transport is great (Kosov et al. 1981). Therefore, to evaluate its effect on the diffusion of two main components is undoubtedly important.

If two main gases are diluted equally by different ballast gases, then the diffusion coefficients of the main gases will depend on which diluent gas (light or heavy) is in the mixture. By appropriately selecting the diluent gas, one can either accelerate or slow down the diffusion mass transfer of the main components.

A numerical study of the instability of mechanical equilibrium in systems with ballast gas can be carried out on basis of the approach described in (Kosov et al. 2017). However, the possibilities of this method are limited. In the study of nonstationary processes, the proposed approach does not allow to determine accurately the critical conditions for the "diffusion-convection" transition. It is also difficult to describe the dynamics of convective currents on basis of the stability theory and to estimate the kinetics of multicomponent mass transfer under conditions of developed instability. Such questions can be solved with the help of numerical methods of mathematical modeling.

The macroscopic motion of an isothermal three-component gas mixture is described by the general system of equations involving the Navier-Stokes equations, conservation equations of the particle number of mixture and components in the Boussinesq approximation. For the numerical solution of this equations system is used the splitting scheme on physical parameters. The spatial derivatives are approximated on the uniform spatial grid. The time derivatives are approximated by differences ahead with the first order. On the first stage, the transference of the number of motion is done due to the convection and diffusion. The intermediate velocity field is solved by the five-point sweep method specified by Navon (1987) with the fourth order of accuracy in space and the third order of accuracy with respect to time using the explicit scheme of Adams-Bachfort for convective terms and implicit scheme of Crank-Nicolson for the diffusion members defined by Kim and Moin (1985). On the second stage, based on the found intermediate velocity field, there is the pressure field. Intermediate velocity field is at the use of fractional step method. By analogy with Abdibekova et al. (2014) we have used the sweep method at each stage of sweep fractional step method to find the stage significance of intermediate field speed. On the third stage, it is assumed that transference is done only due to pressure gradient, where the final velocity field is recalculated. On the fourth stage the concentration of components mixture are calculated on basis of five-point sweep method using the Adam-Bachfort scheme taking into account the found velocity fields. The calculations were carried out on a uniform rectangular staggered grid. The calculations are done for actual physical parameters of geometrical characteristics of the channel. The main assumption in modeling is the two-dimensional flows limitation.

The results of numerical experiment have shown that by appropriately selecting the diluent gas, one can either intensify or slow down, or leave without change the process of transfer of those gases that diffuse in its medium.

The work was supported by the Science Committee of the Ministry of Education and Science of the Republic of Kazakhstan (project no. AP05130712).

References

- A.U. Abdibekova, D.B. Zhakebayev, B.T. Zhumagulov, *Magnetohydrodynamics*, **50**, 121 (2014)
- J.B. Duncan, H.L. Toor, *A. I. Ch. E. Journal* **8**, 38 (1962)
- V.V. Dil'man, O.A. Kashirskaya, V.A. Lotkhov, *Theor. Found. Chem. Eng.* **44**, 379 (2010)
- J. Kim, P. Moin, *J. Comp. Phys.* **59**, 308 (1985)
- V. Kossov, S. Krasikov, O. Fedorenko, *Eur. Phys. J. Special Topics* **226**, 1177 (2017)
- N.D. Kossov, Y.I. Zhavrin, D.U. Kulzhanov, *Zhur. Tekhn. Fiz.* **51**, 645 (1981)
- M. Navon, *Commun. in Applied Numer. Methods* **3**, 63(1987)
- H.L. Toor, *A. I. Ch. E. Journal* **39**, 725 (1957)

Modelling of heat transfer and mass transfer in cryogenic propellant tank pressurization process under microgravity environment

WANG Yanhui^{1,2}, GA Yongjing³, LUO Shu³, WANG Haosu³, ZHOU Binghong²

1, University of Chinese Academy of Sciences, Nanertiao NO.1, Zhongguancun, Haidian, Beijing, 100190, China

2, National Space Science Center, Chinese Academy of Sciences, bhzhou@nssc.ac.cn

3, Beijing Institute of Space System Engineering, Beijing, 100076, China

Many launch vehicles, such as Ariane V, HII, ATLAS V and DELTA IV, use cryogenic propellant to increase performance in their upper stages. Under microgravity environment, the development of the pressure and temperature of cryogenic liquid propellant would probably be different from the experiments' results under normal gravity[1]. On the other hand, propellant sloshing in launch vehicles can have challenging and detrimental effects on the performance of the vehicle. In optimizing the design of cryogenic tank, the self-pressurization rates must be accurately predicted for different g-levels and for a variety of initial sloshing conditions.

In this study, the sloshing phenomenon is analyzed under different initial amplitudes while the launch vehicle main engine cut-off. Different amplitudes of sloshing are described with a CFD model. This paper focuses on the pressure change of the tank and thermal desertification at the interface after sloshing happened. Comparison of different amplitude of sloshing by computations is performed to help us have a better understanding of this phenomenon. The result shows that it is crucial to control the amplitude of sloshing and too large amplitude may cause fatal situations. At the same time, the possible influences of Marangoni convection in several conditions are discussed.

References

[1] M.Utsumi. A Mechanical Model for Low-Gravity Sloshing in an Axisymmetric Tank[J]. Transactions of the ASME. 2004(71):724-730.

Instabilities of thermocapillary-buoyancy-driven flow in a rotating annular pool of medium Prandtl number liquid

Wan-Yuan Shi^{a,b}, Han-Ming Li^a and Michael Ermakov^c

^a College of Power Engineering, Chongqing University, Chongqing 400044, China

^b Key Laboratory of Low-grade Energy Utilization Technologies and Systems, Ministry of Education, Chongqing 400044, China

^c Ishlinsky Institute for Problems in Mechanics of RAS, Moscow, 117526, Russia

shiwuy@cqu.edu.cn

Linear stability of thermocapillary-buoyancy-driven flow in a rotating annular pool (aspect ratio $\Gamma=d/(r_o-r_i)=0.25$, $r_i/r_o=0.5$) of a medium Prandtl number liquid ($Pr=6.7$) is investigated. The neutral Reynolds numbers for the incipience of instabilities are determined by linear stability analysis assuming a counterclockwise rotation direction and the underlying mechanisms are analyzed by energy budgets. Within the parameter space ($0 \leq Ta \leq 60$) considered here, there are three ranges can be distinguished obviously. The axisymmetric basic flow first loses its stability to flow instability of type I in the range of $0 \leq Ta \leq 3.35$. The instability curve shows that the critical Reynolds number Re_c increases with increasing Ta , i.e. the pool rotation improves the stability of the axisymmetric flow. In the intermediate Ta range $3.35 \leq Ta \leq 42.5$, flow instability of type II arises and replaces type I as a critical mode. The Re_c decreases at first and then increases when a minimum value $Re_c=642.6$ is attained at $Ta=16.44$. However, the neutral stability curves of type III show that the flow would under transitions repeatedly between axisymmetric flow and oscillatory bifurcation. The critical boundaries separating the stable region and unstable region are determined by calculating the neutral stability curves of each eigenmode, as the blue solid lines shown in Figure 1b. Figure 2 shows the temperature patterns corresponding to different flow instabilities.

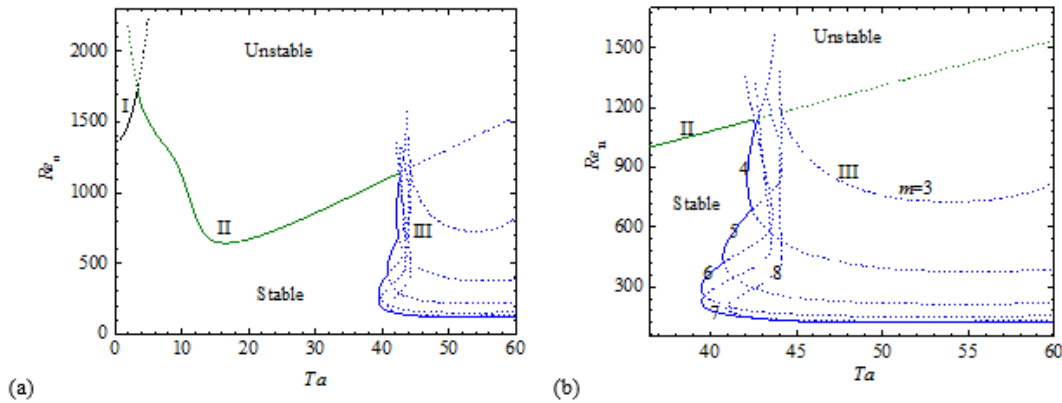


Figure 1: (a) Neutral instability curves and (b) close-up of flow instability type III. The Roman digital signifies different types of flow instability. The Arabic numeral marks the azimuthal wavenumber m . The solid line represents the critical instability boundary while the broken line indicates other neutral boundary.

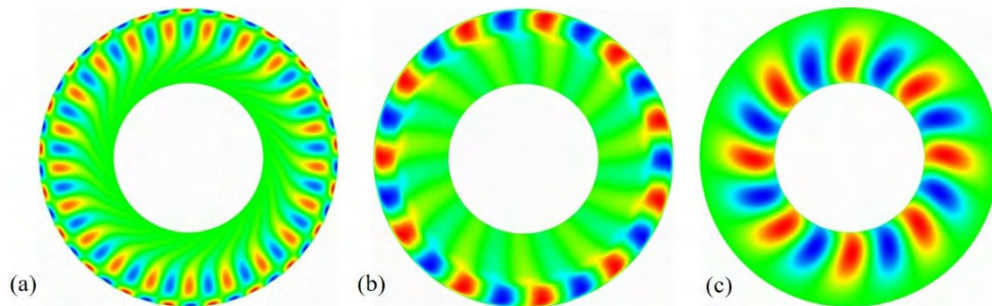


Figure 2: Surface temperature patterns for different flow instabilities. (a) Flow instability type I at $Ta=3.35$, $Re_c=1726.8$. (b) Flow instability type II at $Ta=16.44$, $Re_c=643.8$. (c) Flow instability type III at $Ta=60$, $Re_c=121$.

Acknowledgement: This work was funded by the National Nature Science Foundation of China (No. 51676018).

Growth mechanisms of Breath Figures with a humidity sink

Mathan K. Raja and Wenceslao González-Viñas

Universidad de Navarra,
Complex Systems group and PHYSMED group
Pamplona, Spain
mrja@alumni.unav.es, wens@unav.es

NaCl is highly hygroscopic. Thus, a salty droplet absorbs water vapor from its surrounding and acts as a humidity sink. A humidity sink reduces water vapor concentration and, consequently its corresponding partial vapor pressure. This creates a region of inhibited condensation (RIC). Earlier studies [1], report experimental results on the evolution of the salty drop, the RIC and the BF outside. They were able to estimate the water vapor concentration profile in the nearby atmosphere. Although results can be qualitatively explained, the involved mechanisms are still not clear [2, 3]. Here, we report numerical results where different assumptions have been taken and comparison to the experiments is performed to elucidate the relevant mechanisms. All in all, in our simulations, many of such a controllable characteristics conditions (nucleation density, chemical properties of the condensing surface, growth dynamics) allowed us to investigate the detailed mechanism of Breath Figures formation and evolution in the presence of a humidity sink.

References

- [1] J. Guadarrama-Cetina, R. D. Narhe, D. A. Beysens, and W. González-Viñas, *Phys. Rev. E* **89**, 012402 (2014).
- [2] D. Beysens, *Comptes Rendus Physique* **7**, 1082 (2006).
- [3] M. Sokuler, G. K. Auernhammer, C. J. Liu, E. Bonaccorso, and H.-J. Butt, *EPL* **89**, 36004 (2010).

A Method of Measuring Gas Density By Digital Holography

Wei Song¹, Qiu-Sheng Liu^{1,2*}, Jin-Chang Xie¹, Yong-Xiang Xv¹, Wen-Jun Liu, Li-Li Qiao¹

¹Institute of Mechanics, Chinese Academy of Sciences, Beijing 100190, China

²University of Chinese Academy of Sciences, Beijing 100049, China

*liu@imech.ac.cn

To describe the process of significantly evaporation, the non-equilibrium vapor/liquid interface model has been built up based on the assumption of the uniform gas density distribution [1~3]. In this way, a constant of gas density would represent the whole three-dimensional distribution of the vapor layer and it is obviously not agreed with the actual reality. Meanwhile, it is noticed that there are already various of detecting method for the liquid layer [4~6], such as PIV for the velocity distribution of liquid, infrared thermometer for the temperature distribution of liquid, microscope imager for the appearance of liquid. On the contrary, there is rarely methods mentioned just for the vapor layer's temperature, density, or pressure distribution. By those incomplete experimental data, a physical model describing both sides of the liquid and vapor layer is hardly built up to get closer to the physical reality. So, it is necessary to develop a measurement method for the gas density distribution in the vapor layer, which will compensate the experimental data on the vapor side and contribute to the establishment and modification of the non-equilibrium vapor/liquid interface model.

In this paper, we proposed to apply digital holographic method in the gas density distribution measurement and a preliminary experiment (Fig.1) has been done. As shown in the Fig.1, a digital holography setup has been built up in Mach-Zehnder interferometer style. The recording beam wavelength is 633nm. The object and reference beam are both plane wave generated by the Expander and Lens 1. The PBS 2 is to split the plane beam into two beams (Object Beam and Reference Beam). The holograms attained by the two beams interfering each other and were recorded by the CCD. Through some algorithm processing, the phase distribution around the flame of candle(Fig.2), which is linear correlation to the gas density distribution, has been experimentally detected(Fig.3). As shown in the Fig.2, the objective beam (diameter 10mm) goes through the flame (the longest width 25mm). So, the results only show partial gas density distribution around the candle wick inside the flame.

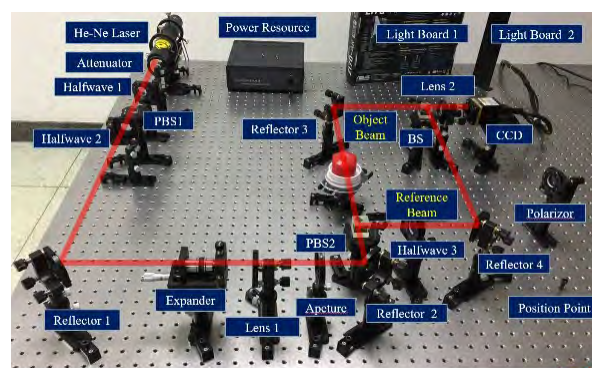


Fig. 1. Setup of the measurement device.



Fig. 2. Flame of Candle with Object Beam Passing through

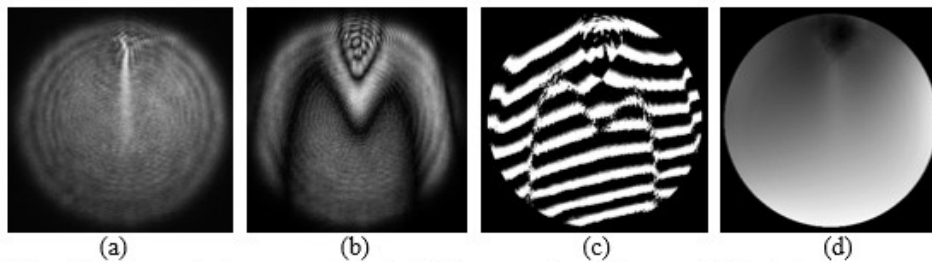


Fig. 3. Result of the preliminary experiments, (a) the recording hologram, (b) the hologram removed the background, (c) the wrapped phase distribution, (d) the unwrapped phase distribution

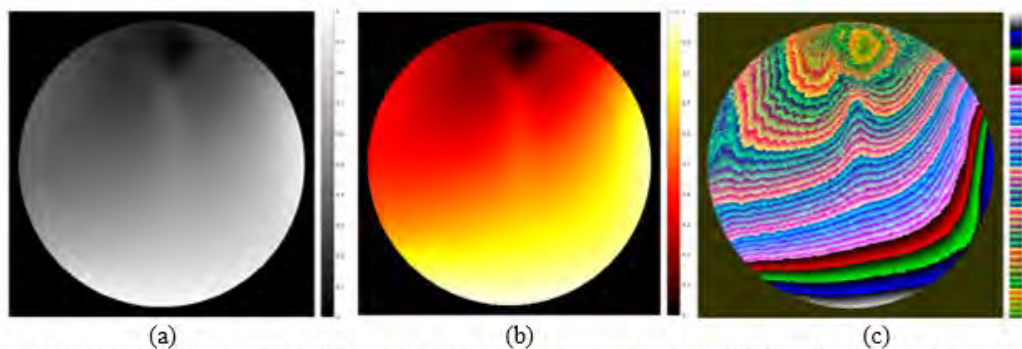


Fig. 3. Colormap of the normalized phase distribution, (a) grey analysis, (b) black-red-yellow analysis, (c) the contour lines of the phase distribution

The Fig.3(b) equals to the result of the traditional holographic interferometry method, a cluster of massive and twisted fringes would reveal the refractive index changes occur as the candle burning. By contrast, more detailed information (Fig.4) is capable to get through the digital holographic method results by much more analysis.

In the next step, the view field of the setup will be extended to contain the whole flame. Then, according to the Gladstone-Dale law, the gas density distribution will come out and the calibration of the gas density also will be finished.

Acknowledgements

This research was financially supported by the National Natural Science Foundation of China (Grants Nos. 11532015, U1738119) and the China's Manned Space Program (TZ-1).

References

- J. Margerit, P. Colinet, G. Lebon, C. S. Iorio and J. C. Legros, Interfacial nonequilibrium and Benard-Marangoni instability of a liquid-vapor system. *Physical Review E*, 2003, 68: 041601-1~041601-14.
- Liu Rong, Liu Qiu-Sheng and Hu Wen-Rui. Marangoni-Benard Instability with the Exchange of Evaporation at Liquid-Vapour. *Interface. Chin Phys Lett*, 2005, vol 22(2), 402-404.
- LIU Rong, LIU Qiu-Sheng. Vapour Recoil Effect on a Vapour-Liquid System with a Deformable Interface. *Chin Phys Lett*, 2006, Vol.23(4), 879-883.
- A Saha, S Basu, R Kumar. Particle image velocimetry and infrared thermography in a levitated droplet with nanosilica suspensions. *Experiments in Fluids*. 2012, 52: 795~807.
- S Bauerecker, P Ulbig, V Buch, L Vrbka, P Jungworth. Monitoring ice nucleation in pure and salty water via high speed imaging and computer simulations. *Journal of Physical Chemistry C*, 2008, 112(20): 7631~7636.
- F Tavakoli, SH Davis, HP Kavehpour. Freezing of supercooled water drops on cold solid substrates: initiation and mechanism. *Journal of Coatings Technology & Research*, 2015, 12(5): 869~875.

Experimental Investigation of Quasi-Static Liquid Layer Evaporation

Wen-Jun Liu^{1,2} and Qiu-Sheng Liu^{1,2*}

¹Institute of Mechanics, Chinese Academy of Sciences, Beijing 100190, China

²University of Chinese Academy of Sciences, Beijing 100049, China

*liu@imech.ac.cn

Thermal convective flow instability in liquid layer has been extensively studied in the past few decades. The temperature gradient in all directions of the liquid layer affects the pattern and structure of the convection vortex. T. Watanabe et al.[1] experimentally investigated the thermocapillary-driven flow in a liquid film with two free gas-liquid interfaces. The flow exhibited a transition from two-dimensional steady flow state to three-dimensional oscillatory state. If the working fluid is a volatile liquid, the problem will become more complicated as the evaporation effect is added [2]. It was shown experimentally in the work of Y. Lyulin et al. [3] that evaporative convection within horizontal liquid layer under shear–stress gas flow occurred in the direction opposite to the gas flow. And the average evaporation flow rate has close relationship with the gas velocity, the gas/liquid temperature and the liquid depth. The regular and irregular Marangoni convection patterns were recognized by infrared camera at the free surface of ethanol layers in deep and shallow vessels [4].

This paper describes the experimental investigation of a quasi-static evaporating liquid layer under two-direction temperature gradient. Depth of the liquid layer (about 2 mm) maintained quasi-changeless with the evaporation rate and liquid-injection rate approximately equal. Comparative experiments were carried out with different working fluids (FC-72, Ethanol and HFE7500), heating modes (constant substrate temperature heating and constant heat flow heating) applying combined observation methods (infrared camera, thickness meter, CCD, etc.). When the vertical temperature difference in the liquid layer (ΔT) increased, Marangoni (Ma) and Rayleigh (Ra) numbers were accompanying changed, and the critical state of thermal flow pattern, related to the critical Marangoni number (Mac) and Rayleigh number (Rac) was investigated to study the influence of evaporation on the convection instability of the liquid layer.

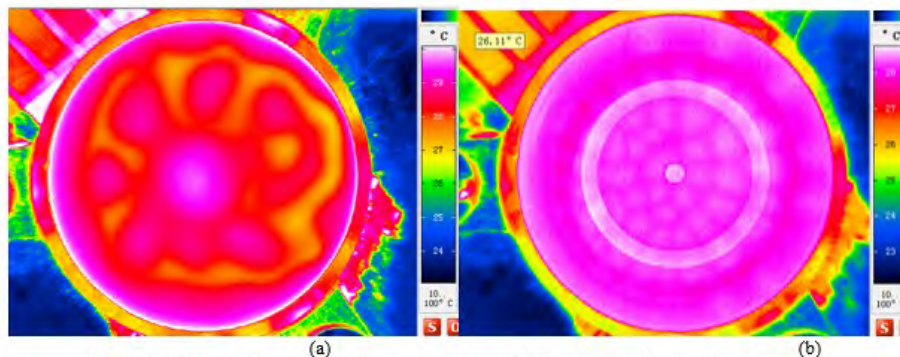


Figure 1: Thermal Convective of evaporation layer of Ethanol (a) and layer of HFE7500 (b).

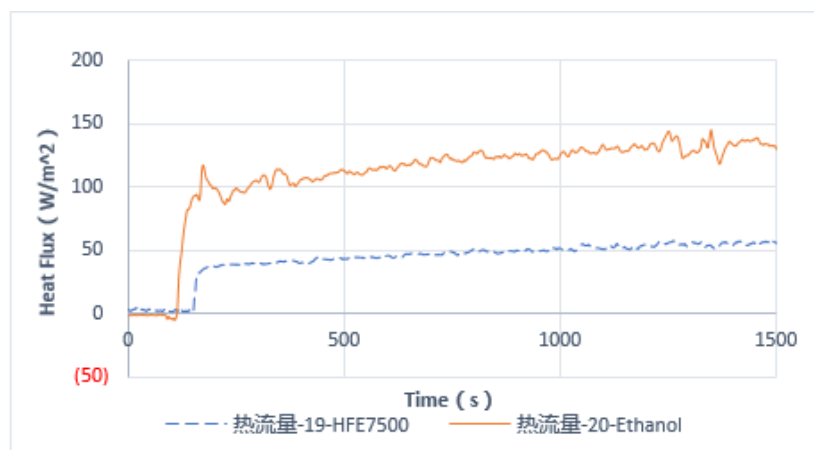


Figure 2: Heat Flux evolution of evaporation layer of Ethanol and HFE7500.

It is shown that the average evaporation rate of Ethanol layer is greater than HFE7500. Judging from the interface temperature distribution obtained by the top view infrared camera, convection flow in the Ethanol liquid layer is easier to destabilize. That is, evaporation effect makes critical Marangoni number (Ma_c) smaller. Moreover, for liquids with different evaporation physical properties, the thermal flow pattern exhibits different characteristics in the terms of cell size, lifetime and transition stage etc.

Acknowledgements

This research was financially supported by the China's Manned Space Program (TZ-1), the National Natural Science Foundation of China (Grants No. 11532015), and the United funding of the National Natural Science Foundation of China and the SJ10 Satellite Research Program on Space Science, the Chinese Academy of Sciences (Grants No.U1738119).

References

- [1] T. Watanabe T. Watanabe, Y. Kowata, I. Ueno, International Journal of Heat and Mass Transfer 116 (2018) 635–641
- [2] P. J. Sáenz, P. Valluri, K. Sefiane et al. Physics of Fluids 26, 024114 (2014)
- [3] Y. Lyulin, O. Kabov, International Journal of Heat and Mass Transfer 70 (2014) 599–609
- [4] A. Sankaran, A.L. Yarin, International Journal of Heat and Mass Transfer 122 (2018) 504–514

The influence of different scale on thermocapillary convection in sessile droplet: experimental study

Xue CHEN^{1,2,*}, Zhiqiang ZHU², Qiusheng LIU^{2,3}

¹ Guilin University of Electronic Technology, School of Mechanical and Electrical Engineering, Guilin, 541004, China

²Institute of Mechanics, Chinese Academy of Sciences, Beijing 100190, China

³University of Chinese Academy of Sciences, Beijing 100049, China

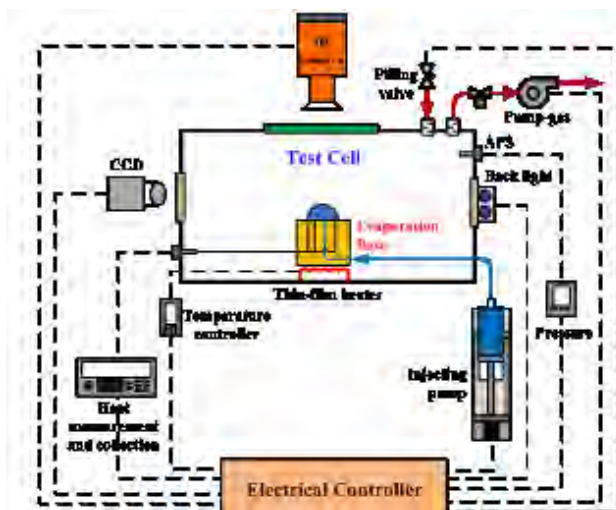
*E-mail: chenxue@imech.ac.cn

The evaporation of a liquid drop resting on a solid substrate is of great importance in a wide variety of industrial and scientific applications, such as evaporative self-assembly technique (DNA mapping, MEMS cooling), evaporation-induced particle deposition (thin film coating, ink-jet printing) and the design of more efficient heat transfer devices (Micro Heat Pipes and Capillary Pumped Loop). Among the mechanisms involved, the behavior of thermo-capillary convection inside the drop induced by temperature gradient along the liquid-gas interface can significantly influence the flow instability. For this reason, understanding the flow characteristics inside the drop plays a vital role in evaporating droplet.

In the past decades, evaporating drops were attracted more and more scientific interests. Most researches concerned on the evolution of drop's contour, influence of the evaporation rate and heat transfer properties. For instance, Sobac, B. and Brutin, D. [1] revealed the influence of the substrate temperature and substrate thermal properties on the evaporation process. However, there is rare experimental studies focusing on the influence of different scale on thermocapillary convection in sessile drop. In fact, such scale effect plays a crucial role in the interfacial phenomena and heat transfer process during evaporation [2]. Therefore, the present study aims to establish the influence mechanisms of different scale on the thermocapillary convection in droplet evaporation.

To investigate the interfacial phenomena during evaporating, the infrared camera was used and the experimental apparatus was designed as shown in Figure 1. It is consisting of an enclosed test cell, injecting system, heat measurement and collection system, pressure controller and observation devices including CCD camera and IR camera [3]. Experiments were performed as a preliminary work for the future space experiments on board the Chinese Space Station (CSS) to investigate the internal flow instability with free interface and phase-change process.

On the basis of this system, we conducted a series of ground experiments. The underlying mechanism of heat and mass transfer involved in the droplet evaporation with different volatile fluids was studied. Taking advantage of infrared thermal imaging technology, evidence on the various convective instabilities is then obtained, depending on the nature convection and the length scale of droplets. It is found that there are two distinct convective patterns appearing during free evaporation: one is in the form of hydrothermal waves and the other one is in the form of Rayleigh-Bénard convective cells. Owing to the scale effect, the surface-tension-driven flow may be divided into four kinds of patterns. The more detailed results will be discussed in the following article.



Acknowledgements

This research was financially supported by National Natural Science Foundation of China (Grants No. 11532015), and the United funding of the National Natural Science Foundation of China and the SJ10 Satellite Research Program on Space Science, the Chinese Academy of Sciences (Grants No.U1738119).

References

- [1] Sobac, B., Brutin, D., Thermal effects of the substrate on water droplet evaporation[J]. *Physical Review E*, 2012, 86(2): 021602.
- [2] Saada M. A., Chikh S., Tadrist L., Evaporation of a sessile drop with pinned or receding contact line on a substrate with different thermophysical properties[J]. *International Journal of Heat and Mass Transfer*, 2013, 58(1-2): 197-208.
- [3] Chen X., Zhu Z. Q., Liu Q. S., Wang X. W., Thermodynamic behaviors of macroscopic liquid droplets evaporation from heated substrates[J]. *Microgravity Science and Technology*, 2015, 27(5): 353-360.

Effect of Rotation on Thermal-Solutal Capillary Convection of Binary Fluid Mixture in a Czochralski Configuration

Wu Chunmei, Yuan Bo, Li Yourong and Lin Ding

Key Laboratory of Low-grade Energy Utilization Technologies and Systems of Ministry of Education,
College of Power Engineering, Chongqing University, Chongqing 400044, China
E-mail: chunmeiwu@cqu.edu.cn

Thermal-solutal capillary convection in a binary mixture fluid is one of the most common types of fluid flow in nature and industrial processes. In the past few decades, it has attracted the attention of many researchers from various fields, not only for its fundamental interest in structures and pattern formation but also for its practical importance in the performance improvement of many industrial devices^[1-3]. In the material processing industry, an important example is the Czochralski crystal growth technology^[4], where both the crucible containing the melt and crystal growing at the melt surface are rotated. Therefore, the coupling among the capillary and buoyancy forces, centrifugal and Coriolis forces drives the undesired convections and ensuing instabilities, which directly affect the quality of semiconductors grown from binary compounds.

In order to gain a fundamental understanding of the complex flow during Czochralski crystal growth, a series of unsteady three-dimensional numerical simulations results are presented in this paper. The silicon-germanium melt with an initial silicon mass fraction of 1.99% is adopted as test fluid. The capillary ratio is -0.2, the radius ratio and aspect ratio of the Czochralski configuration are 0.5 and 0.1, respectively. The rotation Reynolds numbers for the crystal and crucible range from 0 to ± 1870 and 0 to 1402, respectively. Minus means that rotation direction of the crystal is contrary to one of the crucible. To extract the coupled thermal-solutal and rotation effect, buoyancy effect is neglected. Results show that the basic flow is axisymmetric and steady at small rotation rate and temperature gradient. The flow structures are represented as meridian circulations rotating in different directions, which are dependent on the differential rotation rates of the crystal and the crucible. However, with the increase of rotation and thermocapillary Reynolds numbers, the flow will undergo a transition to a three-dimensional oscillatory flow. The critical conditions for the flow transitions are determined and the stability diagrams are mapped. When the thermal-solutal capillary flow is dominated, the critical thermocapillary Reynolds number increases firstly, and then decreases; when the rotation driven flow is much stronger, the thermo-solutal effect can promote the flow instabilities; For the flow pattern, the three-dimensional thermal-solutal capillary flow is shown as standing waves with fluctuations in space. When the crucible and crystal rotate, several spoke patterns with fluctuations travelling the azimuthal directions are captured. The characteristics of the flow instabilities, such as the fluctuation amplitude, wave number and propagation velocity, are dependent on the interactions of the thermal-solutal capillary, centrifugal and Coriolis forces.

References

- [1] S. Saravanan, T. Sivakumar, Combined influence of throughflow and Soret effect on the onset of Marangoni convection, *J. of Eng. Math.*, **85**, 55-64(2014).
- [2] J. J. Yu, Y. R. Li, J. C. Chen, Y.Zhang, C. M. Wu, Thermal-solutal capillary-buoyancy flow of a low Prandtl number binary mixture with various capillary ratios in an annular pool, *Int. J. Heat Mass Trans.*, **113**, 40-52(2017).
- [3] J. C. Chen, C. M. Wu, Y. R. Li, J. J. Yu, Effect of capillary ratio on thermal-solutal capillary-buoyancy convection in a shallow annular pool with radial temperature and concentration gradients, *Int. J. Heat Mass Trans.*, **109**, 367-377(2017).
- [4] S. Abbasoglu, I. Sezai, Three-dimensional modelling of melt flow and segregation during Czochralski growth of $\text{Ge}_x\text{Si}_{1-x}$ single crystals, *Int. J. Thermal Sci.*, **46**, 561-572(2007).



Unsteady flow and heat transfer of MHD nanofluid thin film over a stretching sheet with Marangoni convection

Yan Zhang¹, Bo Yuan², Min Zhang³ and Yu Bai⁴

1,2,3,4 School of Science, Beijing University of Civil Engineering and Architecture, Beijing 100044, China

1,2,3,4 Beijing Key Laboratory of Functional Materials for Building Structure and Environment Remediation, Beijing University of Civil Engineering and Architecture, Beijing 100044, China

E-mail of Yan Zhang: zhangyan1@bucea.edu.cn

E-mail of Bo Yuan: 2430399189@qq.com

E-mail of Min Zhang: 839367870@qq.com

E-mail of Yu Bai: baiyu@bucea.edu.cn

Abstract: The unsteady boundary layer flow and heat transfer of Cu-water nanofluid thin film over a stretching sheet have been investigated. The Marangoni convection driven by a temperature gradient is taken into consideration. The governing partial differential equations are transformed into the nonlinear ordinary differential equations by appropriate similarity transformation. The numerical and analytical solutions are obtained simultaneously using the shooting technique and homotopy analysis method (HAM). It can be seen that metal nanoparticles have remarkable effect on enhancing heat transfer of pure fluids. Marangoni convection can enhance the velocity of the thin film surface so that the velocity profiles doesn't always decrease monotonically from stretching sheet to free surface of the film in the cases of Marangoni number $Ma > 0$.

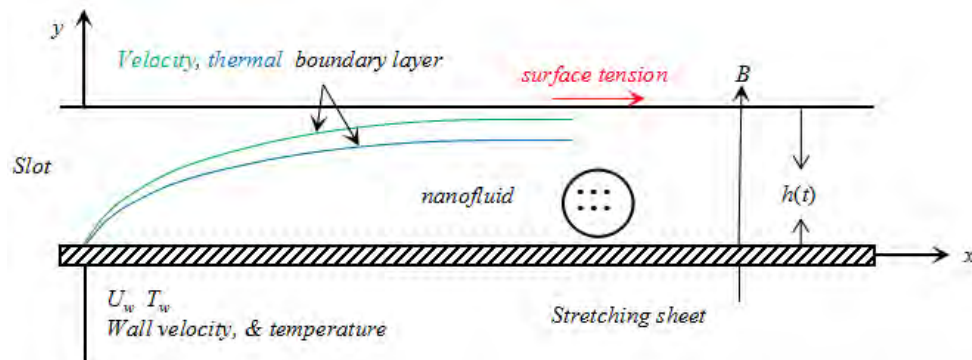


Figure 1: Flow configurations and coordinate system.

References

1. Wang CY (1990) Liquid film on an unsteady stretching sheet. *Q Appl Math* 48:601-610
2. Wang C (2006) Analytic solutions for a liquid thin film on an unsteady stretching surface. *Heat Mass Transf* 42:759-766
3. Liu IC, Andersson HI (2008) Heat transfer in a liquid film on an unsteady stretching sheet. *Int J Therm Sci* 47:766-772
4. Noor NFM, Abdulaziz O, Hashim I (2010) MHD flow and heat transfer in a thin liquid film on an unsteady stretching sheet by the homotopy analysis method. *Int J Numer Methods Fluids* 63:357-373
5. Noor NFM, Hashim I (2010) Thermocapillarity and magnetic field effects in a thin liquid film on an unsteady stretching surface. *Int J Heat Mass Transf* 53:2044-2051
6. Ravindran R, Samyuktha N (2015) Unsteady mixed convection flow over stretching sheet in presence of chemical reaction and heat generation or absorption with non-uniform slot suction or injection. *Appl Math Mech* 36:1253-1272
7. Pal D, Saha P (2016) Influence of nonlinear thermal radiation and variable viscosity on hydromagnetic heat and mass transfer in a thin liquid film over an unsteady stretching surface. *Int J Mech Sci* 119:208-216
8. Nasr A (2018) Heat and mass transfer for liquid film condensation along a vertical channel covered with a thin porous layer. *Int J Therm Sci* 124:288-299
9. Wang C, Pop I (2006) Analysis of the flow of a power-law fluid film on an unsteady stretching surface by means of homotopy analysis method. *J Non-Newtonian Fluid Mech* 138:161-172
10. Lin YH, Zheng LC, Ma LX (2016) Heat transfer characteristics of thin power-law liquid films over horizontal stretching sheet with internal heating and variable thermal coefficient. *Appl Math Mech -Engl Ed* 37:1587-1596
11. Si XH, Zhu XD, Zheng LC, Zhang XX, Lin P (2016) Laminar film condensation of pseudo-plastic non-Newtonian fluid with variable thermal conductivity on an isothermal vertical plate. *Int J Heat Mass Transf* 92:979-986
12. Shaha RC, Katariab RC (2016) On the squeeze film characteristics between a sphere and a flat porous plate using ferro fluid. *Appl Math Model* 40:2473-2484
13. Lin JR, Chu LM, Hung TC, Wang PY (2016) Derivation of two-dimensional non-Newtonian Reynolds equation and application to power-law film slider bearings: Rabinowitsch fluid model. *Appl Math Model* 40:8832-8841

14. Sandeep N, Chamkha AJ, Animasaun IL (2017) Numerical exploration of magnetohydrodynamic nanofluid flow suspended with magnetite nanoparticles. *J Braz Soc Mech Sci Eng* 39:3635-3644.
15. Choi SUS (1995) Enhancing thermal conductivity of fluids with nanoparticles. ASME San Francisco USA 66:99-105
16. Mustafa M, Hina S, Hayat T, Alsaedi A (2012) Influence of wall properties on the peristaltic flow of a nanofluid: Analytic and numerical solutions. *Int J Heat Mass Transf* 55:4871-4877
17. Bachok N, Ishak A, Pop I (2012) Unsteady boundary-layer flow and heat transfer of a nanofluid over a permeable stretching/shrinking sheet. *Int J Heat Mass Transf* 55:2102-2109
18. Narayana M, Sibanda P (2012) Laminar flow of a nanoliquid film over an unsteady stretching sheet. *Int J Heat Mass Transf* 55:7552-7560
19. Xu H, Pop I, You XC (2013) Flow and heat transfer in a nano-liquid film over an unsteady stretching surface. *Int J Heat Mass Transf* 60:646-652
20. Haq RU, Khan ZH, Khan WA (2014) Thermophysical effects of carbon nanotubes on MHD flow over a stretching surface. *Physica E* 63:215-222
21. Junaid Ahmad Khan, Mustafa M, Hayat T, Alsaedi A (2015) Three-dimensional flow of nanofluid over a non-linearly stretchingsheet: An application to solar energy. *Int J Heat Mass Transf* 86:158-164
22. Rida Ahmad, Mustafa M, Hayat T, Alsaedi A (2016) Numerical study of MHD nanofluid flow and heat transfer past abidirectional exponentially stretching sheet. *J Magn Magn Mater* 407:69-74
23. Lin YH, Zheng LC, Zhang XX, Ma LX, ChenG (2015) MHD pseudo-plastic nanofluid unsteady flow and heat transfer in a finite thin film over stretching surface with internal heat generation. *Int J Heat Mass Transf* 84:903-911
24. Lin YH, Zheng LC, ChenG (2015) Unsteady flow and heat transfer of pseudo-plastic nanoliquid in a finite thin film on a stretching surface with variable thermal conductivity and viscous dissipation. *Powder Technol* 274:324-332
25. Zhang Y, Zhang M, Bai Y (2017) Unsteady flow and heat transfer of power-law nanofluid thin film over a stretching sheet with variable magnetic field and power-law velocity slip effect. *J Taiwan Inst Chem Eng* 70:104-110
26. Tamim H, Dinarvand S, Hosseini R, Pop I (2014) MHD mixed convection stagnation-point flow of a nanofluid over a vertical permeable surface: A comprehensive report of dual solutions. *Heat Mass Transf* 50:639-650
27. Malvandi A, Ganji DD (2014) Brownian motion and thermophoresis effects on slip flow of alumina/water nanofluid inside a circular microchannel in the presence of a magnetic field. *Int J Therm Sci* 84:196-206
28. M. Sheikholeslami Kandelousi (2014) KKL correlation for simulation of nanofluid flow and heat transfer in a permeable channel. *Phys Lett A* 378:3331-3339
29. Xu H, Pop I, You XC (2013) Flow and heat transfer in a nano-liquid film over an unsteady stretching surface. *Int J Heat Mass Transf* 60:646-652
30. Pal D, Mandal G, Vajravelu K (2014) Flow and heat transfer of nanofluids at a stagnation point flow over a stretching/shrinking surface in a porous medium with thermal radiation. *Appl Math Comput* 238:208-224
31. Freidoonimehr N, Rashidi MM, Mahmud S (2015) Unsteady MHD free convective flow past a permeable stretching vertical surface in a nano-fluid. *Int J Therm Sci* 87:136-145
32. Hap RU, Nadeem S, Khan ZH, Akbar NS(2015) Thermal radiation and slip effects on MHD stagnation point flow of nanofluid over a stretching sheet. *Physica E* 65:17-23
33. Zhang Y, Zhang M, Bai Y (2016) Flow and heat transfer of an Oldroyd-B nanofluid thin film over an unsteady stretching sheet. *J Mol Liq* 220:665-670
34. Sandeep N, Malvandi A (2016) Enhanced heat transfer in liquid thin film flow of non-Newtonian nanofluids embedded with graphene nanoparticles. *Adv Powder Technol* 6:2448-2456
35. Hayat T, Muhammad T, Sabir Ali Shehzad, Alsaedi A (2017) An analytical solution for magnetohydrodynamic Oldroyd-B nanofluidflow induced by a stretching sheet with heat generation/absorption. *Int J Therm Sci* 11:274-288
36. Kumar R, Kumar R, Shehzad SA, Sheikholeslami M (2018) Rotating frame analysis of radiating and reacting ferro-nanofluid considering Joule heating and viscous dissipation. *Int J Heat Mass Transf* 120:540-551
37. Christopher DM, Wang BX (2001) Prandtl number effects for Marangoni convection over a flat surface. *Int J Therm Sci* 40(6):564-570
38. Christopher DM, Wang BX (2001) Similarity simulation for Marangoni convection around a vapor bubble during nucleation and growth. *Int J Heat MassTransf* 4:799-810
39. Zhang Y, Zheng LC(2012) Analysis of MHD thermosolutal Marangoni convection with the heat generation and a first-order chemical reaction. *Chem Eng Sci* 1:449-455
40. Das K, Acharya N, Kundu P (2015) Thin film flow over an unsteady stretching sheet with thermocapillarity in presence of magnetic field. *Therm Sci* 0:141
41. Lin YH, Zheng LC, ZhangXX (2014) Radiation effects on Marangoni convection flow and heat transfer in pseudo-plastic non-Newtonian nanofluids with variable thermal conductivity. *Int J Heat MassTransf* 77:708-716
42. Dandapat BS, Santra B, Andersson HI (2003) Thermocapillarity in a liquid film on an unsteady stretching surface. *Int J Heat Mass Transf* 16:3009-3015
43. Dandapat BS, Santra B, Vajravelu K (2007) The effects of variable fluid properties and thermocapillarity on the



flow of a thin film on an unsteady stretching sheet. *Int J Heat Mass Transf* 5: 991-996

44. Chen CH (2007) Marangoni effects on forced convection of power-law liquids in a thin film over a stretching surface. *Phys Lett* 1:51-57
45. Saleh H, Hashim I (2015) Buoyant Marangoni convection of nanofluids in square cavity. *Appl Math Mech-Engl Ed* 36(9):1169-1184. doi:10.1007/s10483-015-1973-6
46. Hayat T, Ijaz Khan M, Farooq M, Alsaedi A, Yasmeen T (2017) Impact of Marangoni convection in the flow of carbon–water nanofluid with thermal radiation. *Int J Heat Mass Transf* 106:810-815
47. Hamad MAA (2011) Analytical solution of natural convection flow of a nanofluid over a linearly stretching sheet in the presence of magnetic field. *Int Commun Heat Mass Transfer* 38:487-492
48. Li BT, Chen X, Zheng LC, Zhu LL, Zhou JL, Wang TT (2014) Precipitation phenomenon of nanoparticles in power-law fluids over a rotating disk. *Microfluid. Nanofluid* 17:107-114

Influence of confinement on the linear stability of a falling liquid film

Yiqin Li¹, Sophie Mergui¹, Gianluca Lavallo² and Georg F. Dietze¹

1. Univ Paris-Sud, CNRS, Lab FAST, Bât 502, Orsay, F-91405, France

2 Univ Paris-Sud, CNRS, Lab LIMSI, Bât 508, Orsay, F-91405, France yiqin.li@u-psud.fr

Instability of falling liquid films has been extensively studied in the past due to its relevance for the industrial applications such as evaporators, chemical reactors and distillation columns. A number of experimental works have focused on the linear stability of such flows both in the case of a quiescent atmosphere (Pierson and Whitaker 1977, Liu et al. 1993) and in the case of a counter-current gas flow (Aleksenko et al., 2009). However, to the best of our knowledge, there are no experimental works dealing with the case of a strongly-confined gas flow. The current experimental work focuses on this scenario by studying the influence of confinement on the linear stability of a falling liquid film. Our results are compared with linear stability calculations.

The experimental set-up is based on the one used in Kofman et al. 2017 and is sketched in Figure 1. The working fluid (water) emerges from an upstream tank and flows down an inclined glass plate (150 cm long, 27 cm wide) placed on a rigid framework. A temporal periodic forcing is introduced at the liquid inlet to trigger sinusoidal surface waves of prescribed frequency, f , and amplitude. The gas above the film surface is confined by a second glass plate (70 cm long, 27 cm wide), which is positioned at a distance H from the bottom plate. We consider two situations: (i) a virtually unconfined gas, where $H=17$ mm and (ii) a strongly confined gas, where $H=5.1$ mm. Experiments are performed for a Reynolds number in the range $Re = 18-42$ and a fixed inclination angle $\beta = 1.68^\circ$. A one-point temporal measurement of the film thickness based on a Confocal Chromatic Imaging technique is performed at mid-width of the channel at different locations from the inlet along the flow direction. From this, the spatial growth rate of the surface waves resulting from the so-called Kapitza instability (Kapitza, 1948) is determined in the linear regime and the neutral stability curve for a fixed inclination angle is obtained.

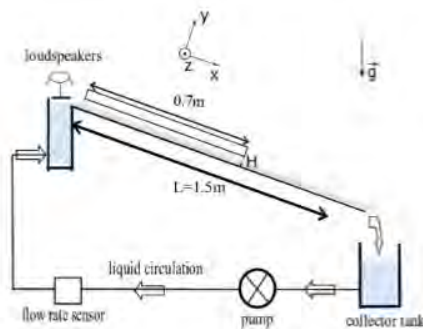


Figure 1: Sketch of the experimental set-up

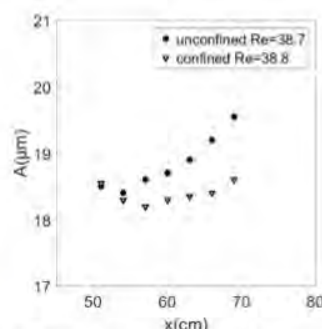


Figure 2: Evolution of the wave amplitude ($f=3.6$ Hz, $\beta=1.68^\circ$)

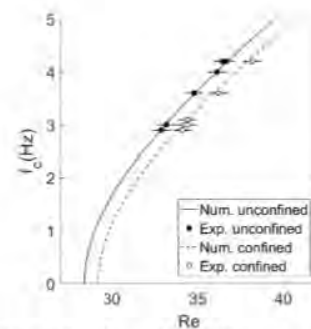


Figure 3: Neutral stability curves for the unconfined and confined configurations ($\beta=1.68^\circ$)

Figure 2 displays the evolution of the wave amplitude along the channel for the unconfined and confined configurations, all other parameters being equal (Re , β , forcing frequency and amplitude). The film is unstable in both configurations but the spatial growth is slower in the confined case, showing a stabilizing effect of the confinement. The cut-off frequency of the instability as a function of the Reynolds number has also been determined and compared with the neutral stability curves based on the linear theory in Figure 3. This stability diagram shows that the stability threshold is located at higher Re at fixed frequency, and at lower frequency at fixed Re in the confined configuration, confirming the stabilizing effect of the confinement.

References

- Aleksenko, S. V., Aktershev, S. P., Cherdantsev, A. V., Kharlamov, S. M. and Markovich, D. M. Primary instabilities of liquid film flow sheared by turbulent gas stream. *International Journal of Multiphase Flow*. 2009, 35, 617-627.
- Kapitza, P. L. Wave Flow of Thin Layer of Viscous Fluid (in Russian). *Zhurn. Eksper. Teor. Fiz.* 1948, 18, 3-28.
- Kofman, N., Mergui, S., and Ruyer-Quil, C. Characteristics of solitary waves on a falling liquid film sheared by a turbulent counter-current gas flow. *International Journal of Multiphase Flow*. 2017, 95, 22-34.
- Liu, J., Paul, J. D., and Gollub, J. P. Measurements of the primary instabilities of film flows. *Journal of Fluid Mechanics*. 1993, 250, 69-101.
- Pierson, F. W., and Whitaker, S. Some theoretical and experimental observations of the wave structure of falling liquid films. *Industrial & Engineering Chemistry Fundamentals*. 1977, 16, 401-408.

Effect of gas temperature on instability in liquid bridge

Yury Gaponenko, Viktor Yasnou, Aliaksandr Mialdun and Valentina Shevtsova

Microgravity Research Center, Université Libre de Bruxelles

F. Roosvelet 50, Brussels, 1050, Belgium

ygaponen@ulb.ac.be

The topic of our study is the influence of gas flow temperature on the dynamics of the liquid bridge induced by interfacial phenomena via thermocapillary (Marangoni). The aim of this investigation is concerned to the space experiment JEREMI (Japanese European Space Research Experiment on Marangoni Instabilities) which is devoted to the study of the threshold of hydrothermal instabilities in two-phase systems in cylindrical geometry. This experiment is planned to be performed in the Japanese module on the ISS using the dedicated FPEF (Fluid Physics Experiment Facility).

In the present study gas-liquid flows induced by Marangoni convection on a free surface and buoyancy due to Earth's gravity are analyzed for fluids in presence of evaporation through the interface. N-decane and air have been used as experimental fluids. We consider the system when gas surrounds the liquid bridge (see Fig.1, left). Depending on the gas temperature, the blowing flow rate and the temperature difference between the rods different flow regimes have been classified including 3D oscillatory.

The problem is solved numerically in 3D geometry, which corresponds to a liquid bridge axially placed into an outer cylinder with solid walls. The internal core consists of solid rods at the bottom and top, while the central part is a relatively short liquid zone filled with viscous liquid and kept in its position by surface tension. The experimental results of this problem have been recently published, Yasnou et al. (2018).

Our previous results (Shevtsova et al., 2013) have demonstrated the influence of shear-stress impact of a gas flow blowing along the interface, but now we examine the influence of gas temperature on the instability in the liquid bridge via heat transfer. Depending on the gas flow temperature we observe a wide variety of flow patterns which correspond to different modes of an oscillatory flow. In Fig. 1, (central and right part) the temperature fields are shown for the case of the oscillatory flow when the temperature difference between the hot and cold rods is the same ($\Delta T = 7^\circ \text{C}$) but the temperature of the gas flow is different. An intensive numerical study has been performed in a large range of gas flow temperatures and temperature differences. For each flow regime the heat fluxes through the surface as well as the flow pattern have been analyzed.

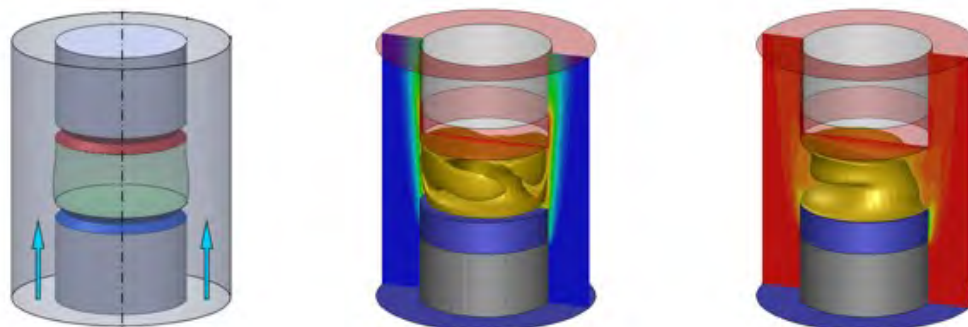


Figure 1: Left: geometry of the problem; Centre: temperature field for cold blowing gas ($T_{\text{gas}} = 15^\circ \text{C}$); Right: temperature field for hot blowing gas ($T_{\text{gas}} = 28^\circ \text{C}$).

References

1. V. Yasnou, Yu. Gaponenko, A. Mialdun, V. Shevtsova. Influence of a coaxial gas flow on the evolution of oscillatory states in a liquid bridge. Accepted to International Journal of Heat and Mass Transfer, 2018.
2. V. Shevtsova, Yu. Gaponenko, A. Nepomnyashchy. Thermocapillary flow regimes and instability caused by a gas stream along the interface. JFM, vol. 714, pp. 644-670, 2013.

Numerical Simulation of Marangoni Convection in a Sessile Droplet Evaporating in Pure Vapor

Yu Zhang, You-Rong Li and Jia-Jia Yu

Key Laboratory of Low-grade Energy Utilization Technologies and Systems of Ministry of Education,
 College of Power Engineering, Chongqing University
 No.174 Shazhengjie, Shapingba, Chongqing, 400044, China
 E-mail: liyounon@cqu.edu.cn

Evaporation of sessile droplets is a very common phenomena in nature and industry, and has extensive applications such as electronic cooling, thin film coating, DNA chip manufacturing, medical diagnose and ink-jet printing. During the process of droplet evaporation, Marangoni convection induced by surface temperature gradient occurs. In order to understand the effect of Marangoni convection on the evaporation rate and flow pattern, a series of three-dimensional numerical simulation on evaporation of sessile water droplet were performed. Temperature T_w of substrate varied from 298K to 302K and the pressure ratio η that is defined as the ratio of vapor pressure P^v to saturation pressure P^v_{sat} at T_w varied between 0.96 to 0.99. The contact radius of the water droplet on the substrate is 2.5 mm. Results show that the axisymmetric temperature distribution on droplet surface transits a serrated temperature distribution on account of the enhancing Marangoni convection with the increase of substrate temperature. The total evaporation rate q_m increases when the temperature of solid substrate increases. Also, the decrease of vapor pressure will intensify the Marangoni effect, and then increase the total evaporation rate of droplet surface, as shown in Figure 1. At the same time, the flow inside the water droplet will become more complex with the decrease of contact angle. As shown in Figure 2, the flow pattern is the axisymmetric at $\theta=90^\circ$, but it becomes a multi-cellular pattern with the decrease of contact angle because of the competition of heat transfer between from substrate and evaporation.

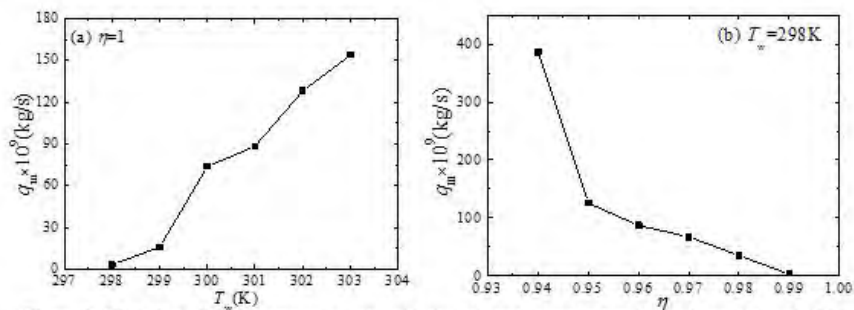


Figure 1: Variation of total evaporation rate with the substrate temperature (a) and contact angle (b).

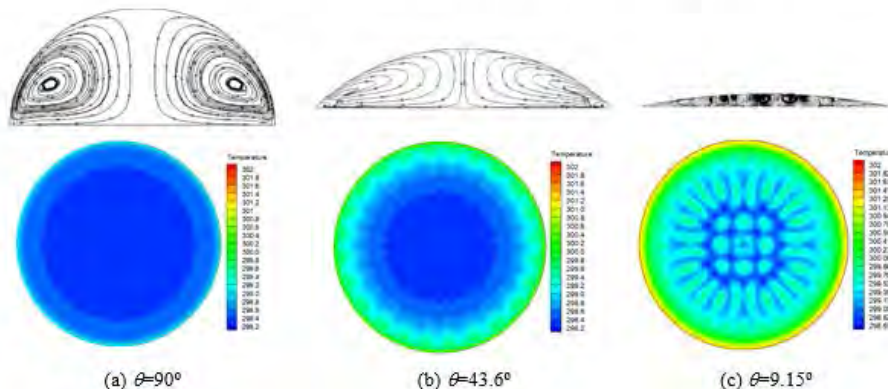


Figure 2: Evolution of flow pattern with the contact angle. Upper: meridional views of path-lines in the vertical center plane; Down: surface temperature distribution.

Spontaneous motion of a floating droplet on liquid layer

Zhenzhen Wang^{1,2}, Jie Chen^{1,2*}, Anjun Liu^{2,3}, Chao Yang^{1,2*}, and Zai-Sha Mao¹

¹ CAS Key Laboratory of Green Process and Engineering, Institute of Process Engineering, Chinese Academy of Sciences, Beijing 100190, China;

² University of Chinese Academy of Sciences, Beijing 100049, China

³ School of Chemical Engineering and Technology, Tianjin University, Tianjin 300350, China;

*Corresponding authors: jchen@ipe.ac.cn (J. Chen), chaoyang@ipe.ac.cn (C. Yang)

The spontaneous motion of an oil-droplet floating on an aqueous layer can be induced by surface instabilities [1]. The droplet would perform complex behaviors including irregular drifting, shrinking, vertical motion, severe deformation and fission. It is a resultant phenomenon influenced by evaporation, dissolution, interphase mass transfer, even the effect of container wall. A MIBK (methyl isobutyl ketone) drop was deposited on aqueous phase saturated by n-hexanol in a circular Petri dish. The evolution of the droplet behavior is showed in Figure 1. The periphery of the droplet slightly deformed under small perturbation. The deformation became more intense and accompanied with vertical acceleration after 1559 s, and the droplet split into small ones with different sizes. The different behavior modes may result from the interphase mass transfer of n-hexanol and MIBK, leading to surface tension gradient on the contact line of oil-gas-water system.

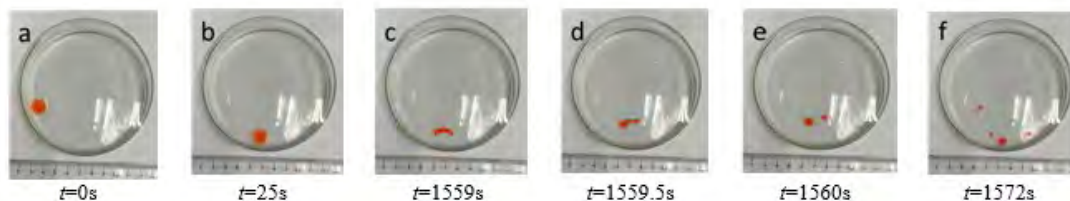


Figure 1: Behavior evolution of a MIBK droplet (100 μ L) floating on an aqueous layer, a-b: irregular motion, c-f: fission motion.

Acknowledgment: This work was financially supported by the National Key Research and Development Program (2016YFB0301702), National Natural Science Foundation of China (21606234, 21490584) and Instrument Developing Project of Chinese Academy of Sciences (YZ201641).

References

[1] Chen Y J, Nagamine Y, Yoshikawa K. Self-propelled motion of a droplet induced by Marangoni-driven spreading. *Physical Review E*, 2012, 80: 016303.

The double-diffusive Marangoni convection in opened two-layer rectangular cavity

Zheng Feng, Zheng Lin*

MIIT Key Laboratory of Thermal Control of Electronic Equipment, School of energy and power engineering,
Nanjing University of Science and Technology, NanJing, 210094, P. R. China

lz@njust.edu.cn

Crystal materials have been playing an important role in our daily life and industrial production with the progress of modern science and technology. With the development of space technology, a vital discovery is that the stripes of crystals are greatly reduced in the microgravity environment (Pimputkar et al. 1981). However, the Marangoni effect becomes an important factor to the quality of crystals. Recently, the double-diffusive Marangoni convection in single layer system has received lots of attention (Shklyaev et al. 2009 and Minakuchi et al. 2014), but for two-layer or multiple-layer system, it still has been paid less attention. The main purpose of present work is to investigate the transport mechanism and transformation route of double-diffused Marangoni convection in composite system. The physical problem is identified in Fig. 1.

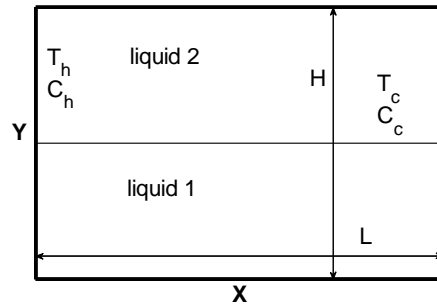


Figure 1: The physical model of double-diffusive Marangoni convection in a two-layer cavity.

The cavity is filled with two immiscible solvent and the same solute. The constant temperature and concentration are specified at the vertical walls, where $T_h > T_c$, $C_h > C_c$, and no-slip boundary is used for all solid walls. The surface tension σ is assumed to vary linearly with temperature and solute concentration as (Chen et al. 2010):

$$\sigma(T, C) = \sigma_0 - \gamma_T(T - T_0) - \gamma_C(C - C_0). \quad (1)$$

In our simulation, the Pr , Le at each layers are assumed at 1.0 and 100, and the physical parameters are kept equally at each layer, except for Re . Six cases are conducted with the surface Reynolds number $Re_2=200, 400, 600, 800, 1000$ and 1200, the corresponding interface Reynolds number $Re_1=100, 200, 300, 400, 500$ and 600. Where the Re is defined

as $Re = Re_T = \frac{\gamma_T \Delta T L}{\mu \nu} = -Re_C$, and the subscript 2 and 1 represent top layer and bottom layer, respectively. Then the

lattice Boltzmann method is applied to investigate the effect of Reynolds number on the transport mechanism of double-diffused Marangoni convection. For example, with $Re_2=200Re_1=100$ and $Re_2=400Re_1=200$, similar power spectra and phase diagrams with Fig. 4(a) in Ref. K. Li (2016) could be depicted. This indicates that periodic Marangoni convection could be observed at free surface and interface with same fundamental frequency f_1 as shown in Fig. 2. However, in the case of $Re_2=400$ and $Re_1=200$, it is characterized with $f_1=17$ and larger velocity amplitude.

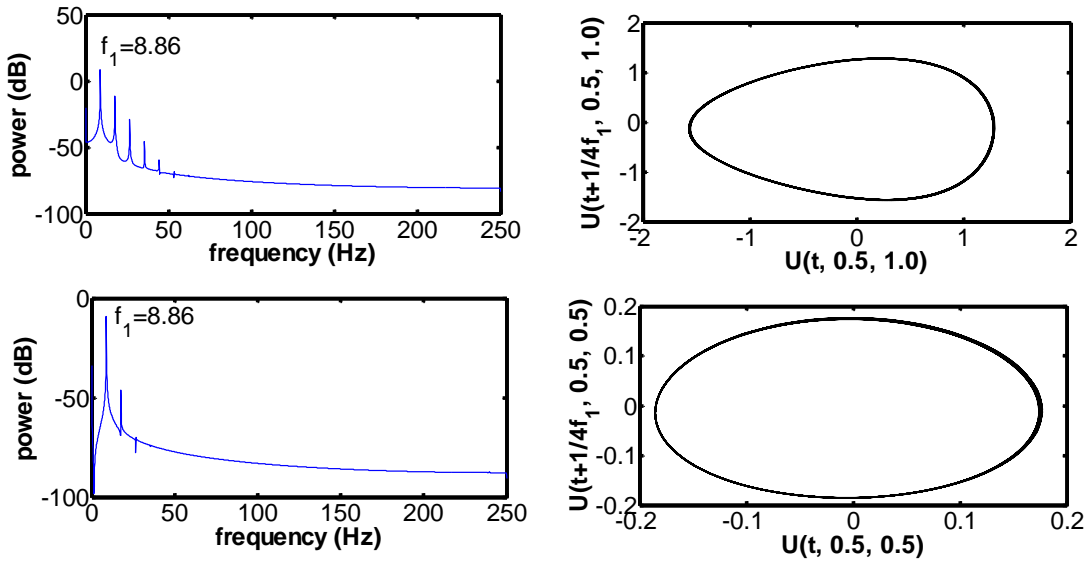


Figure 2: Power spectra (left) and phase diagrams (right) with $Re_2=200$, $Re_1=100$

With Reynolds numbers increased, as shown in Fig. 3, the power spectra with two fundamental frequencies and two-torus phase diagrams indicate that the double-diffusive Marangoni convection will transit from periodic oscillation to quasi-periodic mode. This provides a clear proof that the flow state of double-diffusive Marangoni convection in two layers rectangular cavities will transform along the quasi-periodic bifurcation route as shown in Fig. 2 of Li et al (2010).

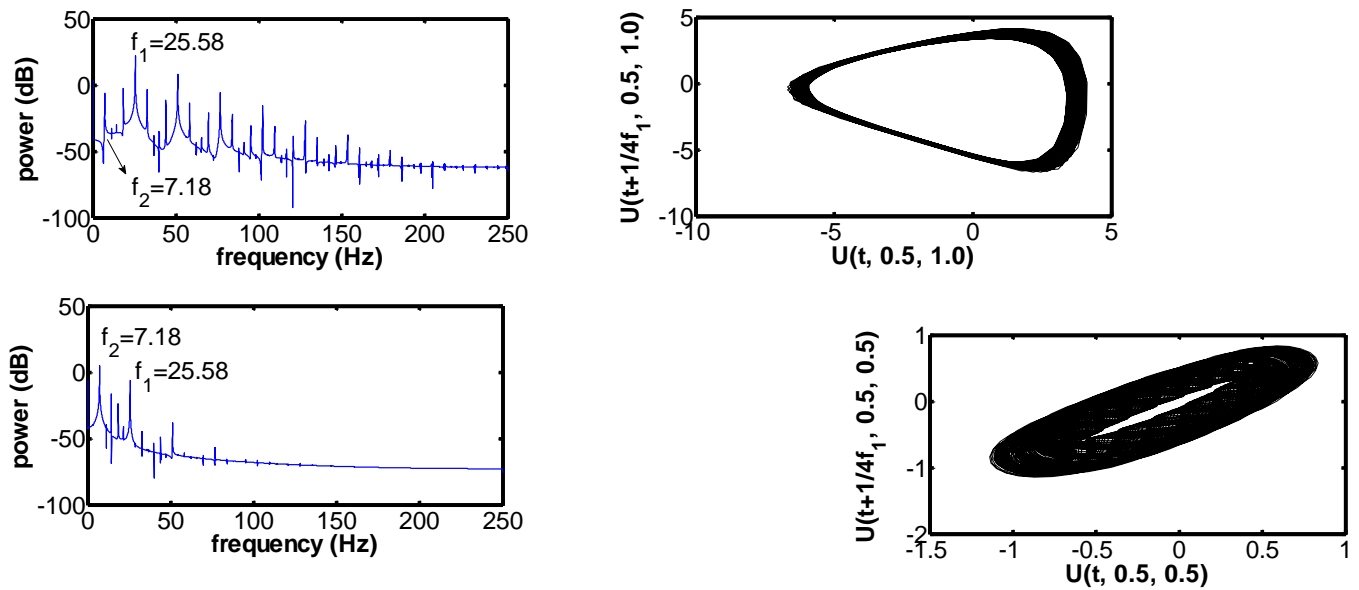


Figure 3: Power spectra (left) and phase diagrams (right) with $Re_2=600$, $Re_1=300$

The relationship between frequencies and Reynolds numbers of the six cases is summarized as Fig. 4. The fundamental frequencies increase with Re . the second fundamental frequency f_2 will appear at particular Re , which means the onset of quasi-periodic mode.

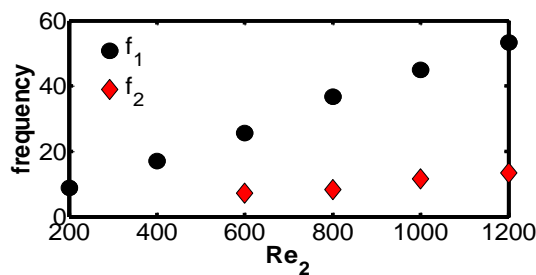


Figure 4: Simulated oscillation frequencies of all cases

Our numerical results show that the velocity amplitude of the monitoring point and the flow intensity will be enhanced with Re increased, and the transformation of double-diffusive Marangoni convection in open composite rectangular cavity is classified as quasi-periodic bifurcation route.

References

- [1] Pimputkar S M, Ostrach S. Convective effects in crystals grown from melt[J]. Journal of Crystal Growth, 1981, 55(3):614-646.
- [2] Shklyaev S, Nepomnyashchy A A, Oron A. Marangoni convection in a binary liquid layer with Soret effect at small Lewis number: Linear stability analysis[J]. Physics of Fluids, 2009, 21(5): 838.
- [3] Minakuchi H, Takagi Y, Okano Y, et al. The relative contributions of thermo-solutal Marangoni convections on flow patterns in a liquid bridge[J]. Journal of Crystal Growth, 2014, 385(2): 61-65.
- [4] Chen Z W, Li Y, Zhan J M. Double-diffusive Marangoni convection in a rectangular cavity: Onset of convection[J]. Physics of Fluids, 2010, 22(3):37.
- [5] Li K, Xun B, Hu W R. Some bifurcation routes to chaos of thermocapillary convection in two-dimensional liquid layers of finite extent[J]. Physics of Fluids, 2016, 28(5):130.
- [6] Li Y S, Chen Z W, Zhan J M. Double-diffusive Marangoni convection in a rectangular cavity: Transition to chaos[J]. International Journal of Heat & Mass Transfer, 2010, 53(23–24):5223-5231.

Preliminary Results of Droplet Evaporation Experiments onboard TZ-1 Cargo Spaceship

Wen-Jun Liu^{1,2}, Zhi-Qiang Zhu^{1*} and Qiu-Sheng Liu^{1,2*}

¹Institute of Mechanics, Chinese Academy of Sciences, Beijing 100190, China

²University of Chinese Academy of Sciences, Beijing 100049, China

*zhuzhiqiang@imech.ac.cn; **liu@imech.ac.cn

Droplet evaporation is commonly encountered in not only daily life but industry processes, for instance, drying of water droplets on a rainy day, cooling of electronic micro-processors[1] and management of space thermal engineering, etc. Most research interests are attracted to the thermal convection and heat transfer of evaporative droplet. F. Carle et al.[2] have developed an empirical model to accurately describe the evaporation rate and contribution of convective transport to evaporation of sessile droplets. The number of carbon atoms and its length in the molecular chain of the liquids were also believed to have a strong influence on the evaporation. What's more, nanofluid droplet is a new branch of droplet evaporation research. In the work of M. Parsa, R. Boubaker et al.[3], the pattern of evaporating binary-based nanofluid sessile droplets deposited on a substrate at different temperature was explored. Recently, due to the development and needs of aerospace industry, the research of evaporating droplets coupling with heat and mass transfer, evaporative convection and interfacial effects in microgravity has become a frontier issue in the field of international microgravity fluid physics.

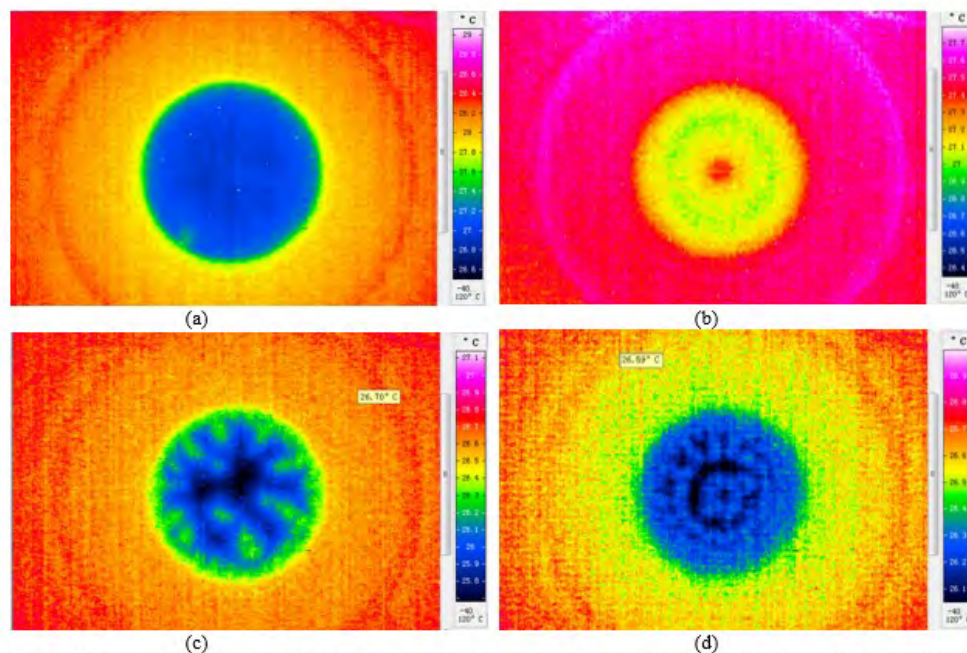


Figure 1: Thermal pattern of evaporation droplet in space (a),(b) and ground-based (c),(d) obtained by infrared camera.

TZ-1 cargo spaceship of CMSA (China's Manned Space Administration) was successfully launched in April 2017. Experiments were carried out to focus on liquid droplet and layer evaporation under various working conditions (different substrate temperatures, injecting liquid volume and cavity pressures for liquid evaporating). The present article will show some preliminary results during droplet evaporation. The average evaporation rate, convective and thermal pattern of evaporative FC-72 liquid droplet, injected from the bottom hole of a certain temperature substrate by an injection pump, was investigated using an infrared thermography. Comparison of temperature fields, average evaporation rate and heat flux during evaporating both in space and on ground were also performed to analyze the influence of gravity effect.

The compared results showed that due to the gravity-free constraints, the height of droplets in space would be

higher than that on ground for same injection volume. The average evaporation rate of FC-72 droplet in space is much slower than the ground tests in the same working conditions (temperatures, volume and pressures), which was thought of the large contribution of buoyancy convection to evaporation on the ground. In addition, in the space experiment, the evaporating vapor of FC72 itself is not easy to diffuse and accumulate to coat the interface of the droplet, which makes the gradient of the vapor concentration at the droplet interface become smaller, resulting in a slower evaporation rate. To a certain extent, the sharpness of the infrared camera observation will also be affected. In both space and ground conditions, The higher the temperature of the evaporation substrate, the greater average evaporation rate, and the more prone to bubbles at the top of the droplet during the evaporating process.

Acknowledgements

This research was financially supported by the China's Manned Space Program (TZ-1), the National Natural Science Foundation of China (Grants No. 11532015, U1738119).

References

- [1] S. Chakraborty, M. A. Rosen, B. D. MacDonald, *Applied Thermal Engineering* 125 (2017) 104–110
- [2] F. Carle, S. Semenov, M. Medale, D. Brutin, *International Journal of Thermal Sciences* 101 (2016) 35e47.
- [3] M. Parsa, R. Boubaker, S. Harmand, K. Sefiane, M. Biggerelle, R. Deltombe, *J Nanopart Res* (2017) 19:268.



Part III

LIST OF PARTICIPANTS



LIST OF PARTICIPANTS

Alexander ORON

Faculty of Mechanical Engineering,
Technion-Israel Institute of Technology,
Haifa.

meroron@technion.ac.il

Alexey Rednikov

Université Libre de Bruxelles,
Avenue F.D. Roosevelt,
50, Brussels, Belgium.

amirgat@technion.ac.il

Alexey Fedyushkin

Ishlinsky Institute for Problems in Mechanics
RAS

Vernadskogo prospect 101, b.1,
IPM RAS, 119526, Moscow, Russia

fai@ipmnet.ru

Alla Ovcharova

Lavrentyev Institute of Hydrodynamics of SB
RAS
Russia.

ovcharova@hydro.nsc.ru

An-Jun Liu

School of Chemical Engineering and
Technology,
Tianjin University,
Tianjin, China.

1015207036@tju.edu.cn

Antonio VERGA

European Space Agency
Keplerlaan 1, 2200 AG Noordwijk,
The Netherlands.

Antonio.Verga@esa.int

Antonio Viviani

Dept. of Industrial and Information
Engineering
Via Roma 29, 81031 Aversa, Italy.

antonio.viviani@unicampania.it

Amir Gat

Faculty of Mechanical Engineering,
Technion-Israel Institute of Technology,
Technion City, Haifa.

amirgat@technion.ac.il

Bing-Hong Zhou

University of Chinese Academy of Sciences,
Nanertiao NO.1, Zhongguancun, Haidian,
100190 Beijing, China.

bhzhou@nssc.ac.cn

Chao YANG

CAS Key Laboratory of Green Process and
Engineering,

Institute of Process Engineering, Chinese
Academy of Sciences,

100190 Beijing, China.

chaoyang@ipe.ac.cn

Cheng-Zhi Zhu

Key Laboratory of Low-grade Energy
College of Power Engineering,
Chongqing University.

zhuzc@cqu.edu.cn

Chen-Yi Yan

Ningbo University, School of Mechanical
Engineering and Mechanics
Ningbo,

Zhejiang, 315211, China

156001547@nbu.edu.cn

Chevtsova (Shevtsova) Valentina

University of Brussels
MRC. CP 165/92, ULB, 50, av.F.D. Roosevelt,
1050 Brussels

vshev@ulb.ac.be

Chun-Mei Wu

Key Laboratory of Low-grade Energy
Utilization Technologies and Systems



Ministry of Education, College of Power
Engineering,
Chongqing University,
Chongqing 400044 China.
liyourong@cqu.edu.cn

Dominika Zabiegaj

Mechanical and Construction
Engineering, Faculty of Engineering and
Environment,
Northumbria University
Wynne-Jones Building,
Newcastle upon Tyne, NE1 8ST, United
Kingdom
dominika.zabiegaj@northumbria.ac.uk

Evgeniy Boyko

Faculty of Mechanical Engineering,
Technion – Israel Institute of Technology
HAHASHMONAIM 63, KIRYAT MOZKIN,
ISRAEL
evgboyko@campus.technion.ac.il

Fei Duan

School of Mechanical and Aerospace
Engineering,
Nanyang Technological University
50 Nanyang Ave. Singapore, 639798
feiduan@ntu.edu.sg

Feng Zheng

MIIT Key Laboratory of Thermal Control of
Electronic Equipment, School of energy and
power engineering, Nanjing University of
Science and Technology,
NanJing, 210094, P. R. China
zheng1261310331@163.com

Guo-Feng Xu

Institute of Mechanics, Chinese Academy of
Sciences,
No.15 Bei-Si-Huan West Road,
Haidian District, Beijing 100190, China.
xuguofeng@imech.ac.cn

Hans Riegler

MAX-PLANCK-INSTITUTE OF COLLOIDS
AND INTERFACES MPIKG
Wissenschaftspark Potsdam-Golm
Am Muehlenberg 1 OT Golm
14476 Potsdam, Germany.
Hans.Riegler@mpikg.mpg.de

Hao Liu

Department of Engineering Mechanics,
College of Aerospace Engineering,
Chongqing University,
400044, Chongqing, China.
zzeng@cqu.edu.cn

Hao Yan

Institute of Mechanics, Chinese Academy of
Sciences,
No.15 Bei-Si-Huan West Road, Haidian
District, Beijing 100190, China.
yanhao@csu.ac.cn

Ion Dan Borcia

Department of Computational Physics,
Brandenburg University of Technology
(BTU)
Cottbus-Senftenberg,
Erich-Weinert-Straße 1 03046 Cottbus,
Germany
borciai@b-tu.de

Jalil Ouazzani

ArcoFluid Consulting LLC
390 N Orange Ave #2300,
Orlando, FL 32801 USA
jalil.ouazzani@gmail.com

Jie Chen

CAS Key Laboratory of Green Process and
Engineering,
Institute of Process Engineering, Chinese
Academy of Sciences,
100190 Beijing, China.

jchen@ipe.ac.cn

Ji-Long Zhu

College of Power Engineering,
Chongqing University,
400044 Chongqing, China.
892498678@qq.com

Joschka M.Schulz

Technische Universität Berlin,
Chair of Chemical and Process Engineering
Ackerstraße 76,
13355 Berlin, ACK 7,
Hof III, Treppe H, Germany.
j.schulz@tu-berlin.de

Kai-Xin Hu

Ningbo University,
School of Mechanical Engineering and
Mechanics
Ningbo,
Zhejiang, 315211, China
hukaixin@nbu.edu.cn

Kerem Uguz

Bogazici University,
Department of Chemical Engineering, Bebek
Bogazici University,
Istanbul, 34342, Turkey
Kerem.uguz@boun.edu.tr

Li Zhang

Key Laboratory of Low-grade Energy
Utilization Technologies and Systems of
Ministry of Education,
College of Power Engineering,
Chongqing University,
Chongqing 400044, China.
liyourong@cqu.edu.cn

Li-Li Qiao

Institute of Mechanics, Chinese Academy of
Sciences,
No.15 Bei-Si-Huan West Road,

Haidian District, Beijing 100190, China.
liu@imech.ac.cn

Lin Zheng

Nanjing University of Science and
Technology,
NanJing, 210094, P. R.China
zheng1261310331@163.com

Lu Qiu

School of Energy and Power Engineering,
Beihang University,
Beijing, 100191, P. R. China
luqiu@buaa.edu.cn

Mei-Lan Zhou

Guilin University of Electronic Technology,
School of Mechanical and Electrical
Engineering,
Mechanical Engineering, Jinji road,
Guilin, 541004, China
lianghang@guet.edu.cn

Michael Bestehorn

Chair of Statistical Physics and Nonlinear
Dynamics,
Brandenburg University of Technology
Cottbus-Senftenberg
Erich-Weinert-Str. 1, 03046 Cottbus
Germany
bestehorn@b-tu.de

Natalia Ivanova

Tyumen State University,
Photonics and Microfluidics Laboratory,
6 volodarskogo st., Tyumen, 625003
Russia
ivanova@utmn.ru

Nikolay Kubochkin

Tyumen State University,
Photonics and Microfluidics Laboratory,
6 volodarskogo st., Tyumen, 625003
Russia
nikolavkubochkin@gmail.com



Nobuhiro Shitomi

Department of Mechanical Engineering,
Yokohama National University
79-5 Tokiwadai, Hodogaya-ku,
Yokohama, Kanagawa 240-8501, Japan.
shitomi-nobuhiro-nk@ynu.jp

Nobuyuki Imaishi

Kyushu University
6-1 Kasuga-koen, Kasuga 816-8580, Japan
imaishi@cm.kyushu-u.ac.jp

Olga Fedorenko

Institute of Experimental and Theoretical
Physics,
Al-Farabi Kazakh National University
al-Farabi Ave. 71, 050040 Almaty,
Republic of Kazakhstan.
fedor23.04@mail.ru

Olivier Minster

European Space Agency
ESTEC HRE Keplerlaan 1,
2200AG Noordwijk, The Netherlands.
Olivier.Minster@esa.int

Oxana A. Frolovskaya

Lavrentyev Institute of Hydrodynamics SB
RAS, Novosibirsk, Lavrentyev pr., 15
630090 Russia.
oksana@hydro.nsc.ru

Paul Gang Chen

Aix-Marseille University, Centrale Marseille,
CNRS, M2P2
38, rue Frederic Joliot-Curie,
13451 Marseille Cedex 20, France
gang.chen@univ-amu.fr

Perrine Freydier

Lab. FAST, Université Paris-Sud,
CNRS, Université Paris-Saclay, Bâtiment 502,
Campus Universitaire, F-91405, Orsay,
France.

perrine.freydier@u-psud.fr

Qiang YU

University of Chinese Academy of Sciences,
Nanertiao NO.1, Zhongguancun, Haidian,
Beijing, 100190, China.
yuqiang@nssc.ac.cn

Qi-Sheng Chen

Institute of Mechanics, Chinese Academy of
Sciences,
No.15 Bei-Si-Huan West Road,
Haidian District, Beijing 100190,
China.
qschen@imech.ac.cn

Qing-Yong Zhu

School of Engineering,
Sun Yat-sen University
China.
mcszqy@mail.sysu.edu.cn

Qiu-Sheng Liu

Institute of Mechanics, Chinese Academy of
Sciences,
No.15 Bei-Si-Huan West Road,
Haidian District, Beijing 100190,
China.
liu@imech.ac.cn

Ranganathan Narayanan

UNIVERSITY OF FLORIDA
P.O. BOX 116 005, UNIVERSITY OF
FLORIDA, GAINESVILLE,
FL 32611, USA
RANGA@UFL.EDU

Rodica Borcia

Venia legendi for Theoretical Physics
Brandenburg University of Technology
Cottbus-Senftenberg
Dept. Statistical Physics and Nonlinear
Dynamics Erich-Weinert-Str. 1 D-03046

Cottbus, Germany
borciar@b-tu.de

Ruddy Eglee Urbina Sulbarán

University of Navarra,
Irunlarrea, 1B, Physics and Mathematics
Department, 31008, Pamplona, Navarra
rurbina@alumni.unav.es

Santiago Madruga

Universidad Politécnica de Madrid,
ETSI Aeronáutica y del Espacio
Plaza Cardenal Cisneros 3,
28040 Madrid, Spain
santiago.madruga@upm.es

Sebastian Richter

Brandenburg University of Technology
(BTU)
Cottbus-Senftenberg
Erich-weinert-str.1,
03046 Cottbus Germany
Sebastian.Richter@b-tu.de

Seyed Iman Nejati

Institute for Technical Thermodynamics,
TU Darmstadt, L206,
Alarich-Weiss-Strasse 10,
64287 Darmstadt, Germany
nejati@ttd.tu-darmstadt.de

Taishi Yano

Department of Mechanical Engineering
Yokohama National University,
79-5 Tokiwadai, Hodogaya-ku,
Yokohama, 240-8501, Japan
yano-taishi-gh@ynu.ac.jp

Tatyana Lyubimova

Institute of Continuous Media Mechanics UB
RAS, Koroleva Str 1., 614013 Perm
Russia.
lyubimova@psu.ru

Valeri Frumkin

Technion – Israel Institute of Technology
Yokohama National University 79-5
Tokiwadai,
Hodogaya-ku, Technion – Israel Institute of
Technology,
Haifa, 32000, Israel.
valeri@technion.ac.il

Victoria Bekezhanova

Institute of Computational Modelling SB
RAS, Department of Differential Equations
Mechanics,
Akademgorodok 50/44, Krasnoyarsk, 660036
Russia.
bekezhanova@mail.ru

Viktor M. Fliagin

Tyumen State University,
Photonics and Microfluidics Laboratory 6
Volodarskogo st.,
Tyumen, 625003, Russia
v.m.flyagin@utmn.ru

Wan-Yuan Shi

Key Laboratory of Low-grade Energy
Utilization Technologies and Systems,
Ministry of Education,
Chongqing 400044, China.
shiwuy@cqu.edu.cn

Wei Song

Institute of Mechanics, Chinese Academy of
Sciences,
No.15 Bei-Si-Huan West Road, Haidian
District, Beijing 100190, China.
davidwsong@126.com

Wei Zhang

Technology and Engineering Center for
Space Utilization
Chinese Academy of Sciences
No.9 Dengzhuang South Rd
Haidian District, Beijing, 100094



China

zhangwei@csu.ac.cn

Wen-Jun Liu

Institute of Mechanics, Chinese Academy of Sciences,

No.15 Bei-Si-Huan West Road,
Haidian District, Beijing 100190,
China.

liuwenjun@imech.ac.cn

Xue Chen

Guilin University of Electronic Technology,
School of Mechanical and Electrical
Engineering, Guilin, 541004, China

²Institute of Mechanics, Chinese Academy of
Sciences, Beijing 100190, China

³University of Chinese Academy of Sciences,
Beijing 100049, China

chenxue@imech.ac.cn

Xu-Zhi Li

Technology and Engineering Center for
Space Utilization

Chinese Academy of Sciences

No.9 Dengzhuang South Rd

Haidian District, Beijing, 100094

China

xzhli@csu.ac.cn

Yan-Hui WANG

University of Chinese Academy of Sciences,
Nanertiao NO.1, Zhongguancun, Haidian,

Beijing, 100190 China.

bhzhou@nssc.ac.cn

Yan Zhang

School of Science,

Beijing University of Civil Engineering and
Architecture,

Beijing 100044, China.

zhangyan1@bucea.edu.cn

Ya-Sha Liu

Institute of Mechanics, Chinese Academy of
Sciences,

No.15 Bei-Si-Huan West Road,

Haidian District, Beijing 100190,

China.

liuyasha@imech.ac.cn

Yi-Qin Li

CNRS, Lab FAST, University Paris-sud

Univ Paris-Sud, CNRS, Lab FAST, Bat 502,

Orsay, F-91405, France

yiqin.li@u-psud.fr

You-Rong Li

Key Laboratory of Low-grade Energy

Utilization Technologies and Systems

Ministry of Education, College of Power

Engineering,

Chongqing University,

Chongqing 400044 China.

liyurong@cqu.edu.cn

Yury Gaponenko

UNIVERSITY OF BRUSSELS (ULB)

MRC. CP 165/92, ULB, 50, av. F.D.

Roosevelt, 1050 Brussels, Belgium

ygaponen@ulb.ac.be

Yu Zhang

Key Laboratory of Low-grade Energy

Utilization Technologies and Systems

Ministry of Education, College of Power

Engineering,

Chongqing University,

Chongqing 400044 China.

liyurong@cqu.edu.cn

Zeng Zhong

Chongqing University,

College of Aerospace Engineering,

Department of Engineering Mechanics,

Chongqing, 400044, China.

zzeng@cqu.edu.cn

Zhen-Zhen Wang

CAS Key Laboratory of Green Process and
Engineering,
Institute of Process Engineering, Chinese
Academy of Sciences,
Beijing 100190 China.
wangzhenzhen@ipe.ac.cn

Zai-Qiang JU

Spacety Co., Ltd,
No.9 Dengzhuang South Rd

Haidian District, Beijing, 100094
China.

juzaiqiang@spacety.cn

Zhi-Qiang Zhu

Institute of Mechanics, Chinese Academy of
Sciences,
No.15 Bei-Si-Huan West Road,
Haidian District, Beijing 100190,
China.

zhuzhiqiang@imech.ac.cn



